

**NASA
Technical
Paper
2090**

January 1983

NASA
TP
2090
c.1

Airborne Measurements Launch Vehicle Effluent *Launch of Space Shuttle (STS-1, on April 12, 1981*

TECH LIBRARY KAFB, NM
DL34939

Gerald L. Gregory,
David C. Woods, and
Daniel I. Sebacher

LOAN COPY RETURN TO
AFRL TECHNICAL LIBRARY
KIRTLAND AFB, N.M.

NASA



**NASA
Technical
Paper
2090**

1983

TECH LIBRARY KAFB, NM



0134939

**Airborne Measurements of
Launch Vehicle Effluent**
*Launch of Space Shuttle (STS-1)
on April 12, 1981*

Gerald L. Gregory,
David C. Woods, and
Daniel I. Sebacher
*Langley Research Center
Hampton, Virginia*

NASA
National Aeronautics
and Space Administration
**Scientific and Technical
Information Branch**

INTRODUCTION

Since 1972, the National Aeronautics and Space Administration (NASA) has been conducting measurements of launch vehicle effluent (LVE) during selected NASA and Air Force launches for the purpose of investigating the environmental impact of launch vehicle emissions (mainly exhaust of solid-propellant rocket motors) on tropospheric air quality. The LVE program is a multicenter activity involving Langley Research Center (LaRC), George C. Marshall Space Flight Center (MSFC), and John F. Kennedy Space Center (KSC). An initial program goal was to assess the applicability and accuracy of diffusion models for predicting the dispersion of exhaust effluents from NASA launch vehicles and in particular from the Space Shuttle vehicle. Current program goals focus on obtaining data bases to assist in the determination of the environmental effects of Shuttle launches. To meet these goals, measurements are made of the ambient concentrations of rocket exhaust products at the earth's surface and within the ground cloud formed during launch. These exhaust products are primarily hydrogen chloride (HCl) and particulates. Previous LVE measurement activities focused mainly on the Titan III launch vehicle, the country's largest solid-propellant rocket (similar to solid fuel used for Space Shuttle) vehicle prior to the Space Shuttle. Measurements have also been made during Scout and Delta launches (ref. 1) and during Apollo launches (ref. 2).

Results from previous launches (1974 through 1980) have been used to investigate the many facets associated with launch air-quality and environmental impacts, including such areas as comparisons of dispersion model and measurements, HCl partitioning (gas vs aqueous aerosol) in the exhaust cloud, physical growth and behavior of the cloud, meteorological parameters important to cloud dynamics, reaction of exhaust products with ambient air, and potential effects of launch emissions on the environment. The measurement results combined with various model and analytical studies have generated a substantial data base on LVE activities. A comprehensive list of previous publications pertinent to earlier LVE studies is included as appendix A to the report.

The first Space Shuttle (STS-1) was launched from KSC launch complex 39A (LC-39A) at 0700 EST, April 12, 1981. NASA LVE activities included airborne measurements of effluent within the exhaust cloud, measurements on the surface beneath the cloud, photographic documentation of cloud trajectory and growth, and model calculation of down-wind effluent concentrations. This report summarizes the LaRC airborne within-cloud measurements and the observations of exhaust cloud trajectory and volume growth. The within-cloud measurements and the cloud trajectory/volume measurements are used to assess various parameters and assumptions used in the diffusion modeling of the exhaust cloud. The surface measurements provide a basis for assessing the accuracy of the models used to calculate the exhaust effluent deposition beneath the cloud for a given launch. Surface measurements and model calculations, which are not included in this report, were conducted for STS-1 by personnel from the other participating NASA centers. Portions of the within-cloud data have already been summarized at recently held conferences (refs. 3 and 4).

SYMBOLS

B_{scat}	scattering coefficient, m^{-1}
HCl(g)	hydrogen chloride, gaseous state
HCl(t)	hydrogen chloride, total (gaseous plus aqueous)
RH	relative humidity, percent
T +	time referenced to launch (T = 0), min

Abbreviations:

AFETR	Air Force Eastern Test Range
KSC	Kennedy Space Center
LaRC	Langley Research Center
LVE	launch vehicle effluent
MSFC	Marshall Space Flight Center
NASA	National Aeronautics and Space Administration
QCM	quartz crystal microbalance
SEM	scanning electron microscopy
STS-1	Space Transportation System, launch number 1
UCS	universal camera site

DESCRIPTION OF EXHAUST CLOUD

The engine exhaust products of interest in the LVE studies are those portions emitted below the surface mixing layer (typically 1- to 2-km altitude). This exhaust forms one or more clouds within the mixing layer which, as a result of the heat content, rise and stabilize just below the inversion layer (top of mixing layer). Titan III measurements show that stabilization occurs 5 to 10 min after launch, then the cloud diffuses and drifts down-wind depositing effluents at the surface. This "stabilized" exhaust cloud contains engine exhaust (solid- and liquid-fueled engines), pad debris, pad deluge water, and entrained ambient air and can remain visible for periods of 1 to 2 hr after launch.

Engine exhaust products from the Shuttle solid- and liquid-fueled engines include HCl, Al_2O_3 , H_2O , CO_2 , N_2 , NO, and other minor species. Shown in table I are the approximate compositions of the exhaust products by major species, including: (1) the estimated total mass of exhaust products injected into the cloud, (2) the mass percentage of species at the nozzle exit plane of the Space Shuttle engines, (3) the mass percentage of species following afterburning entrained ambient air. The data of table I are from references 5 to 7. Not included in the estimates of table I

are species entrained into the cloud from such sources as the pad deluge water, pad and soil debris, and entrained ambient air. The range of exhaust mass in the cloud takes into account two cases: 1-km stabilization altitude and 15 sec of engine exhaust, and 2-km stabilization altitude and 24 sec of engine exhaust. By the time of stabilization, over 99 percent of the cloud mass is attributed to entrained ambient air. Photographs of the exhaust cloud during the STS-1 launch are shown in figure 1.

MEASUREMENT PROGRAM

The airborne sampling strategy and instrumentation used in the LVE program have been previously discussed (refs. 8 to 12). Descriptions of the photographic data and analysis of the cloud trajectory and growth calculations are available from references 9 and 13. A summary of the measurement program for STS-1 is given herein. The surface-level-measurement and diffusion-modeling activities are not addressed in this document.

Aircraft Sampling Plan

The sampling platform, a twin-engine light aircraft (Cessna 402, fig. 2) was airborne 30 min prior to launch and positioned in a holding pattern approximately 10 km west of the launch pad. Approximately 1 min after launch, the aircraft was released from its holding pattern by the Range Safety Officer and the sampling mission was begun. The first sampling pass occurred at T + 9 min. (See table II.) The sampling plan consisted of a series of along-wind and cross-wind penetrations (fig. 3) of the cloud. All passes (except pass 4) were intended to be through the centroid of the cloud as determined visually by the flight crew. By design, pass 4 was approximately 100 m below the visible cloud. Predictions and observations of the stabilization altitude and the transport direction of the cloud centroid were provided by radio to assist the flight crew in initializing the flight sequences. Modifications to the flight plan were made as necessary by the flight crew based on their observations, data onboard the aircraft, and cloud behavior. For the STS-1 launch, 31 sampling passes were made before the aircraft landed for fuel. Two clouds were sampled. Passes 1 to 9 (T + 9 min to T + 43 min) sampled a cloud which stabilized at about 900-m altitude and drifted north from the launch pad along the coast. Passes 10 to 31 (T + 50 min to T + 128 min) were through a cloud which stabilized at about 1800-m altitude and drifted inland, west of the launch pad. Flight parameters associated with each sampling pass are listed in table II.

Aircraft Instrumentation

The aircraft (ref. 10) was equipped to monitor HCl (gaseous and gaseous plus aqueous), suspended particulates, temperature, and dewpoint. In subsequent text and figures, gaseous plus aqueous HCl will be referred to as total HCl or HCl(t). Routine flight parameters of altitude, heading, and airspeed were also measured. The aircraft was equipped with an S-band transmitter beacon for positioning; however, radar tracking of the aircraft was not possible because of launch requirements. As discussed in reference 10, the aircraft and its sampling systems were designed specifically for sampling launch effluent. Air samples are taken into the aircraft through inlet probes located in the nose of the aircraft. These probes extend forward of the flow-field disturbance created by the aircraft, thus collecting undisturbed free-stream air. All instruments have been used in previous LVE missions and

the characteristics of the instruments are shown in table III. The instrumentation is discussed in detail in references 8 to 10, 12, and 13.

Two HCl instruments were flown: a gas-filter-correlation instrument sensitive only to gaseous HCl and a chemiluminescent instrument sensitive to gaseous and aqueous aerosol HCl. Comparison of data between the two instruments provides HCl partitioning (between gaseous and aqueous phases) information about the cloud. Suspended particulates were also measured by two techniques, each with a heated inlet to volatilize liquid aerosols. The integrating nephelometer measures total suspended particulates as a function of time using a light (visible) scattering technique. The efficiency at which light is scattered by small particles is size dependent. Particles ranging in size from 0.2 μm to several micrometers in diameter are most efficient at scattering visible light. In this technique, the mass of suspended particulates is related to the measured light scattering coefficient after making certain assumptions (see Data Reduction section) concerning particulate size distribution and particle composition. The 10-stage quartz crystal microbalance (QCM) measures suspended-particulate mass concentration ($\mu\text{g}/\text{m}^3$) in 10 particle-size (aerodynamic) ranges from 0.08 to about 60 μm in diameter. Table IV lists the size characteristic for the QCM stages. The 50-percent sizing cut point for a given stage implies that particles below that diameter are collected on that stage at less than 50-percent efficiency. The QCM uses a cascaded collection system with larger particles being collected on the earlier stages. As such, the effective collection size interval for any given stage is defined by the 50-percent cut point of that stage (lower bound) and the 50-percent cut point of the previous stage. (See table IV.) The geometric mean diameter, which was calculated based on the effective collection size range of each stage, represents the nominal size of the particles collected on any given stage. Figure 4 illustrates the above definitions for stages 7 and 8 of the QCM. Particulate mass concentration and size are determined on a per-cloud-pass basis, and postflight elemental analyses of particulates collected (total from all passes) on each QCM stage provides composition information.

Cloud Photography

The time-sequenced cameras were located at surface sites UCS-2, UCS-6, and UCS-9 (fig. 5) for purposes of obtaining cloud photographs from which cloud track, cloud altitude prior to stabilization time, and cloud volume were calculated. Cameras were time sequenced to the launch and located such that the cloud was within the viewing areas of at least two of the three camera sites. Only the cloud which drifted north of the launch pad was tracked by the camera crews, and photographs were obtained to about T + 25 min. Beyond T + 25 min, the cloud either filled the frame of view of the cameras or was indistinguishable from the ambient background.

DATA REDUCTION

Aircraft Measurements

Data measured onboard the aircraft were recorded on magnetic tape and/or strip charts. Data tapes were later digitized at a rate of 10 records/sec. Most data were reported as 1-sec averages. Data for HCl(g) were computer processed to filter high frequency noise, and relative humidity of the cloud was calculated from the temperature and dewpoint data. Aircraft altitude and heading are reported in meters above

mean sea level (MSL) and degrees clockwise from magnetic north. Gaseous and total HCl are in the conventional units of parts per billion (ppb) by volume.

The nephelometer measures the light scattering coefficient ($B_{\text{scat}}, \text{m}^{-1}$) of suspended particulates with diameters from about $0.2 \mu\text{m}$ to several micrometers. The B_{scat} measurement may be converted to an approximate particle mass concentration ($\mu\text{g}/\text{m}^3$) by making assumptions for particle size distribution, particle composition, and the refractive index of the particles within the instrument's viewing volume. The merits and uncertainties associated with these calculations and assumptions are discussed in the literature (e.g., refs. 14 and 15). Nephelometer data are reported as B_{scat} and as mass concentration. Mass concentrations calculated from these data generally agree with QCM results to within at least a factor of 2.

The QCM measures suspended-particulate mass concentration ($\mu\text{g}/\text{m}^3$) as a function of time in 10 particle-size (aerodynamic sizing) ranges from about $0.08-$ to $60-\mu\text{m}$ particle diameter. Readout problems with the two largest ranges (stages 1 and 2) limited the QCM data to about $15-\mu\text{m}$ diameter or smaller. Particulates were collected on all 10 stages for laboratory analysis. To obtain a statistically significant sample for each cloud penetration, QCM results are reported on a per-pass basis, rather than as a function of time. QCM results are reported as mass concentration, $\mu\text{g}/\text{m}^3$, at the geometric mean diameter of each stage. Particles collected by the QCM were analyzed postlaunch using scanning electron microscopy (SEM) and energy dispersive X-ray techniques to determine particle shape and elemental composition.

Photographic Measurements of Cloud

Cloud photographs taken at the three camera sites were used to calculate cloud trajectory from the launch pad and cloud growth (volume) as a function of time. At selected times after launch, photographs from each camera site were analyzed. Standard triangulation procedures were used to obtain cloud trajectory. Based on previous experience (Titan LVE programs) and an error analysis of the STS-1 cloud photographic data, cloud locations are considered accurate to about 1 km. In addition, the techniques discussed in reference 8 were used to calculate cloud volume using data from paired camera sites (UCS-6/UCS-9 and UCS-6/UCS-2). Based on previous experience, cloud volumes can be estimated to within ± 20 percent.

RESULTS

During the discussion of the STS-1 data, frequent reference will be made to previous Titan III results for the following reasons:

1. A considerable Titan III LVE data base (see appendix A) exists.
2. The historical evidence of more than 30 Titan III launches at KSC indicates that significant adverse environmental effects were not reported.
3. The Titan III was the country's largest launch vehicle using solid-propellant rocket motors prior to Space Shuttle.
4. Titan III exhaust products are similar to those emitted by the Shuttle engines.

Cloud Behavior

As has been observed for some of the Titan III launches, the STS-1 exhaust cloud segmented and broke into multiple pieces. As many as five separate clouds were noted by some ground observers; however, two clouds were prominent and the focus for the aircraft measurements. Cloud segmentation occurred at about $T + 8$ min with one major cloud drifting north (north cloud) and a second major cloud drifting west (west cloud). The north cloud drifted up the coast being influenced by early morning (7 a.m. launch) coastal conditions. It stabilized at 850- to 950-m altitude and was sampled by the aircraft from about $T + 9$ min (pass 1) to about $T + 43$ min (pass 9). The ground track of the north cloud as determined by photographic data from the three camera sites is shown in figure 5. Approximately 25 min of cloud track was available from the cloud photographic data. The west cloud drifted inland, away from the coastal environment. It was not tracked by the camera crews but was sampled by the aircraft from about $T + 50$ min (pass 10) to $T + 128$ min (pass 31). Based upon the aircraft flight altitudes, the west cloud was stabilized at about 1400-m altitude ($T + 50$ min), slowly drifting upwards to an altitude of about 1900 m ($T + 128$ min). Figure 6 shows the aircraft flight altitudes for each of the sampling passes.

The calculated volume of the north cloud is shown in figure 7. The volume envelope (shaded area) shown is the result of two separate (data from different paired camera sites) volume determinations made at each time. Volume calculations beyond 8 min are not shown and are questionable for two reasons. First, the cloud trajectory (fig. 5) was directly towards camera site UCS-9 and when the cloud was within 2 to 3 km of the site ($T + 8$ min), photographic data from the site were of no further use in the volume calculations. Second, during the first 8 to 10 min, data from the camera sites were providing near orthogonal views of the cloud dimensions, but by $T + 10$, the location of the cloud was such that the two remaining sites (UCS-2 and UCS-6) were providing essentially the same view. The technique used in calculating the cloud requires approximate orthogonal views (from two sites) of the cloud in order not to generate large errors in the calculation. Based on the STS-1 data, the camera site locations relative to the cloud track, and an analysis of the volume calculation technique, volumes beyond 8 min may be in error by as much as a factor of 2 or 3.

Aircraft Measurements - North Cloud

Figures 8 and 9 show typical data from samplings of the north cloud. Figure 8 for pass 2 ($T + 15$ min) and figure 9 for pass 9 ($T + 43$ min) show HCl (gaseous and total), particulate (nephelometer), temperature, and relative humidity profiles through the exhaust cloud. As shown by the faster responding instruments, chemiluminescent detector and nephelometer, HCl and particulates exhibit similar profiles within the cloud. Sampling altitudes for these two passes are approximately 940 m (pass 2) and 880 m (pass 9). These data are typical of those observed in each pass through the north cloud. Maximum peak concentrations occurred during pass 1 with an HCl(t) concentration of 14.9 ppm, an HCl(g) concentration of 3.5 ppm, and a particulate loading (nephelometer) of $668 \mu\text{g}/\text{m}^3$ equivalent to a B_{scat} of $17.6 \times 10^{-4} \text{ m}^{-1}$. Minimal peak values occurred during pass 7 and were 2.9 ppm, 0.6 ppm, and $253 \mu\text{g}/\text{m}^3$ ($B_{\text{scat}} = 6.7 \times 10^{-4} \text{ m}^{-1}$), respectively. Pass 4, approximately 100 m below the visible cloud (640-m altitude), showed substantially lower concentrations of 1 ppm HCl(t), 0.2 ppm HCl(g), and $180 \mu\text{g}/\text{m}^3$ ($B_{\text{scat}} = 4.7 \times 10^{-4} \text{ m}^{-1}$) for particulates. For the north cloud, only about 25 percent of the HCl was in the gaseous state. Relative humidity in the cloud was generally 60 to 70 percent (at ambient level) showing some increases up to 80 percent during the first few passes. Temperature within the cloud

was at ambient levels, 15°C to 18°C. Figure 10 shows the species concentration decay (maximum concentrations observed during each pass) with time. Data from pass 4 (under the cloud) are shown for comparison.

Typical QCM data obtained in the north cloud are shown in figure 11. The size distribution spectra of all sampling of the north cloud were similar to those of the figure, including pass 4 under the cloud. Most particles were of small diameter, less than 0.2 μm . For example, at least 55 percent of the particle mass was concentrated in particle sizes at or below 0.11- μm diameter; 85 percent of mass, below diameters of 0.17 μm . QCM results showed, similar to the nephelometer, a gradual decrease in the average particulate concentrations ($\mu\text{g}/\text{m}^3$) within the cloud during the 40-minute sampling period of the north cloud. Increased particulate concentrations observed for a particular sampling pass are attributed to errors of the flight crew in locating the center of the cloud and to local inhomogeneity within the cloud.

North cloud observations can be summarized as follows:

- (1) Cloud humidity was relatively high (60 to 70 percent), but generally at or near ambient levels.
- (2) Cloud temperatures were at ambient levels.
- (3) HCl existed mainly in the aqueous state, only 25 percent of in-cloud HCl was gaseous.
- (4) The particles in the cloud were mainly of the smaller diameter; 85 percent of particle mass was the result of particles with diameters below 0.17 μm .
- (5) Species concentrations gradually decreased during the 40-min sampling period.

Aircraft Measurements - West Cloud

As stated earlier, the west cloud stabilized at a higher altitude (1400 vs 900 m) and in a much drier environment (ambient relative humidity 10 to 15 percent vs 60 to 70 percent) than the north cloud. The west cloud was sampled from T + 50 min (pass 10) to T + 128 min (pass 31). In accordance with the later sampling times and cloud diffusion, west cloud concentrations were generally lower than those observed for the north cloud. For the west cloud, maximum peak concentrations occurred during pass 11 (T + 55 min) and were for HCl(t), HCl(g), and particulates (nephelometer); 6.4 ppm, 4.7 ppm, and 175 $\mu\text{g}/\text{m}^3$ ($B_{\text{scat}} = 4.6 \times 10^{-4} \text{ m}^{-1}$), respectively. By completion of the sampling (T + 128 min), concentrations had decayed to levels of 2 ppm HCl (total and gaseous) and 80 to 100 $\mu\text{g}/\text{m}^3$ ($B_{\text{scat}} = 2 \text{ to } 3 \times 10^{-4} \text{ m}^{-1}$) for particulates. Shown in figures 12 and 13 are typical in-cloud data for the west cloud. Figure 14 shows decay of species with time for the west cloud. The scatter in these maximum concentrations is attributed to a diffuse cloud and associated uncertainties in locating the cloud center for the various aircraft passes. As shown in the figures of appendix B, HCl(g) was observed to be higher than HCl(t) in many of the samplings of the west cloud. These differences were of the order of 0.5 to 1 ppm occurring at concentrations below about 3 ppm. While theoretically impossible for HCl(g) to exceed HCl(t), the observed differences are attributed to instrument errors at these relatively low concentrations which may include some or all of the following: (1) instrument calibration errors, (2) a decrease in the sensitivity for the HCl(t) instrument, and (3) an increase in the sensitivity for the HCl(g) instrument. The HCl instruments showed no sensitivity changes based on laboratory (prelaunch and

postlaunch) calibrations. Neither instrument is calibrated in flight, although various electronic functions are checked. As the result of the different operating principles and sample flowrate requirements of each instrument, different HCl standards are used in the calibration of each instrument. While each standard is carefully prepared and certified (≈ 10 -percent absolute accuracy), concentrations of 1 or 2 ppm are difficult to prepare and certify at the 10-percent level. The HCl(t) instrument can show a sensitivity decrease at low humidities (west cloud humidity was 10 to 15 percent). For example, laboratory data (unpublished) show that HCl in dry nitrogen (≈ 0 percent RH) mixtures are not accurately detected. On the other hand, field tests (ref. 16) in a desert environment (≈ 10 percent RH) showed no sensitivity decrease over several hours of operation. HCl(g) concentrations were generally greater than HCl(t) for west-cloud sampling. This was interpreted as implying that HCl(g) was 80 to 100 percent of the total HCl present. The following are general observations from the west-cloud data:

- (1) Cloud relative humidity is low, but at ambient levels of 10 to 15 percent, and for some passes, in-cloud humidity increases by as much as 10 percent.
- (2) The majority of the HCl present in the cloud is in the gaseous state. Gaseous HCl ranged from 64 to over 100 percent of total HCl. Except for the first few passes of the west cloud (passes 10 to 12), the data indicate that over 80 percent of the HCl is gaseous.
- (3) As was noted for the north cloud, cloud temperatures are at ambient values.

Typical QCM data obtained in the west cloud are shown in figure 15. The size distribution spectra of all west-cloud sampling are similar to those of the figure. In contrast to the north cloud, significant particle mass is observed at the larger diameters. On the average for the west cloud, over 40 percent of the particle mass resides in particles with mean geometric diameters of $5.4 \mu\text{m}$ or larger, and less than 20 percent of the particle mass in particles with diameters less than $0.17 \mu\text{m}$.

Laboratory Analysis - Particle Composition

Particles collected on the various stages of the QCM were analyzed in the laboratory using scanning electron microscopy (SEM) and energy dispersive X-ray techniques. The results, which encompass all cloud samplings (no distinction between the two clouds or among the 31 passes), are summarized and discussed with reference to the geometric mean diameter of the collected particles.

(1) Particles, approximately spherical in shape and containing aluminum, were found in all stages of the QCM. These particles are presumed to be Al_2O_3 (based on X-ray analysis showing aluminum, on the spherical shapes, and on previous Titan results) produced from the burning of the propellant which contains aluminum.

(2) In stages 1 through 3 ($42 \mu\text{m}$ to about $10.7 \mu\text{m}$ in diameter), SEM photographs show agglomerates, consisting of individual particles stuck together. This suggests that coagulation of particles in the cloud may significantly contribute to the observed larger particles. Figure 16 shows an SEM photograph of some of these large agglomerates (some greater than $40\text{-}\mu\text{m}$ diameter) collected on stage 1 of the QCM. Figure 16(a) shows some of the agglomerates (particles A, B, and C) as well as individual spherical particles (particles D, E, and F). Figure 16(b) is an enlargement of particle A shown in figure 16(a). X-ray analyses of these agglomerates show an abundance of aluminum relative to other elements. As stated earlier, it was not

possible to quantify these particles by mass because of the readout problems in stages 1 and 2. As viewed in the laboratory, these large agglomerates are relatively few in number; however, they may account for a measurable fraction of the total particulate mass because of their large sizes.

(3) Shown in figure 17 is an SEM photograph of particles collected on stage 6 (1.3- μm diameter) of the QCM. Particles collected on stages 4 through 7 (5.4- to 0.69- μm geometric mean diameter) were mostly spherical in shape. These spherical particles (particle A, fig. 17) were rich in aluminum content. Amorphous material present on the stages (particles B and C) showed a complex energy-dispersion X-ray spectrum indicating the presence of sodium, magnesium, aluminum, sulfur, chlorine, calcium, and iron.

(4) The morphology of particles on stages 8 through 10 (0.33- to 0.11- μm geometric mean diameter) was complex with many amorphous as well as spherical shaped particles. X-ray analysis showed abundant amounts of sodium, sulfur, chlorine, iron, zinc, and potassium, as well as aluminum.

Summary of Aircraft Data

Table V is a summary of the maximum HCl and particulate concentrations measured for each pass. For comparison, figure 18 combines the decay data of figures 10 and 14. Figure 19 compares the QCM particle size distribution for the north cloud (pass 9) and the west cloud (pass 11). While the time difference between passes 9 and 11 is only 12 min, a significant change in particle size within the two clouds is noted. Included as appendix B are figures showing HCl (total and gaseous), particulates (nephelometer), temperature, and relative humidity data for most of the sampling passes. Also included in the appendix is a tabulation of the QCM sizing results for individual passes.

DISCUSSION OF RESULTS

The results from the first Space Shuttle launch are, perhaps, best discussed by comparison with earlier effluent measurements for the Titan III launch vehicle. The Titan III has been launched from the AFETR, Florida, since the 1960's with no significant adverse environmental effects having been reported. Comparisons of the Shuttle and Titan should provide the reader with a reference point for interpreting the Shuttle data. Two points should be noted before discussing the comparisons. First, only additional Shuttle data sets will determine to what extent this first data set is characteristic of the Shuttle vehicle. Second, the Titan data include results from approximately 12 launches (1973 to 1978) and no attempt has been made to select only those Titan data sets obtained under meteorological conditions similar to those of the first Space Shuttle launch (STS-1).

Cloud Behavior

Observations from the Titan launches have indicated that generally a single exhaust cloud forms within the mixing layer; however, multiple clouds have been noted in a few launches (e.g., December 1974 (ref. 17)). Launch conditions for STS-1, namely an early morning launch and the existence of a maritime atmospheric layer along the coast, would be expected to result in meteorological conditions which might cause cloud segmentation. In addition, the configuration of the launch pad (multiple

exhaust ducts and flame trenches) and the launch vehicle (large liquid and solid engines firing at lift-off) suggest that the Space Shuttle would be more apt to produce multiple clouds rather than one large cloud. The direction of cloud drift and the altitude of stabilization are, as expected, dependent upon existing meteorology.

Shown in figures 20 and 21 are comparisons of cloud-centroid altitude and cloud volume for the Space Shuttle with those of earlier Titan launches. Altitude data (fig. 20) taken up to T + 25 min are shown which cover the period to cloud stabilization (typically 10 min). Up to the time of stabilization, the cloud-centroid altitude as a function of time is dependent on launch vehicle dynamics as well as on the existing meteorology. Beyond stabilization, meteorology is the controlling parameter. As seen from the figure, cloud-centroid altitudes for the Shuttle are very similar to those of Titan III, with the STS-1 north cloud being a little lower than the Titan cloud. From the volume comparisons of figure 21, Shuttle (north cloud) volumes are similar to Titan. One would expect the Shuttle clouds to be larger in volume than Titan clouds (exhaust mass about 2.4 times that of Titan); however, the existence of multiple clouds could account for the volume of the north cloud being little different than observed for Titan.

As discussed earlier, the temperature of the STS-1 launch cloud is essentially ambient. This has been the experience from earlier Titan measurements. Within minutes (typically 10 min), the majority (~99 percent) of the cloud is entrained ambient air; thus, ambient temperature would be expected. Infrared studies of Titan clouds (ref. 18) at the launch site have also shown cloud temperatures to be at ambient levels. For example (from ref. 18), "Radiation intensities from an ambient cloud and from an exhaust cloud were measured simultaneously with a 3 to 5.6 μm scanning radiometer. After the exhaust cloud stabilized, it could not be distinguished from the ambient cloud by their temperatures. However, the radiation intensities from the two clouds at various wavelengths differed. These differences were probably due to compositional differences between the clouds ..."

HCl Concentration in Cloud

Shown in figure 22 is a comparison of STS-1 and Titan HCl measurements. All data are peak, total HCl concentrations measured onboard the aircraft during samplings of the various exhaust clouds. Comparisons are shown for only the first 50 min after launch. The second Titan upper data boundary (fig. 22) reflects the December 1974 data set (ref. 17). During this launch, the aircraft sampled two distinct exhaust clouds. The second cloud, sampled after T + 30 min, showed abnormally high HCl concentrations. Postlaunch analyses of available meteorological data suggested that this second cloud was trapped between two stable layers and, thus, diffused very slowly. The shaded area of the figure includes the remaining Titan data and what is believed to be nominal Titan results. As shown in the figure, STS-1 results compare well with the nominal Titan observations.

As shown earlier for the STS-1 results (figs. 8, 9, 12, and 13), HCl and particulate concentrations are similarly distributed within the cloud. This has also been true for the Titan measurements, as illustrated in figure 23. The concentrations have been normalized based on their peak values.

In terms of partitioning of HCl between the gaseous and aqueous states within the exhaust cloud, references 19 and 20 discuss this for the Titan and probably ade-

quately describe the Shuttle also. Basically, HCl tends to exist mainly in the aqueous state (60 to 80 percent) early after launch (typically the first 20 min). Later, with cloud dilution and lowering of relative humidity within the cloud (provided ambient humidity is not high), the majority of HCl (80 percent or more) is found in the gaseous state. Laboratory and analytical studies (refs. 20 to 23) indicate that ambient temperature and, to a larger degree, relative humidity are important factors influencing HCl partitioning. These studies show that high humidities favor the aqueous phase and aerosol formation, and low humidities, the gaseous phase. These descriptions (Titan data, laboratory work, and analytical studies) compare well qualitatively with the STS-1 observations of the high-humidity north cloud and the low-humidity west cloud.

Particulate Observations

Figure 24 shows a comparison of nephelometer results from Titan with the STS-1 data. Concentrations are peak values as observed from the various aircraft passes. Earlier comments regarding figure 22 and the Titan data also apply to figure 24, since the second Titan upper data boundary in both figures results from the December 1974 Titan measurements. As shown in figure 24, the STS-1 results lie well within the Titan data.

Particle size data (QCM) from the Titan launches have indicated a preference for a bimodal distribution within the cloud. In almost all observations, peak mass loadings have been observed at about 0.1- μm geometric mean diameter. The second mode (peak) normally occurs in the range of 1- to 5- μm diameter. The location of this second peak varies from data set to data set and can vary among the passes of a given data set. Typically, on a mass concentration basis ($\mu\text{g}/\text{m}^3$), the mode at 0.1- μm diameter shows mass equal to or greater than the mass in the second mode. For the STS-1 data, a bimodal distribution is not prevalent. As discussed for Space Shuttle, single-mode distributions were observed with north-cloud peak mass loading occurring in a size range from 0.1- to 0.2- μm diameter, and west-cloud peak mass loading occurring around 5- μm diameter.

Results of particulate composition analyses of collected samples from Titan launches and the STS-1 launch show similar results. Particles, spherical in shape and rich in aluminum, are in existence in all size ranges (0.1- to 40- μm geometric mean diameter). Occurring with these spherical particles are irregular shaped particles consisting of elements of aluminum as well as sodium, sulfur, chlorine, potassium, zinc, calcium, and iron. For Titan and STS-1, more irregular-shaped particles are observed at the smaller sizes (below 1- μm diameter) and the very large particles have appeared to be agglomerates of a number of small spherical particles. These agglomerates, as stated earlier for STS-1 data, are rich in aluminum content.

SUMMARY REMARKS

During the launch of the first Space Shuttle (STS-1) on April 12, 1981, data were obtained on the chemical makeup and physical behavior of the exhaust effluent cloud. The results have been presented and discussed, and comparisons have been made which show the STS-1 results and observations to be similar to Titan results. STS-1 HCl and particulate concentrations fall within the bounds of earlier Titan observations. Major differences between STS-1 and Titan observations were the formation of

multiple STS-1 exhaust clouds and the particulate size distributions within the STS-1 north and west clouds. From these comparisons, the reader can develop a reference frame from which the STS-1 environmental data can be evaluated. Future measurements of Shuttle launch vehicle effluent (LVE) will determine whether the STS-1 results are typical.

Langley Research Center
National Aeronautics and Space Administration
Hampton, VA 23665
November 2, 1982

APPENDIX A

SUMMARY OF REFERENCES ON LAUNCH VEHICLE EFFLUENT

This appendix is a summary of references from the LVE activities. References are listed in one of five subject areas: (1) models and analytical studies, (2) launch site measurements, (3) laboratory studies, (4) instrumentation, and (5) other.

Models and Analytical Studies

1. Dumbauld, R. K.; Bjorklund, J. R.; and Bowers, J. F.: NASA/MSFC Multilayer Diffusion Models and Computer Program for Operational Prediction of Toxic Fuel Hazards. NASA CR-129006, 1973.
2. Stephens, J. Briscoe; Susko, Michael; Kaufman, John W.; and Hill, C. Kelly: An Analytical Analysis of the Dispersion Predictions for Effluents From the Saturn V and Scout-Algol III Rocket Exhausts. NASA TM X-2935, 1973.
3. Stephens, J. Briscoe, ed.: Atmospheric Diffusion Predictions for the Exhaust Effluents From the Launch of a Titan III C, Dec. 13, 1973. NASA TM X-64925, 1974.
4. Pellett, G. L.: Washout of HCl and Application to Solid Rocket Exhaust Clouds. Precipitation Scavenging (1974), ERDA Symp. Ser. 41 (CONF-741003), June 1977, pp. 437-465.
5. Stephens, J. Briscoe; and Hamilton, P. A.: Diffusion Algorithms and Data Reduction Routine for Onsite Launch Predictions for the Transport of Titan III C Exhaust Effluents. NASA TN D-7862, 1974.
6. Stewart, Roger B.; and Grose, William L.: Parametric Studies With an Atmospheric Diffusion Model That Assesses Toxic Fuel Hazards Due to the Ground Clouds Generated by Rocket Launches. NASA TN D-7852, 1975.
7. Pergament, Harold S.; and Thorpe, Roger D.: NO_x Deposited in the Stratosphere by the Space Shuttle. NASA CR-132715, 1975.
8. Dumbauld, R. K.; and Bjorklund, J. R.: NASA/MSFC Multilayer Diffusion Models and Computer Programs - Version 5. NASA CR-2631, 1975.
9. Stewart, Roger B.; and Gomberg, Richard I.: The Production of Nitric Oxide in the Troposphere as a Result of Solid-Rocket-Motor Afterburning. NASA TN D-8137, 1976.
10. Gomberg, Richard I.; and Stewart, Roger B.: A Computer Simulation of the Afterburning Processes Occurring Within Solid Rocket Motor Plumes in the Troposphere. NASA TN D-8303, 1976.
11. Stephens, J. Briscoe: Diffusion Algorithms and Data Reduction Routine for Onsite Real-Time Launch Predictions for the Transport of Delta-Thor Exhaust Effluents. NASA TN D-8194, 1976.

APPENDIX A

12. Bollay, Eugene; Bosart, Lance; Droessler, Earl; Jiusto, James; Lala, G. Garland; Mohnen, Volker; Schaefer, Vincent; and Squires, Patrick: Position Paper on the Potential of Inadvertent Weather Modification of the Florida Peninsula Resulting From the Stabilized Ground Cloud. NASA CR-151199, 1976.
13. Dingle, A. Nelson: Rain Scavenging of Solid Rocket Exhaust Clouds. NASA CR-2928, 1978.
14. Stephens, J. Briscoe; and Stewart, Roger B.: Rocket Exhaust Effluent Modeling for Tropospheric Air Quality and Environmental Assessments. NASA TR R-473, 1977.
15. Hwang, B.; and Mathis, J. J., Jr.: A Comparative Study of Tropospheric Ground Cloud Diffusion Models. Joint Conference on Applications of Air Pollution Meteorology, American Meteorol. Soc., 1978, pp. 261-266.
16. Gomberg, Richard I.; and Wilmoth, Richard G.: Effects of Entrained Water and Strong Turbulence on Afterburning Within Solid Rocket Motor Plumes. NASA TP-1111, 1978.
17. Parungo, Farn P.; and Allee, Paul A.: Rocket Effluent: Its Ice Nucleation Activity and Related Properties. J. Appl. Meteorol., vol. 17, no. 12, Dec. 1978, pp. 1856-1863.
18. Pellett, G. L.; Sebacher, D. I.; Bendura, R. J.; and Wornom, D. E.: HCl in Rocket Exhaust Clouds: Atmospheric Dispersion, Acid Aerosol Characteristics, and Acid Rain Deposition. [Preprint] 80-49.6, Air Pollut. Control Assoc., June 1980.
19. Pellett, G. L.: Analytic Model for Washout of HCl(g) From Dispersing Rocket Exhaust Clouds. NASA TP-1801, 1981.
20. Pellett, G. L.; and Staton, W. L.: Application of a Gaussian Multilayer Diffusion Model To Characterize Dispersion of Vertical HCl Column Density in Rocket Exhaust Clouds. NASA TP-1956, 1981.

Launch Site Measurements

1. Gregory, Gerald L.; Hulten, William C.; and Wornom, Dewey E.: Apollo Saturn 511 Effluent Measurements From the Apollo 16 Launch Operations - An Experiment. NASA TM X-2910, 1974.
2. Hulten, William C.; Storey, Richard W.; Gregory, Gerald L.; Woods, David C.; and Harris, Franklin S., Jr.: Effluent Sampling of Scout "D" and Delta Launch Vehicle Exhausts. NASA TM X-2987, 1974.
3. Gregory, Gerald L.; and Storey, Richard W., Jr.: Effluent Sampling of Titan III C Vehicle Exhaust. NASA TM X-3228, 1975.
4. Wagner, H. S.: Measurement of Solid Rocket Motor Effluents in the Atmosphere. Proceedings of the Sixth Annual Conference on Environmental Toxicology, AMRL-TR-75-125, Dec. 1975, pp. 513-530. (Available from DTIC as AD A024 899.)

APPENDIX A

5. Stewart, Roger B.; Sentell, Ronald J.; and Gregory, Gerald L.: Experimental Measurements of the Ground Cloud Effluents and Cloud Growth During the February 11, 1974 Titan-Centaur Launch at Kennedy Space Center. NASA TM X-72820, 1976.
6. Gregory, Gerald L.; Wornom, Dewey E.; Bendura, Richard J.; and Wagner, H. Scott: Hydrogen Chloride Measurements From Titan III Launches at the Air Force Eastern Test Range, FL 1973 Through 1975. NASA TM X-72832, 1976.
7. Stephens, J. Briscoe; Adelfang, S. I.; and Goldford, A. I.: Compendium of Meteorological Data for the Titan III C Launch in December 1973. NASA TM X-73334, 1976.
8. Stephens, J. Briscoe; Adelfang, S. I.; and Goldford, A. I.: Compendium of Meteorological Data for the Centaur Launch in February 1974. NASA TM X-73335, 1976.
9. Stephens, J. Briscoe; Adelfang, S. I.; and Goldford, A. I.: Compendium of Meteorological Data for the ATS-F Launch in May 1974. NASA TM X-73336, 1976.
10. Stephens, J. Briscoe; Adelfang, S. I.; and Goldford, A. I.: Compendium of Meteorological Data for the Helios A Launch in December 1974. NASA TM X-73337, 1976.
11. Stephens, J. Briscoe; Adelfang, S. I.; and Goldford, A. I.: Compendium of Meteorological Data for the Titan III C (AF-777) Launch in May 1975. NASA TM X-73338, 1976.
12. Stephens, J. B.; Adelfang, S. I.; and Goldford, A. I.: Compendium of Meteorological Data for the Viking A Launch in August 1975. NASA TM X-73339, 1976.
13. Stephens, J. B.; Adelfang, S. I.; and Goldford, A. I.: Compendium of Meteorological Data for the Viking B Launch in September 1975. NASA TM X-73340, 1976.
14. Gomberg, Richard I.; Kantsios, Andronicos G.; and Rosensteel, Frederick J.: Some Physical and Thermodynamic Properties of Rocket Exhaust Clouds Measured With Infrared Scanners. NASA TP-1041, 1977.
15. Gregory, Gerald L.; and Storey, Richard W., Jr.: Experimental Measurements of the Ground Cloud Effluents and Cloud Growth for the May 20, 1975, Titan IIIC Launch at Air Force Eastern Test Range, Florida. NASA TM-74044, 1977.
16. Woods, D. C.: Rocket Effluent Size Distributions Made With a Cascade Quartz Crystal Microbalance. Conference Proceedings - 4th Joint Conference on Sensing of Environmental Pollutants, American Chem. Soc., c.1978, pp. 716-718.
17. Bendura, Richard J.; and Crumbly, Kenneth H.: Ground Cloud Effluent Measurements During the May 30, 1974, Titan III Launch at the Air Force Eastern Test Range. NASA TM X-3539, 1977.
18. Gregory, G. L.; Emerson, Burt R., Jr.; and Hudgins, Charles H.: Summary of Airborne Chlorine and Hydrogen Chloride Gas Measurements for August 20 and September 5, 1977, Voyager Launches at Air Force Eastern Test Range, Florida. NASA TM-78673, 1978.

APPENDIX A

19. Wornom, Dewey E.; and Woods, David C.: Effluent Monitoring of the December 10, 1974, Titan III-E Launch at Air Force Eastern Test Range, Florida. NASA TM-78735, 1978.
20. Chuan, R. L.; and Woods, D. C.: Morphology and Elemental Composition Analysis by Size of Rocket Particulate Effluent. Proceedings of the 4th Joint Conference on Sensing of Environmental Pollutants, American Chem. Soc., c.1978, pp. 610-613.
21. Gregory, Gerald L.; Bendura, Richard J.; and Woods, David C.: Launch Vehicle Effluent Measurements During the May 12, 1977, Titan III Launch at Air Force Eastern Test Range. NASA TM-78753, 1979.
22. Sebacher, Daniel I.; Wornom, Dewey E.; and Bendura, Richard J.: Hydrogen Chloride Partitioning in a Titan III Exhaust Cloud Diluted With Ambient Air. AIAA Paper 79-0299, Jan. 1979.
23. Wornom, Dewey E.; Bendura, Richard J.; and Gregory, Gerald L.: Launch Vehicle Effluent Measurements During the September 5, 1977, Titan III Launch at Air Force Eastern Test Range. NASA TM-80065, 1979.
24. Hindman, Edward E., II; and Radke, Lawrence F.: Cloud Nuclei From Launches of Liquid and Solid Fueled Rockets. Seventh Conference on Inadvertent and Planned Weather Modification (Extended Abstracts), American Meteorol. Soc., c.1979, pp. 18-19.
25. Woods, David C.; Bendura, Richard J.; and Wornom, Dewey E.: Launch Vehicle Effluent Measurements During the August 20, 1977, Titan III Launch at Air Force Eastern Test Range. NASA TM-78778, 1979.
26. Sebacher, Daniel I.; Bendura, Richard J.; and Wornom, Dewey E.: Hydrochloric Acid Aerosol and Gaseous Hydrogen Chloride Partitioning in a Cloud Contaminated by Solid Rocket Exhaust. Atmos. Environ., vol. 14, no. 5, 1980, pp. 543-547.
27. Sebacher, D. I.; Gregory, G. L.; Bendura, R. J.; Woods, D. C.; and Cofer, W. R.: Hydrogen Chloride and Particulate Measurements in the Space Shuttle Exhaust Cloud. 1981 JANNAF Safety & Environmental Protection Subcommittee Meeting, CPIA Publ. 348 (Contract N00024-81-C-5301), Johns Hopkins Univ., Nov. 1981, pp. 251-257.

Laboratory Studies

1. Knutson, Earl O.; and Fenton, Donald L.: Atmospheric Scavenging of Hydrochloric Acid. NASA CR-2598, 1975.
2. Tyree, S. Y., Jr.: Chemistry of the System: $Al_2O_3(c)-HCl \cdot aq.$ 1st Status Report. Grant NSG 1204, College of William and Mary, [1975]. (Available as NASA CR-146309.)
3. Fenton, Donald L.; and Ranade, Madhav B.: Aerosol Formation Threshold for HCl-Water Vapor System. Environ. Sci. & Technol., vol. 10, no. 12, Nov. 1976, pp. 1160-1162.

APPENDIX A

4. Tyree, S. Y., Jr.: Chemistry of the System: $\text{Al}_2\text{O}_3(\text{c})\text{-HCl}\cdot\text{aq}$. 2nd Status Report. Grant NSG 1204, College of William and Mary, [1976]. (Available as NASA CR-146728.)
5. Lerman, S.; Taylor, O. C.; and Darley, E. F.: Phytotoxicity of Hydrogen Chloride Gas With a Short-Term Exposure. *Atmos. Environ.*, vol. 10, no. 10, 1976, pp. 873-878.
6. Cofer, W. R., III; and Pellett, G. L.: Adsorption and Chemical Reaction of Gaseous Mixtures of Hydrogen Chloride and Water on Aluminum Oxide and Application to Solid-Propellant Rocket Exhaust Clouds. NASA TP-1105, 1978.
7. Hindman, Edward E., II; Garvey, Dennis M.; Langer, Gerhard; Odencrantz, F. Kirk; Parungo, Farn P.; and Gregory, Gerald L.: Laboratory Investigations of Cloud Forming Nuclei and Aerosol Particles From Unpressurized Burns of Space Shuttle Propellant. NWC Tech. Memo. 3666, U.S. Navy, Dec. 1978. (Available as NASA CR-160358.)
8. Dawbarn, R.; Kinslow, M.; and Watson, D. J.: Analysis of the Measured Effects of the Principal Exhaust Effluents From Solid Rocket Motors. NASA CR-3136, 1980.
9. Hindman, Edward E., II; Garvey, Dennis M.; Langer, Gerhard; Odencrantz, F. Kirk; and Gregory, Gerald L.: Laboratory Investigations of Cloud Nuclei From Combustion of Space Shuttle Propellant. *J. Appl. Meteorol.*, vol. 19, no. 2, Feb. 1980, pp. 175-184.
10. Heck, Walter W.; Knott, William M.; Stahel, Edward P.; Ambrose, John T.; McCrimmon, James N.; Engle, Madeleine; Romanow, Louse A.; Sawyer, Alan G.; and Tyson, James D.: Response of Selected Plant and Insect Species to Simulated Solid Rocket Exhaust Mixtures and to Exhaust Components From Solid Rocket Fuels. NASA TM-74109, 1980.
11. Kang, Yoonok; Pellett, G. L.; Skiles, Jean Ann; and Wightman, J. P.: Interaction of Gaseous Hydrogen Chloride and Water With Sandy Soil. *J. Colloid & Interface Sci.*, vol. 75, no. 2, June 1980, pp. 313-321.

Instrumentation

1. Gregory, Gerald L.; Hudgins, Charles H.; and Emerson, Burt R., Jr.: Evaluation of a Chemiluminescent Hydrogen Chloride and a NDIR Carbon Monoxide Detector for Environmental Monitoring. 1974 JANNAF Propulsion Meeting, Volume I, Part II, CPIA Publ. 260 (Contract N00017-72-C-4401), Appl. Phys. Lab., Johns Hopkins Univ., Dec. 1974, pp. 681-704. (Available from DTIC as AD B002 590.)
2. Gregory, Gerald L.: Measurement Techniques Investigated for Detection of Hydrogen Chloride Gas in Ambient Air. NASA TN D-8352, 1976.
3. Woods, David C.: The Effects of Particle Size Distribution and Refractive Index on Aerosol Mass Concentration Measurements Made With an Integrating Nephelometer. Blacks in Technology - Beyond the Bicentennial, CP 101, Natl. Tech. Assoc., Aug. 1977.

APPENDIX A

4. Gregory, Gerald L.; and Moyer, Rudolph H.: Evaluation of a Hydrogen Chloride Detector for Environmental Monitoring. Rev. Sci. Instrum., vol. 48, no. 11, Nov. 1977, pp. 1464-1468.
5. Wornom, Dewey E.; Woods, David C.; Thomas, Mitchel E.; and Tyson, Richard W.: Instrumentation of Sampling Aircraft for Measurement of Launch Vehicle Effluents. NASA TM X-3500, 1977.
6. Sebacher, Daniel I.: Airborne Nondispersive Infrared Monitor for Atmospheric Trace Gases, Rev. Sci. Instrum., vol. 49, no. 11, Nov. 1978, pp. 1520-1525.

Other

1. Susko, Michael; and Stephens, J. Briscoe: Baseline Meteorological Soundings for Parametric Environmental Investigations at Kennedy Space Center and Vandenberg Air Force Base. NASA TM X-64986, 1976.
2. Stephens, J. Briscoe; and Sloan, Joseph C.: Meteorological Regimes for the Classification of Aerospace Air Quality Predictions for NASA-Kennedy Space Center. NASA TM X-3450, 1976.
3. Cour-Palais, Burton, G., compiler: Proceedings of the Space Shuttle Environmental Assessment Workshop on Tropospheric Effects. NASA TM X-58199, 1977.
4. Goldford, A. I.; Adelfang, S. I.; Hickey, J. S.; Smith, S. R.; Welty, R. P.; and White, G. L.: Environmental Effects From SRB Exhaust Effluents - Technique Development and Preliminary Assessment. NASA CR-2923, 1977.
5. Thorpe, Roger D.: Definition of Air Quality Measurements for Monitoring Space Shuttle Launches. NASA CR-2942, 1978.
6. Potter, Andrew E.: Environmental Effects of the Space Shuttle, J. Environ. Sci., vol. XXI, no. 2, Mar./Apr. 1978, pp. 15-21.
7. Environmental Impact Statement - Space Shuttle Program. NASA TM-82278, 1978.
8. Bollay, Eugene; Bosart, Lance; Droessler, Earl; Jiusto, James; Lala, G. Garland; Mohnen, Volker; Schaefer, Vincent; and Squires, Patrick: Position Paper on the Potential of Inadvertent Weather Modification of the Florida Peninsula Resulting From Neutralization of Space Shuttle Solid Rocket Booster Exhaust Clouds. NASA CR-3091, 1979.

APPENDIX B

SUMMARIES AND PLOTS OF STS-1 DATA

This appendix summarizes data from the aircraft sampling passes. Shown are plots of HCl(t), HCl(g), particulate concentration (nephelometer), temperature, and relative humidity as a function of time within the cloud. (See figs. B-1 to B-24.) Only plots for passes with complete data sets are presented. Since no HCl(g) data (see table V) were obtained for passes 10, 14, 16, 17, 24, 26, and 28, no plots are shown for these passes. Table B-1 shows the results of the QCM particle sizing measurements.

TABLE B-1.- QCM PARTICLE SIZING RESULTS, STS-1 LAUNCH

Pass number	Particle loading, $\mu\text{g}/\text{m}^3$, for stage ^a -							
	3	4	5	6	7	8	9	10
	with geometric mean diameter of -							
	10.7 μm	5.4 μm	2.6 μm	1.32 μm	0.69 μm	0.33 μm	0.17 μm	0.11 μm
1	10	4	6	5	0	6	52	97
2	2	10	2	2	1	1	48	78
3	1	1	1	2	1	3	44	69
4	0	2	2	1	1	7	27	45
5	0	1	1	1	1	0	24	48
6	0	0	1	2	3	3	40	61
7	0	0	1	2	2	4	30	51
8	0	0	2	3	2	5	68	100
9	0	1	2	4	2	4	45	59
b ₁₀								
11	12	49	20	20	8	3	9	7
12	13	42	16	15	6	3	7	0
13	4	36	15	18	7	2	6	5
14	10	21	6	8	0	2	2	4
15	9	46	21	20	10	2	5	7
b ₁₆								
b ₁₇								
18	15	41	14	16	6	1	4	5
19	17	45	16	12	5	2	6	8
20	5	33	15	7	5	2	2	6
21	28	24	10	5	0	0	0	17
22	7	14	10	8	5	1	13	4
23	2	7	2	1	0	1	0	2
24	3	8	6	7	3	1	2	4
25	0	9	6	4	4	2	2	9
26	2	5	6	8	3	1	3	5
27	3	25	14	14	7	6	4	9
28	8	11	10	8	5	3	5	6
29	2	0	0	0	0	0	2	2
b ₃₀								
31	2	9	6	10	5	2	3	5

^aNo data from stages 1 and 2.

^bData loss.

APPENDIX B

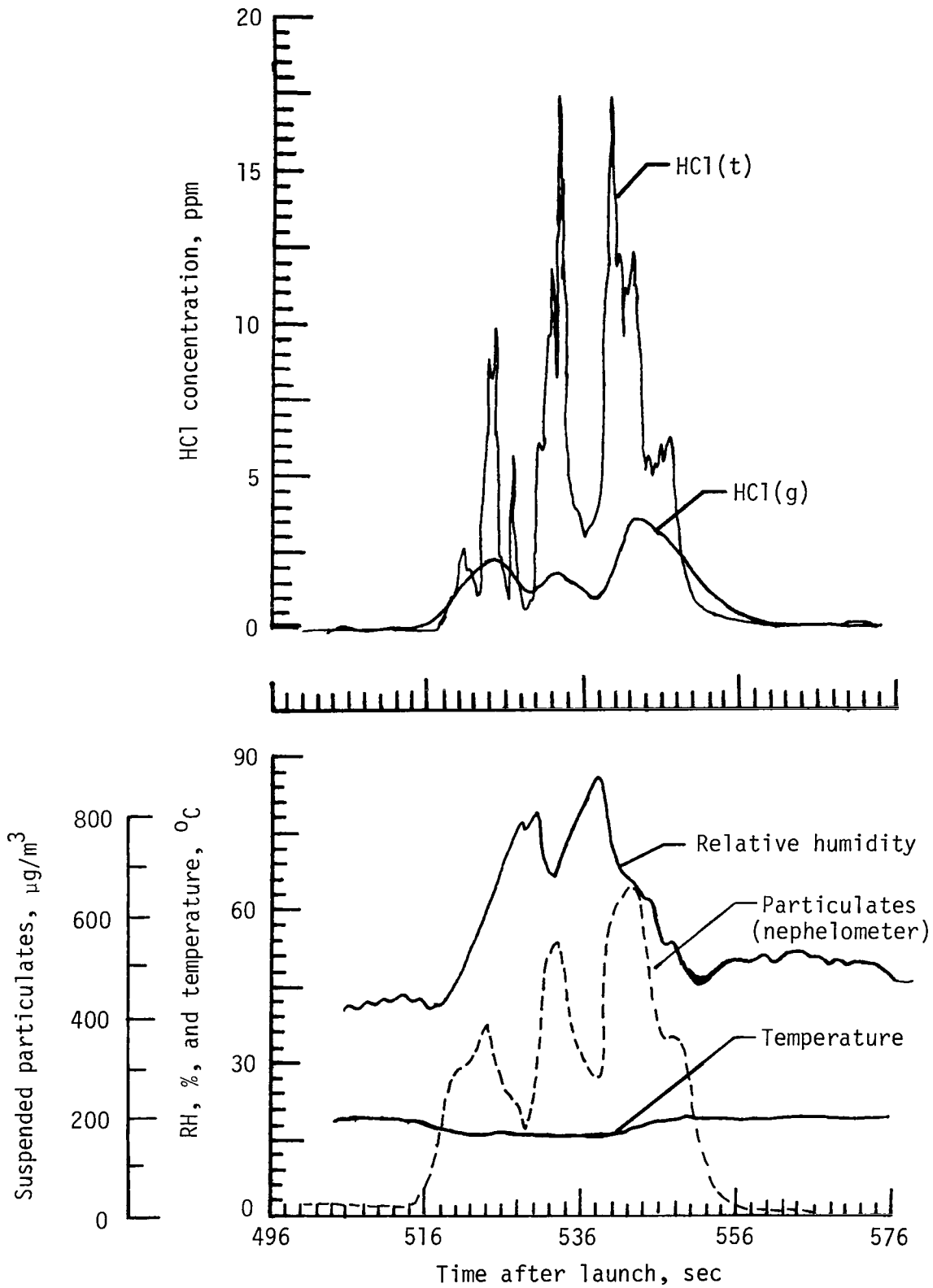


Figure B1.- Data of pass 1, north cloud.

APPENDIX B

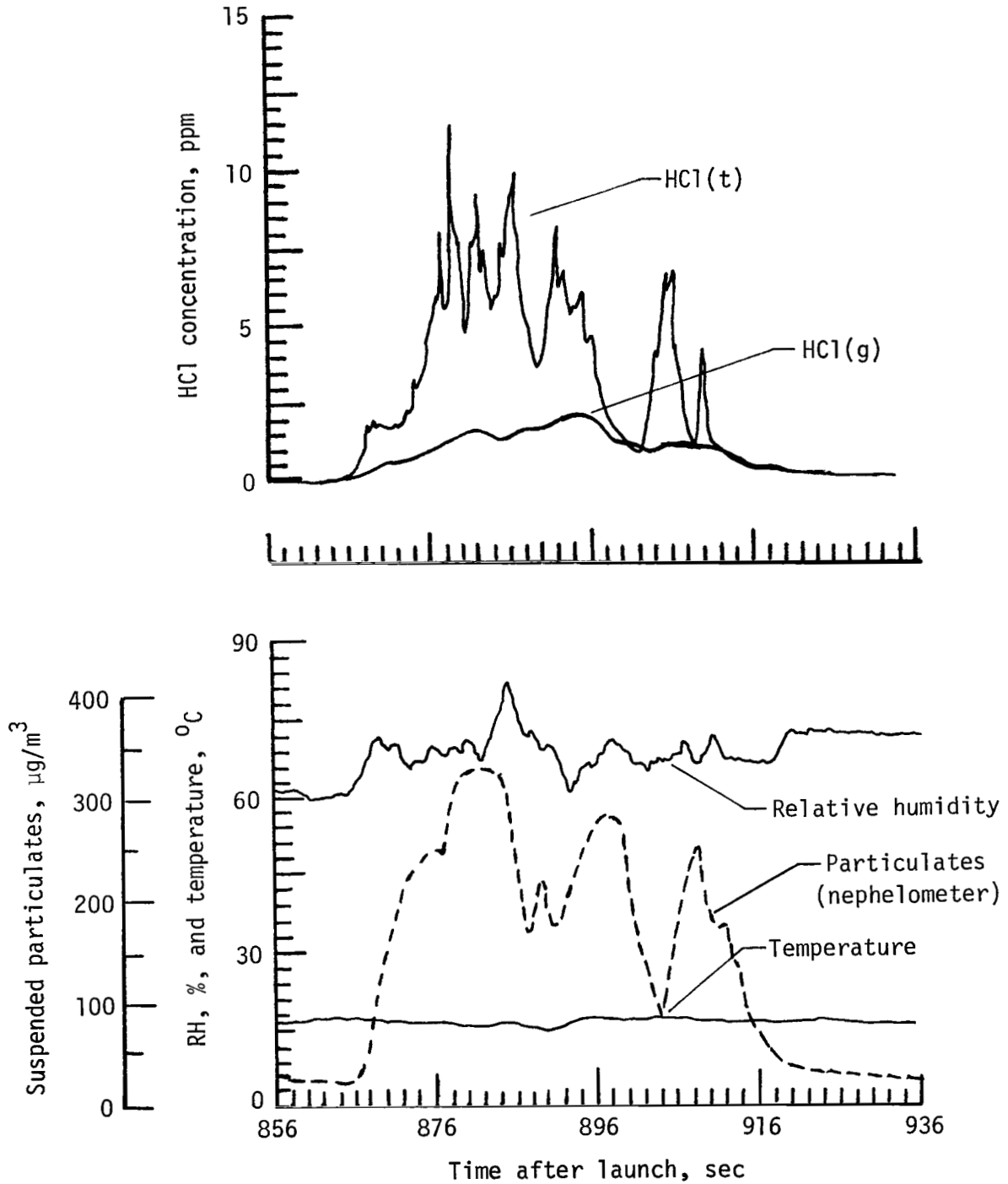


Figure B2.- Data of pass 2, north cloud.

APPENDIX B

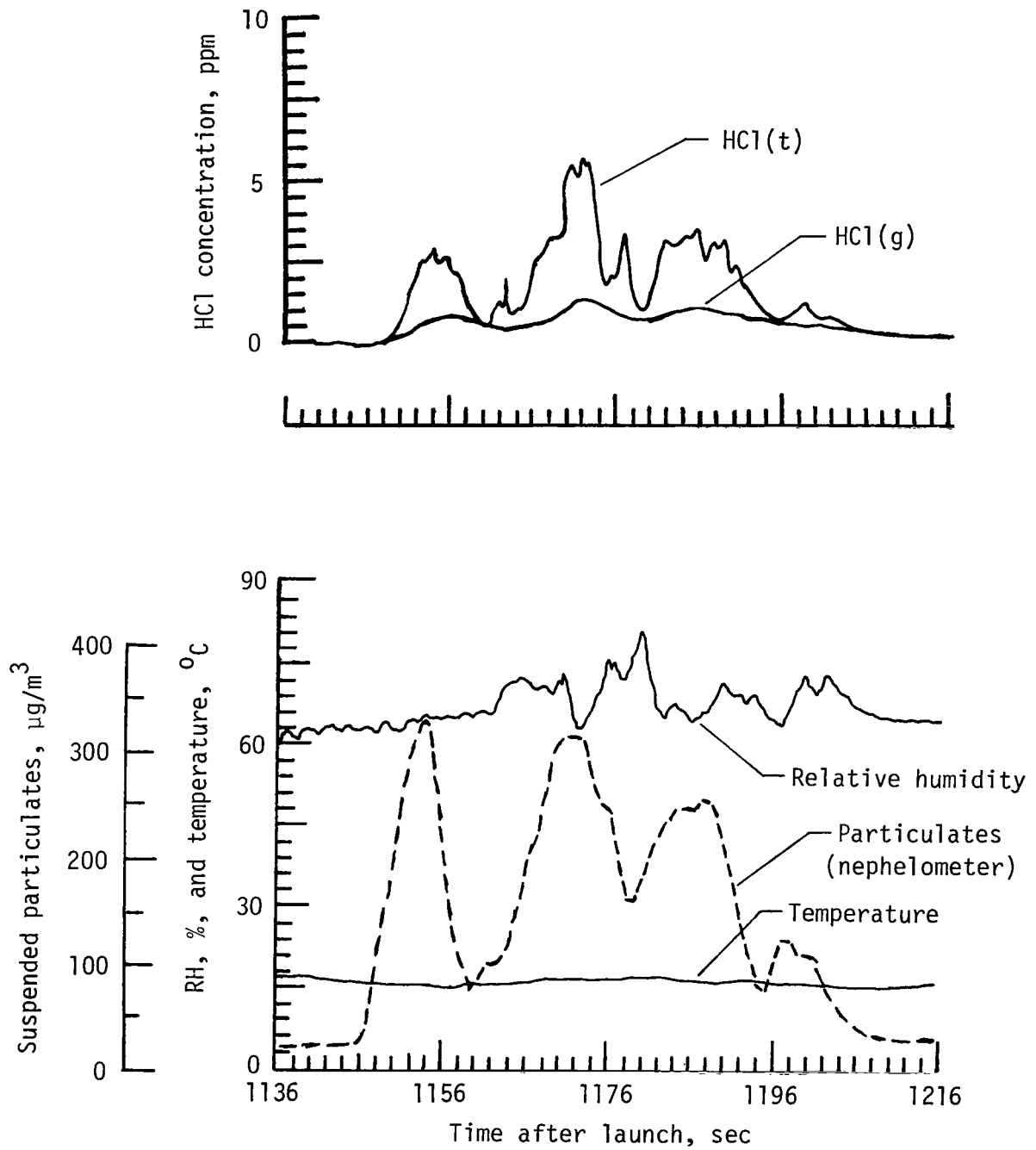


Figure B3.- Data of pass 3, north cloud.

APPENDIX B

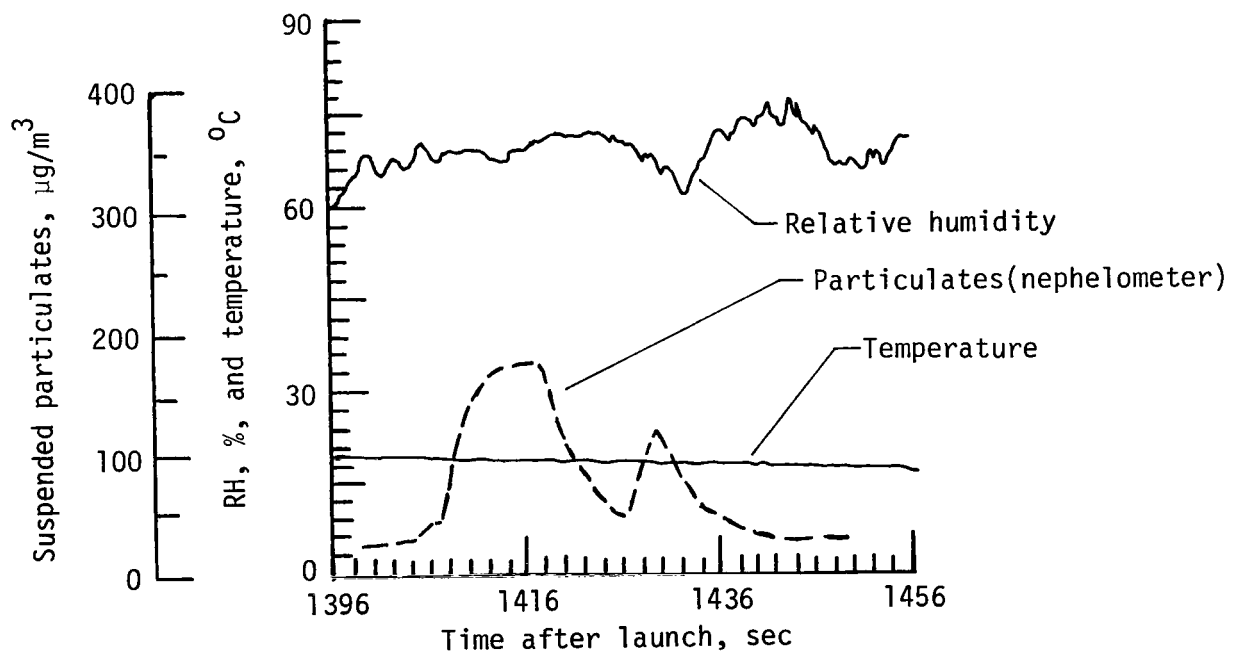
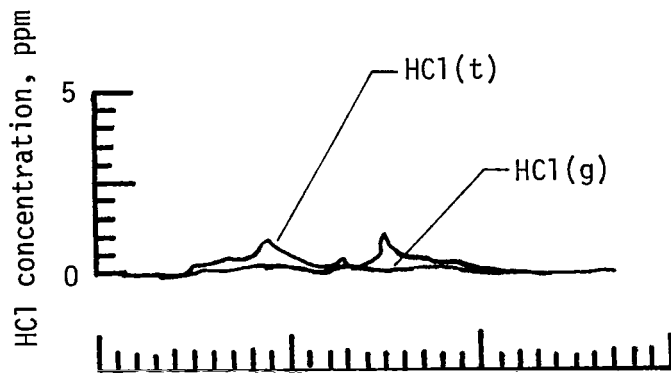


Figure B4.- Data of pass 4, north cloud.

APPENDIX B

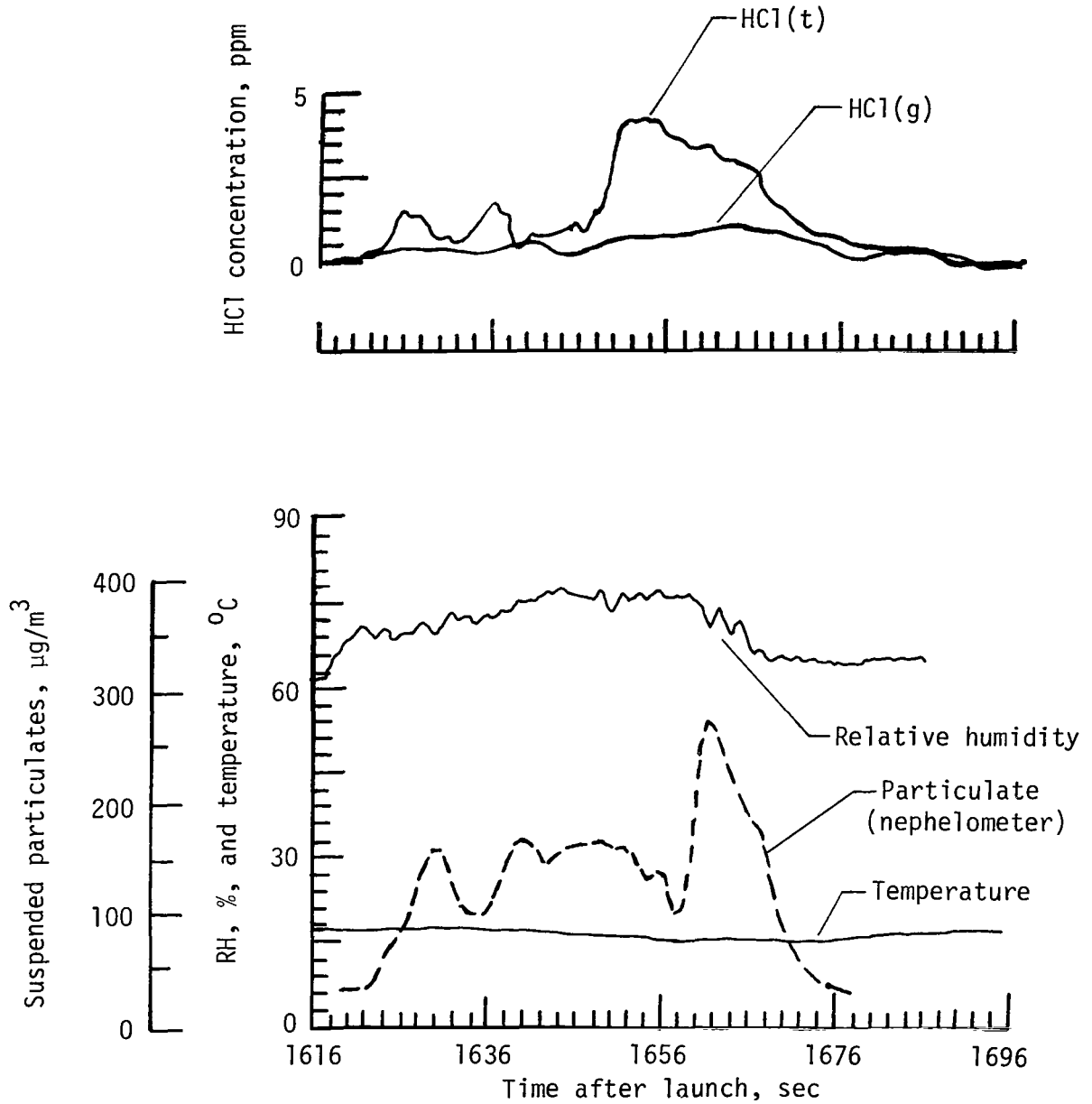


Figure B5.- Data of pass 5, north cloud.

APPENDIX B

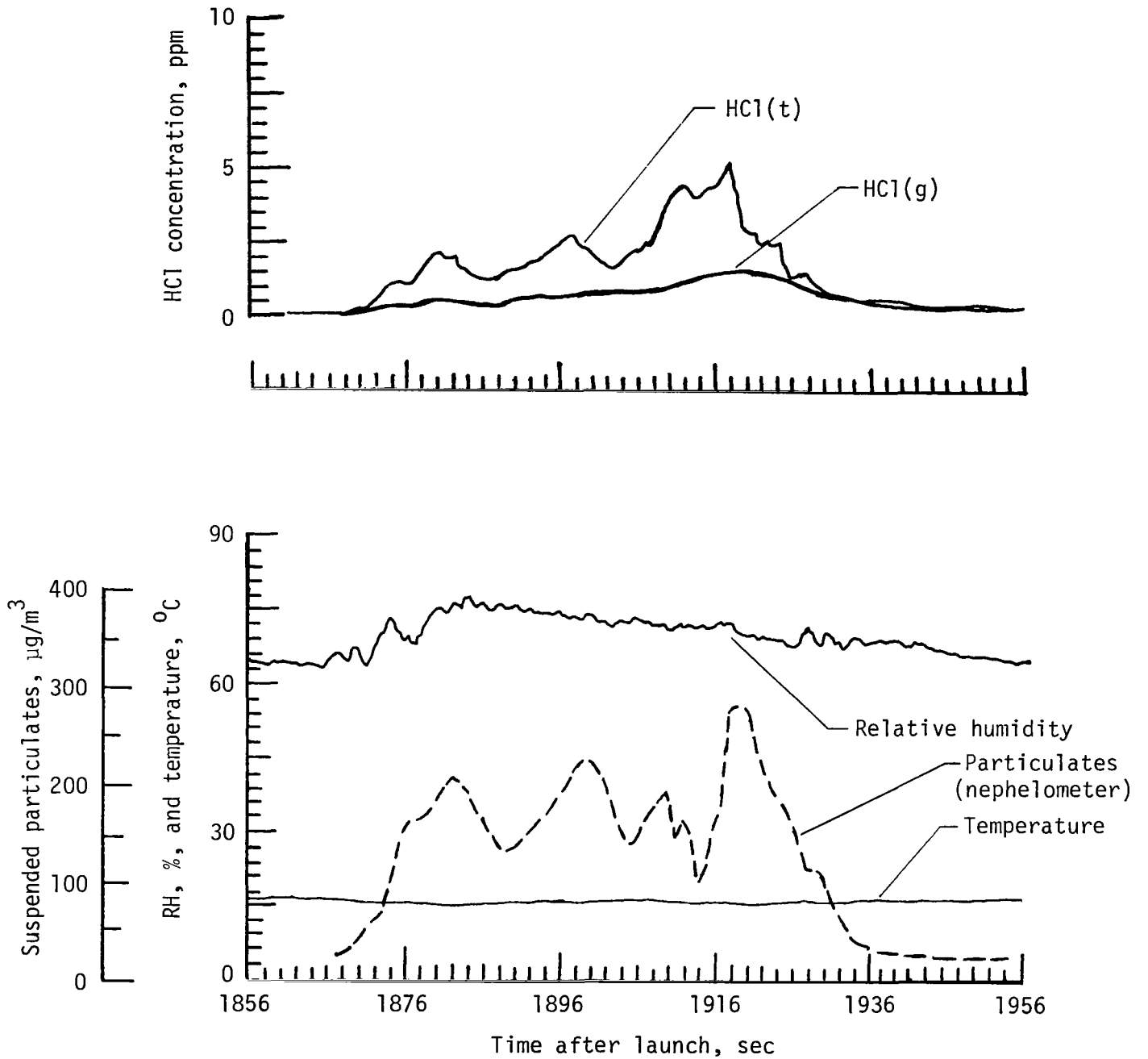


Figure B6.- Data of pass 6, north cloud.

APPENDIX B

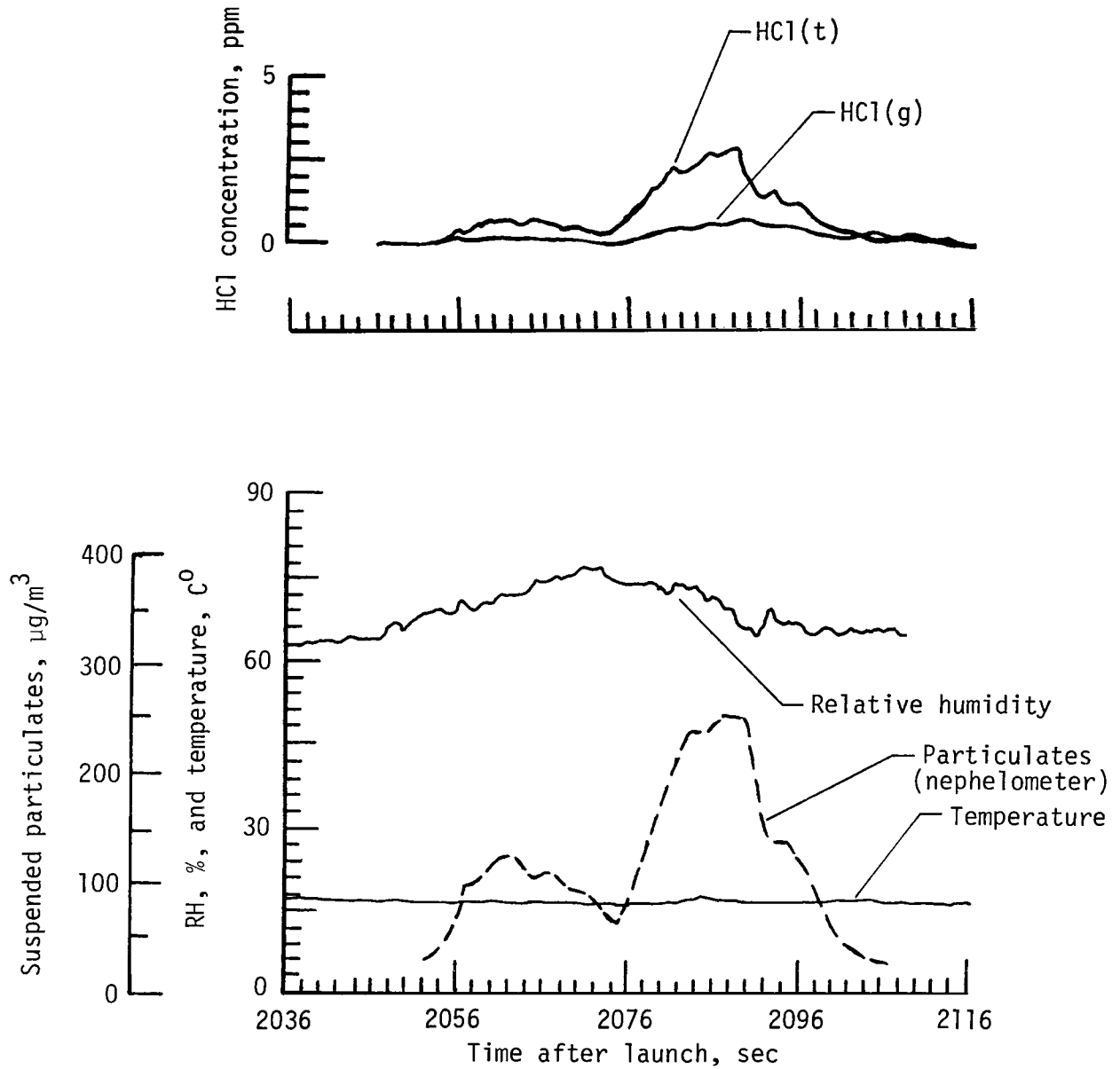


Figure B7.- Data of pass 7, north cloud.

APPENDIX B

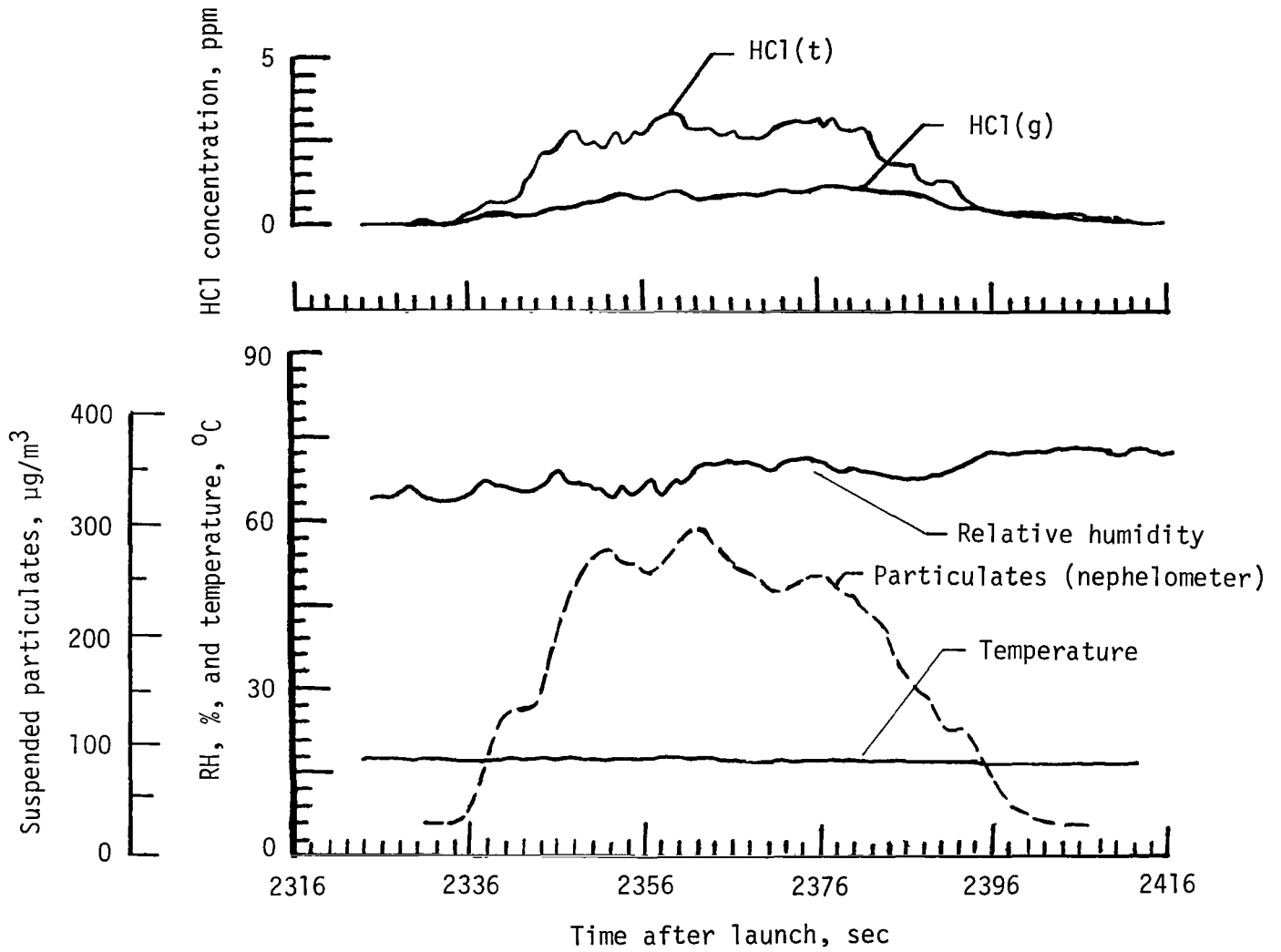


Figure B8.- Data of pass 8, north cloud.

APPENDIX B

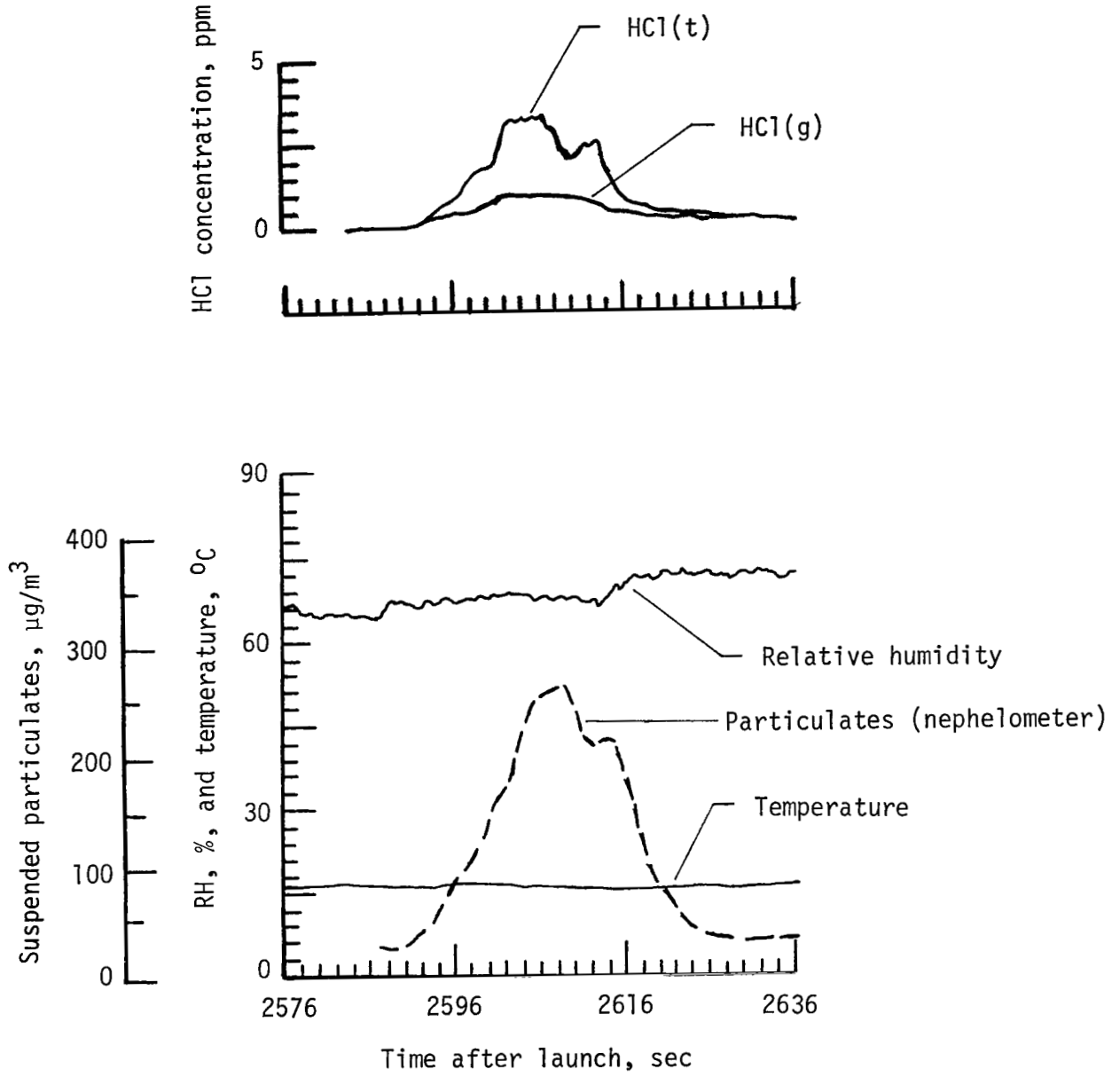


Figure B9.- Data of pass 9, north cloud.

APPENDIX B

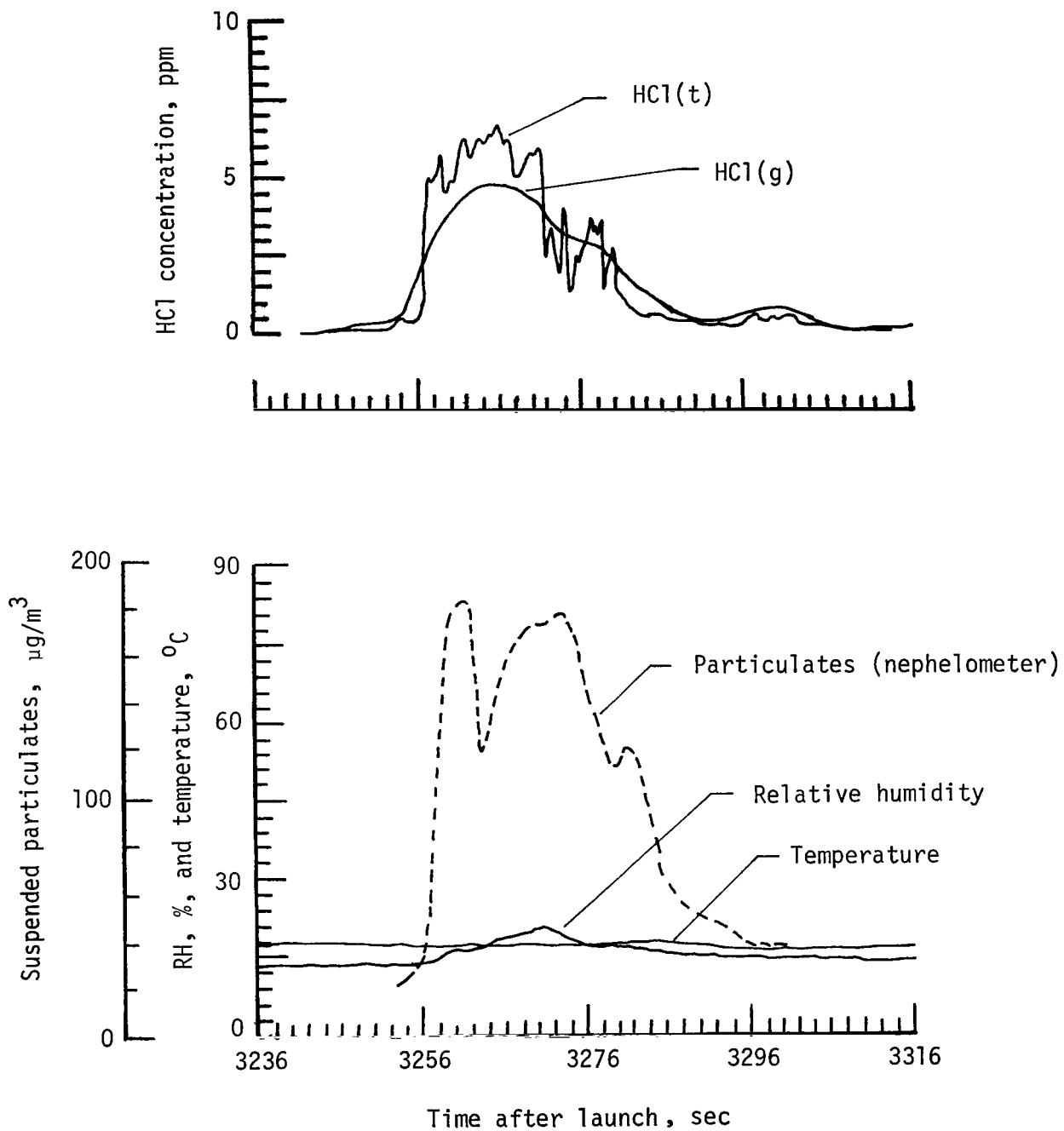


Figure B10.- Data of pass 11, west cloud.

APPENDIX B

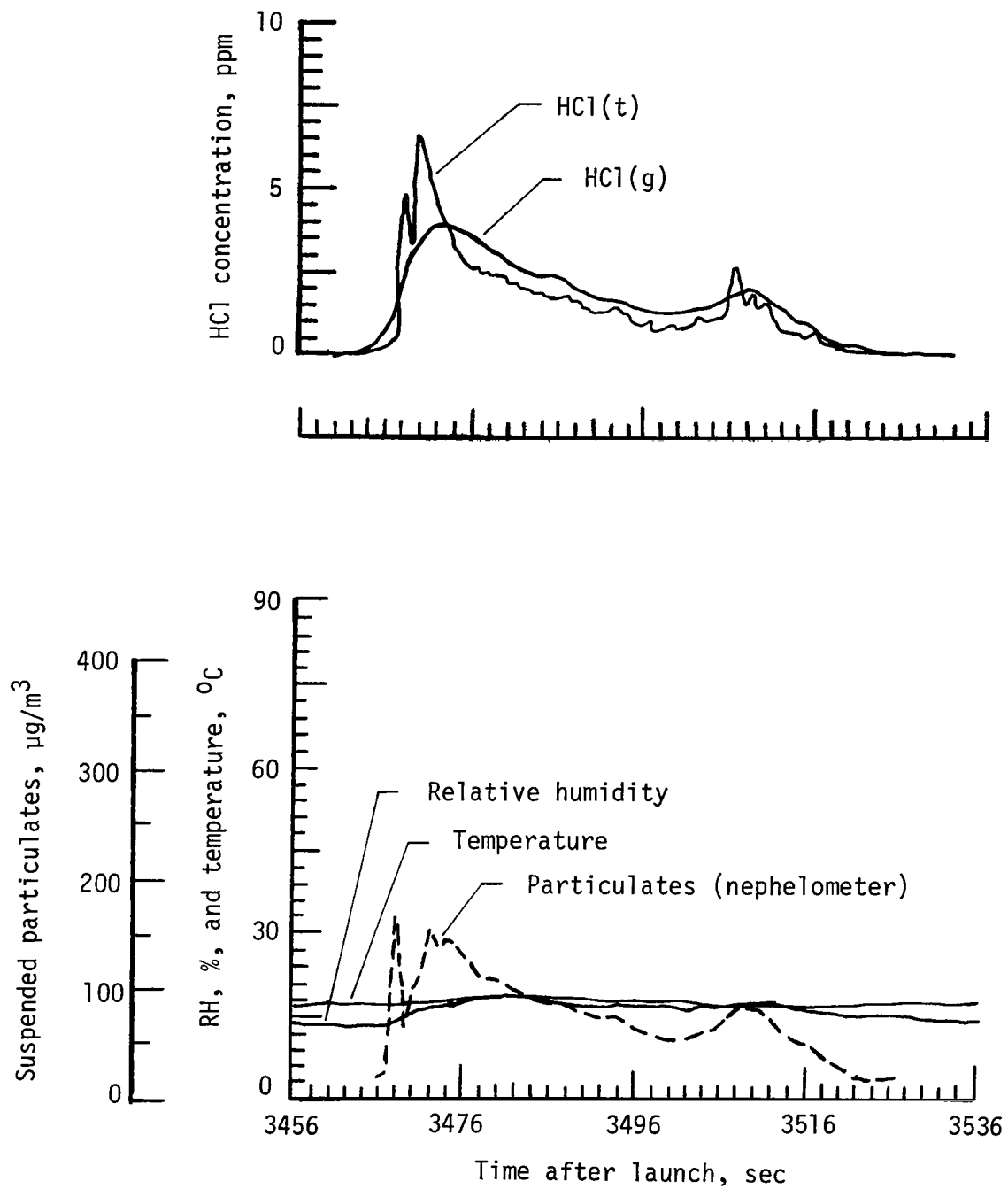


Figure B11.- Data of pass 12, west cloud.

APPENDIX B

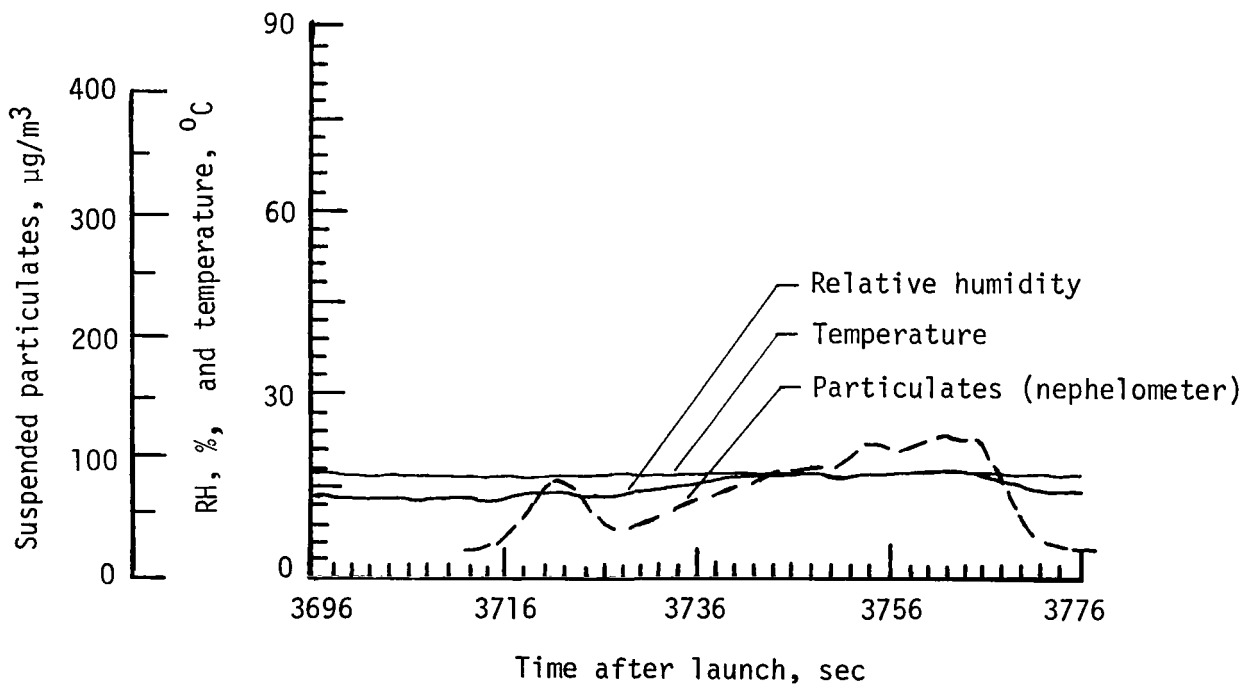
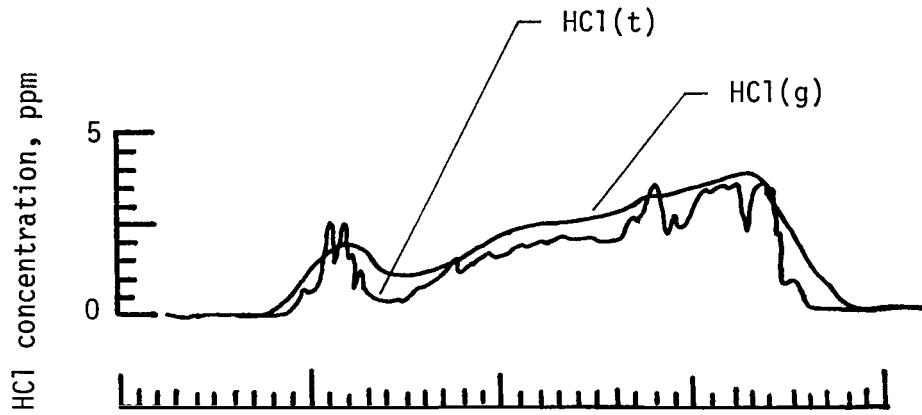


Figure B12.- Data of pass 13, west cloud.

APPENDIX B

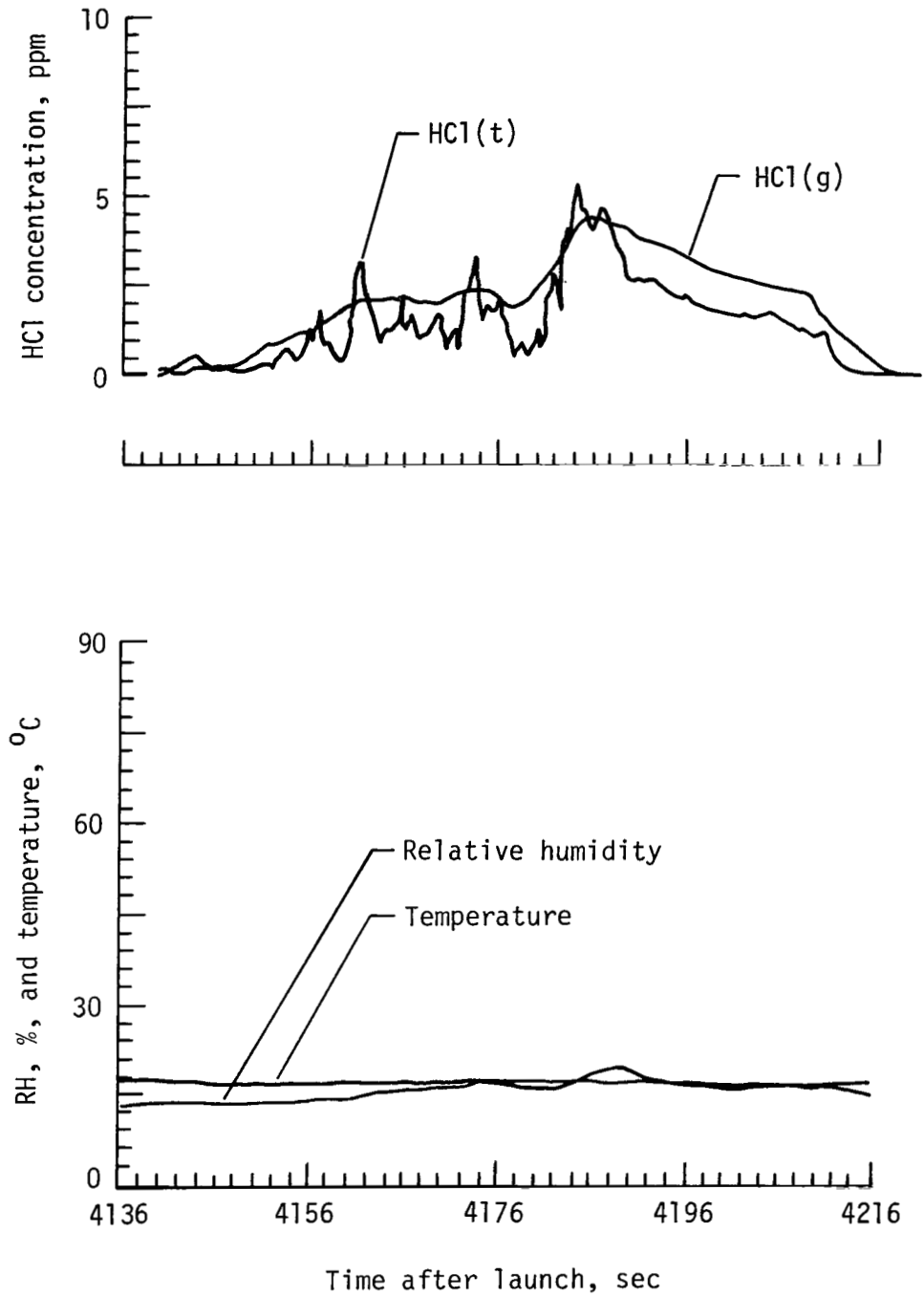


Figure B13.- Data of pass 15, west cloud.

APPENDIX B

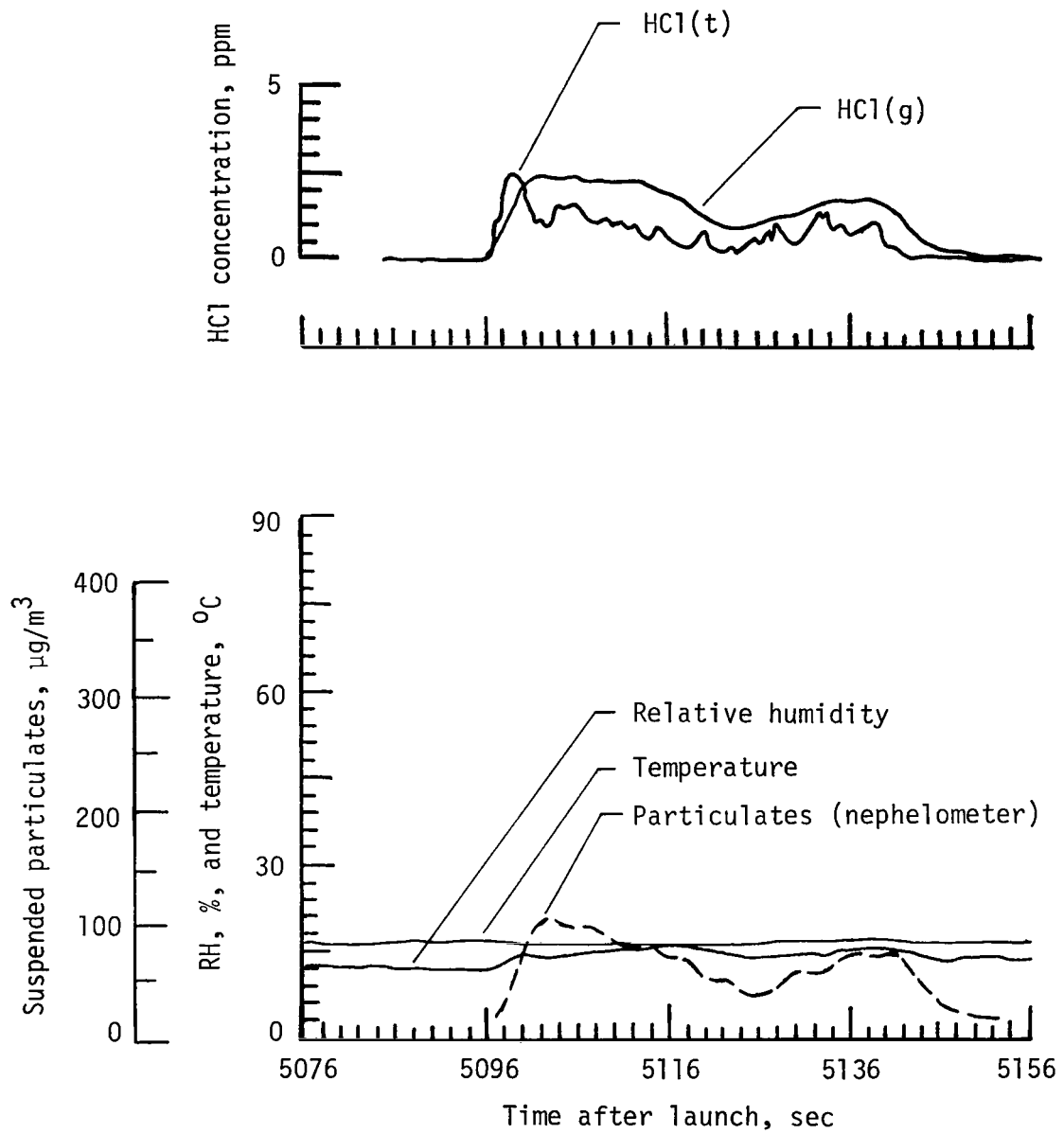


Figure B14.- Data of pass 18, west cloud.

APPENDIX B

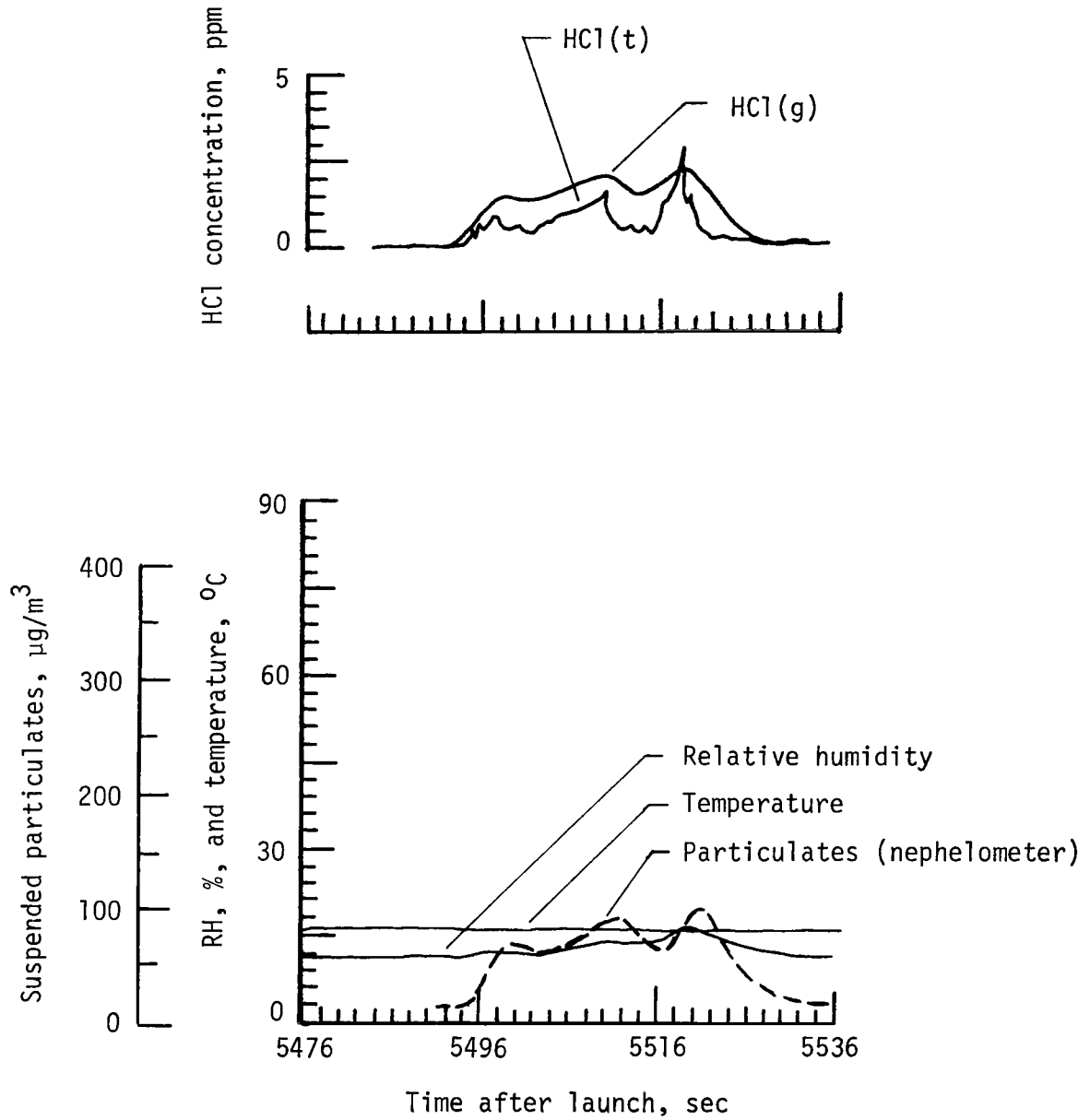


Figure B15.- Data of pass 19, west cloud.

APPENDIX B

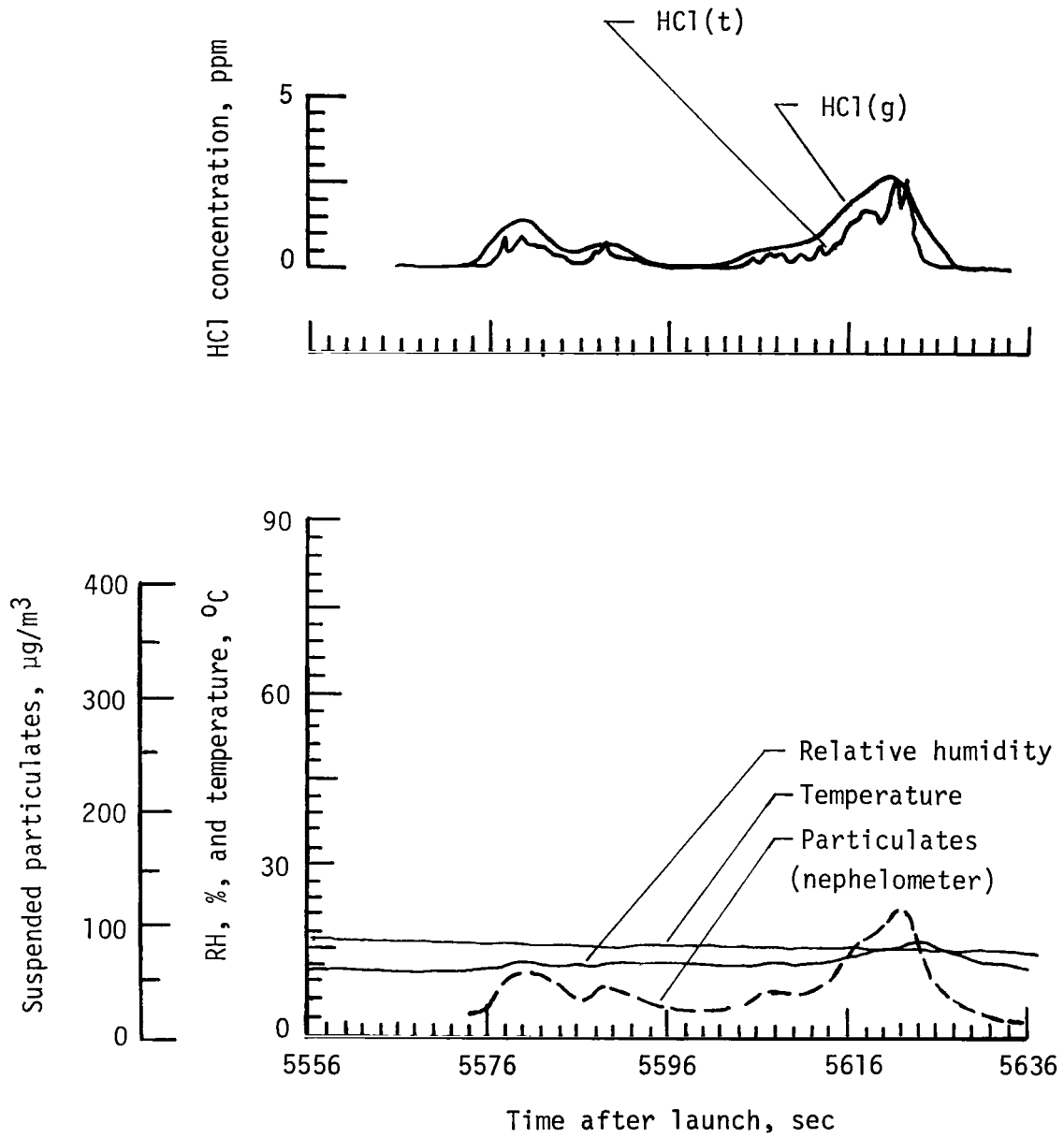


Figure B16.- Data of pass 20, west cloud.

APPENDIX B

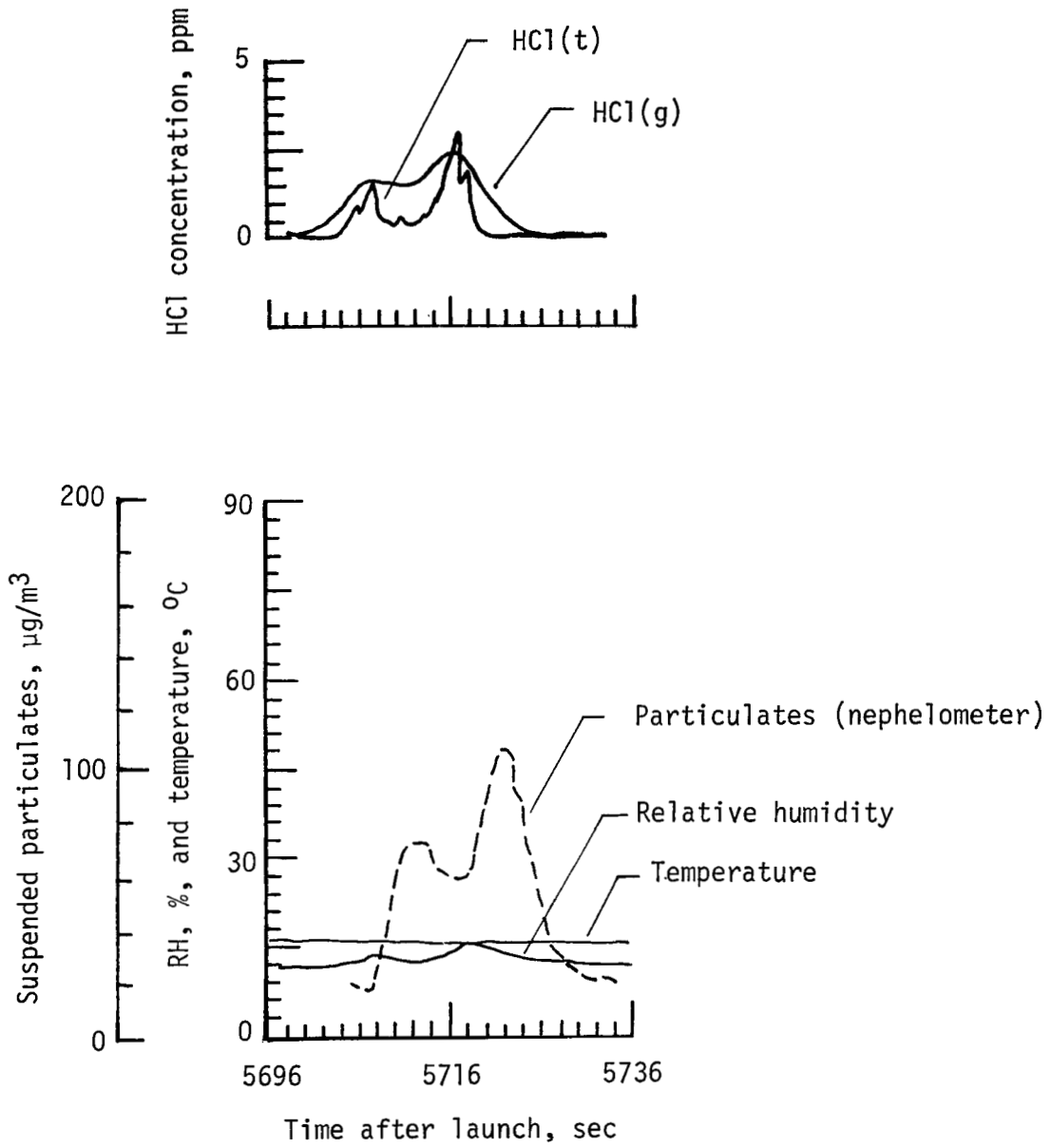


Figure B17.- Data of pass 21, west cloud.

APPENDIX B

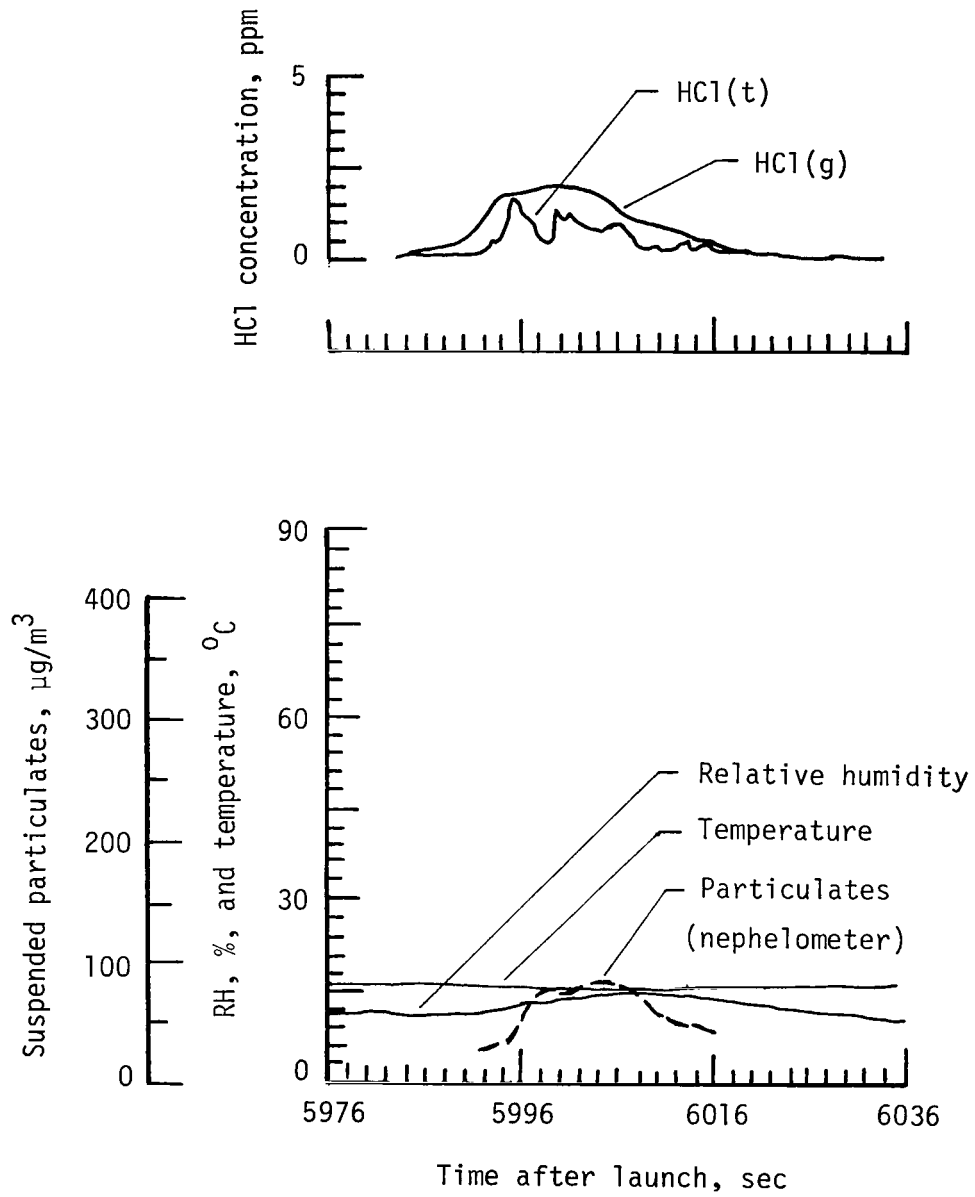


Figure B18.- Data of pass 22, west cloud.

APPENDIX B

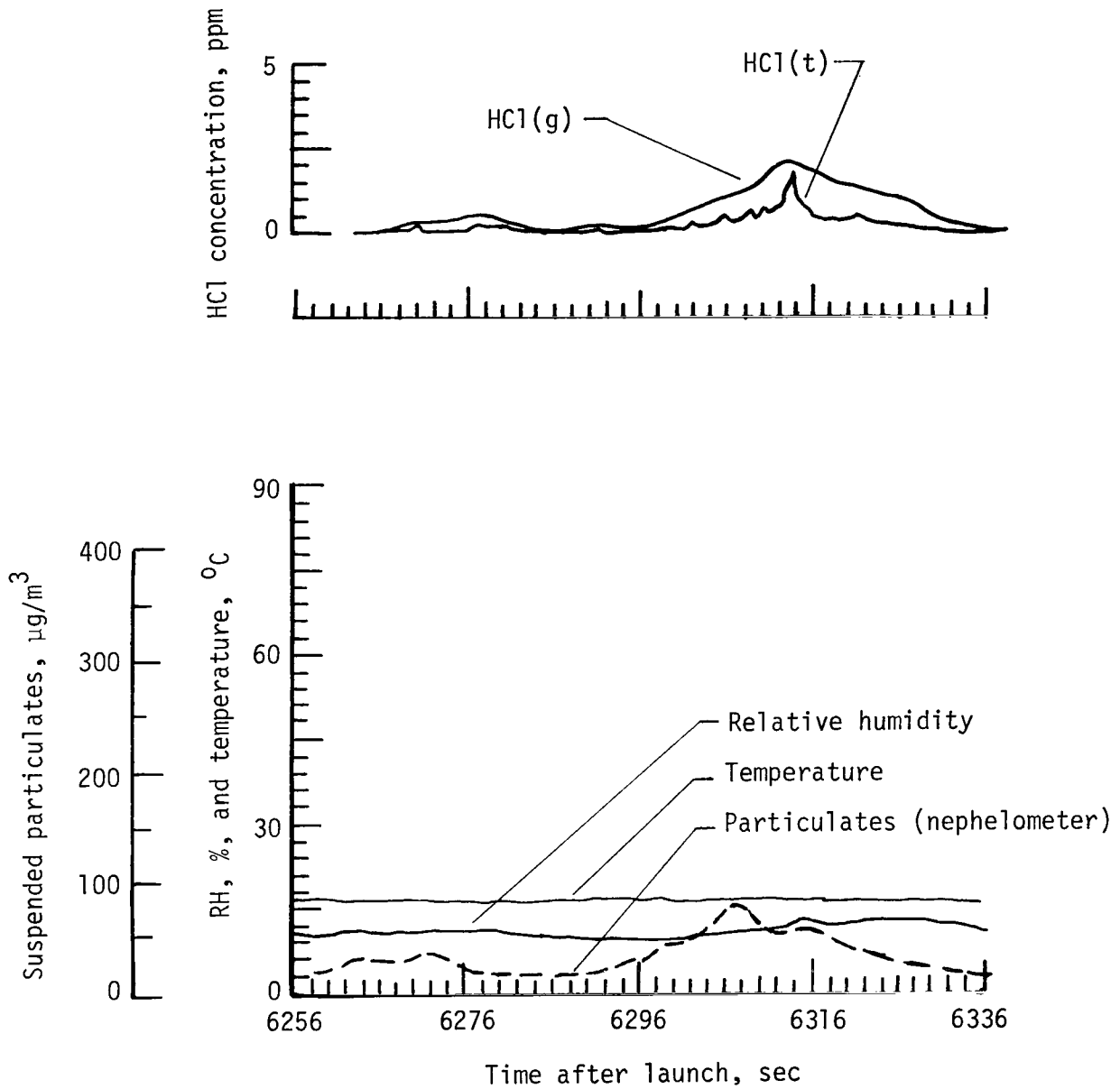


Figure B19.- Data of pass 23, west cloud.

APPENDIX B

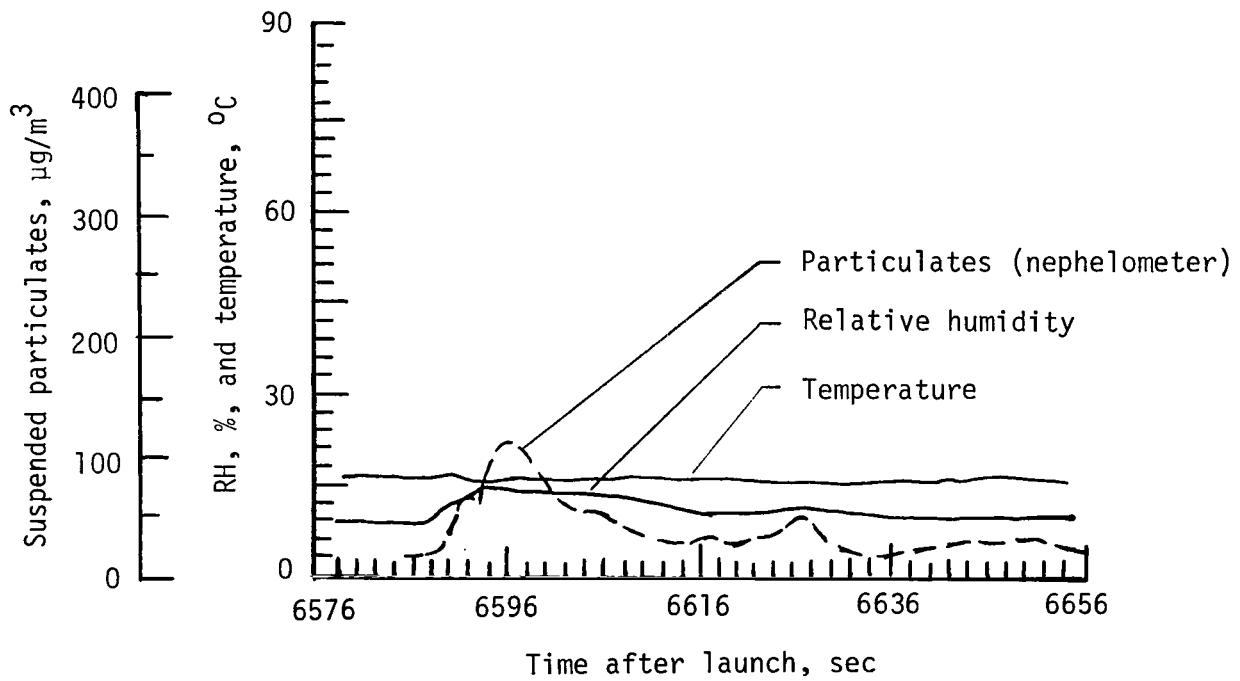
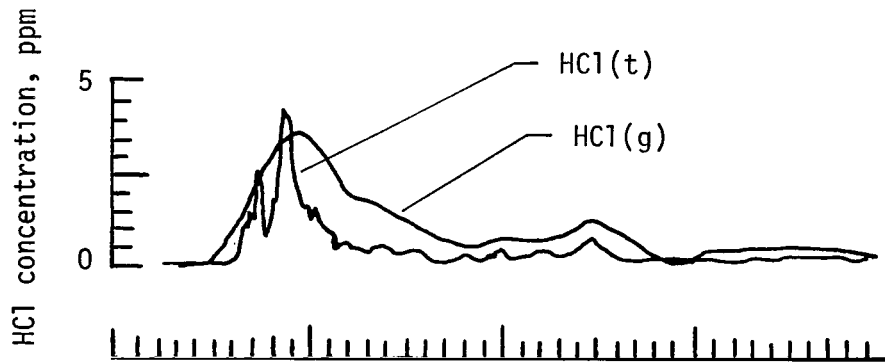


Figure B20.- Data of pass 25, west cloud.

APPENDIX B

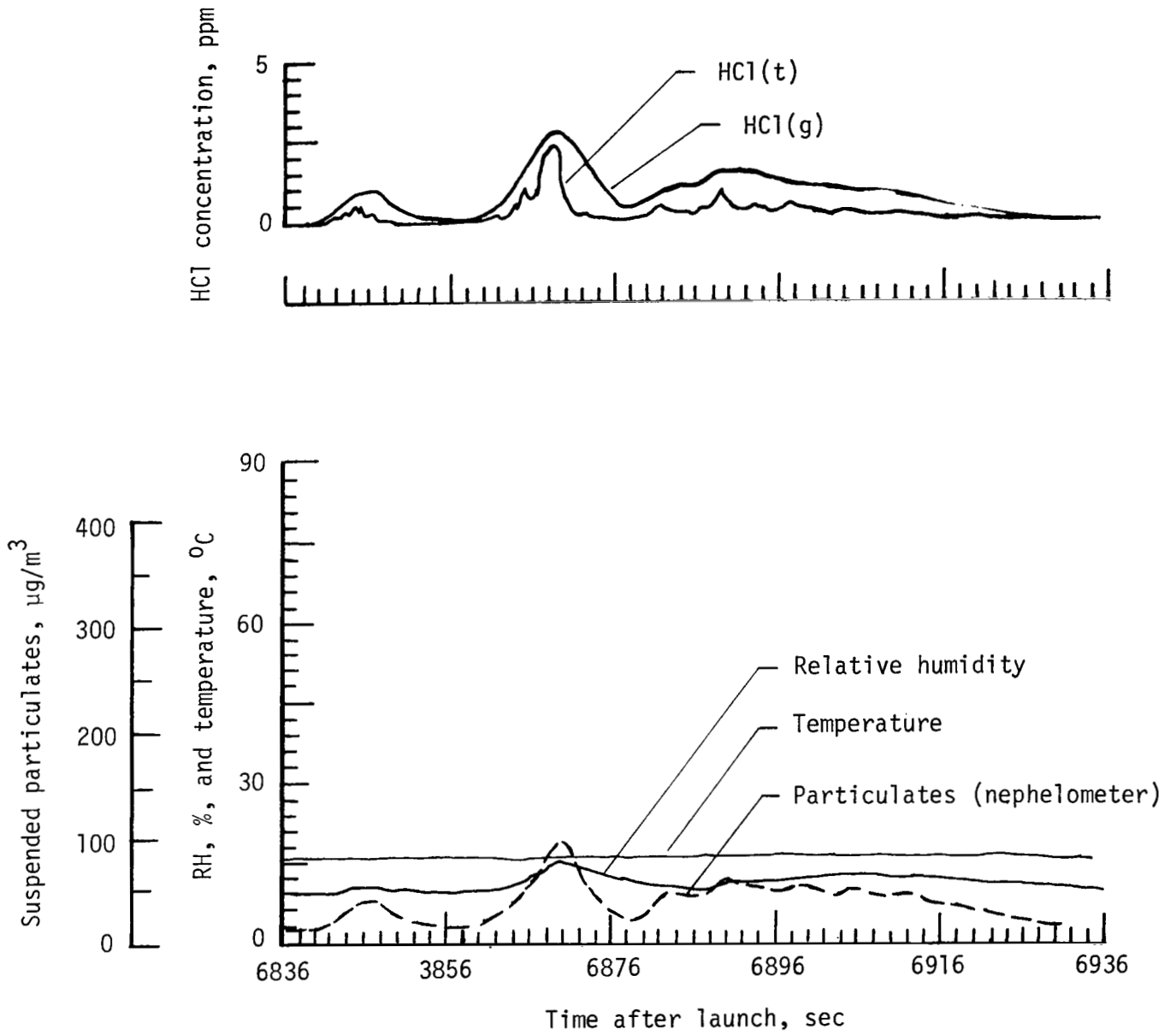


Figure B21.- Data of pass 27, west cloud.

APPENDIX B

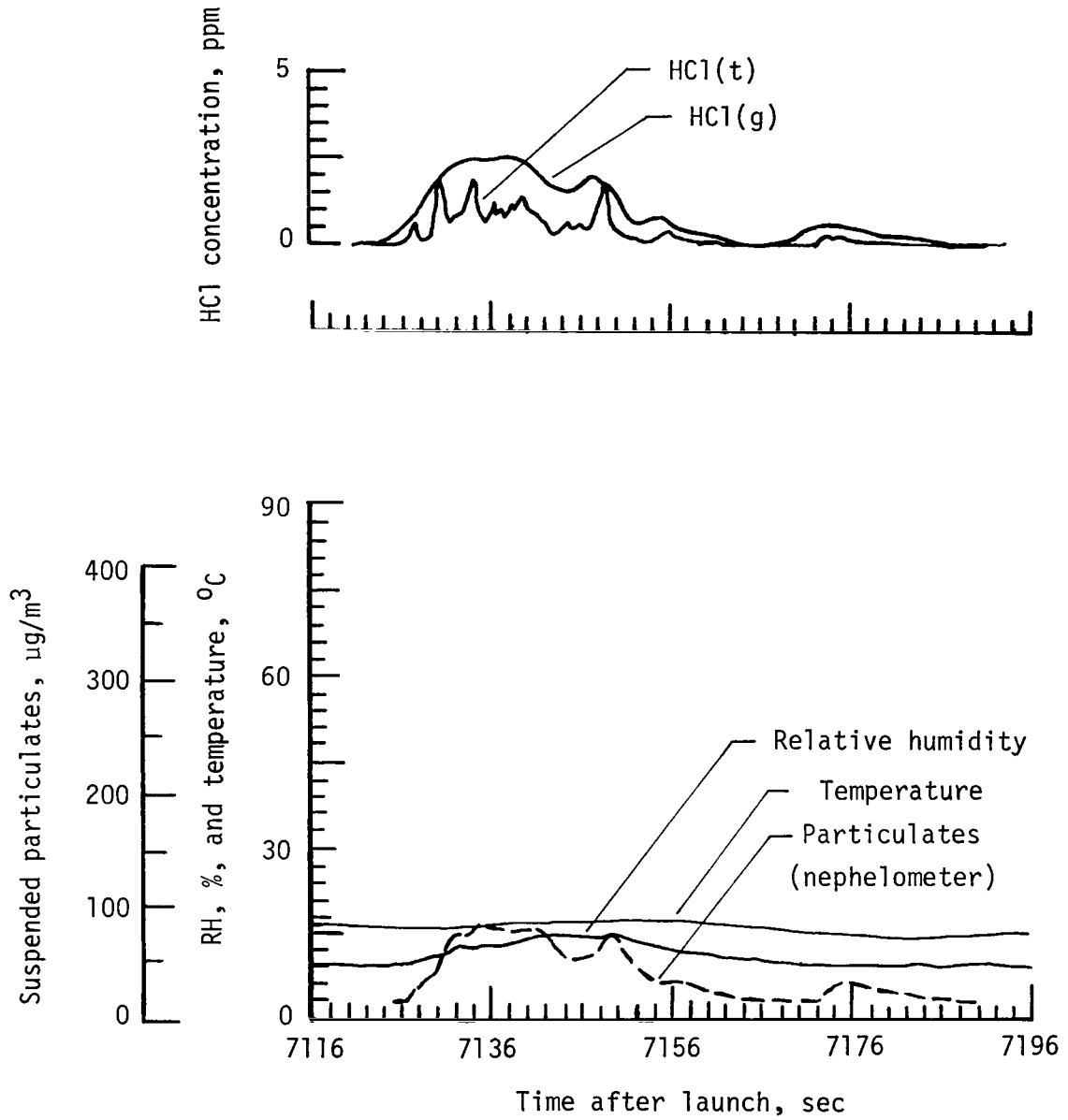


Figure B22.- Data of pass 29, west cloud.

APPENDIX B

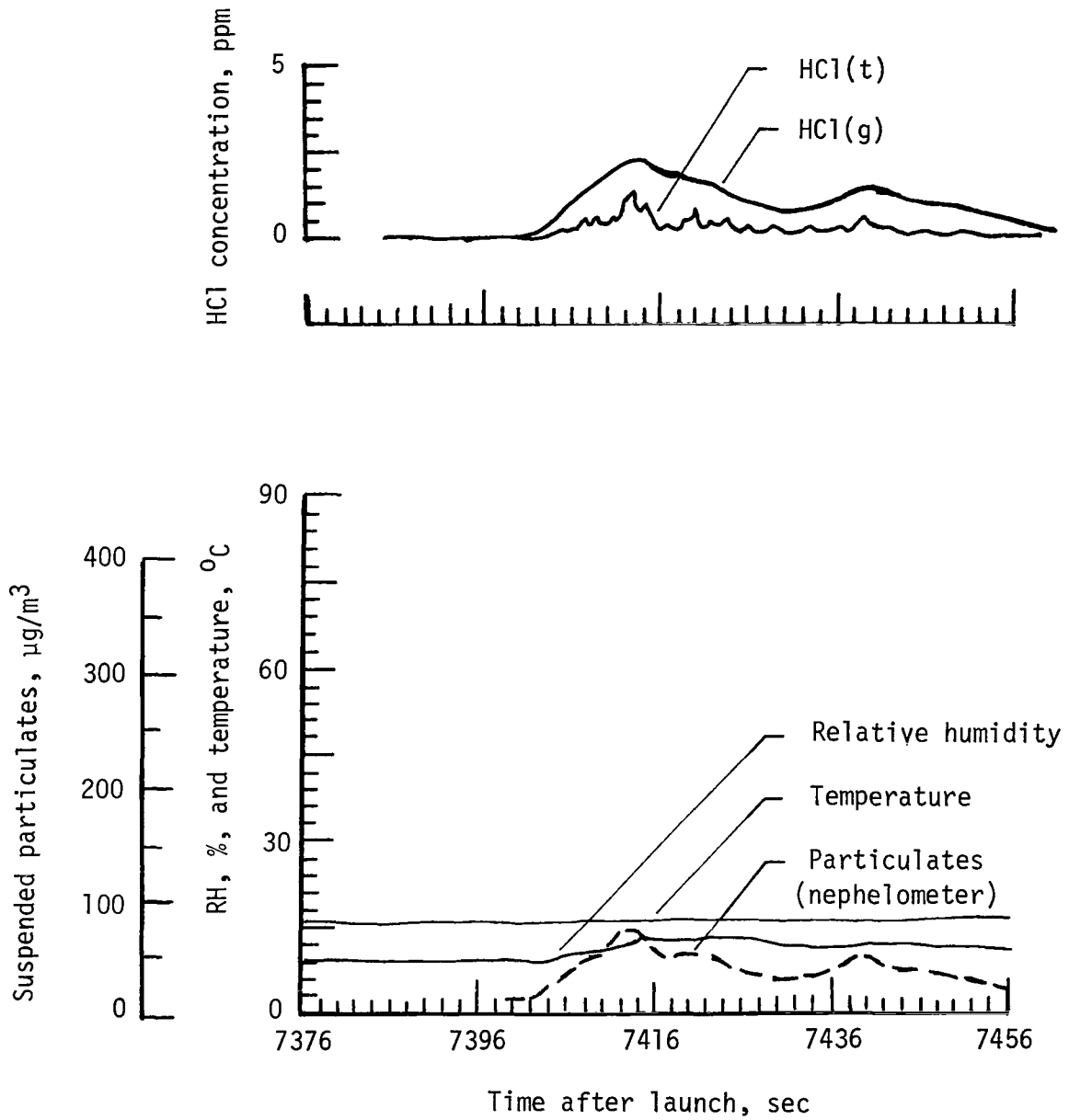


Figure B23.- Data of pass 30, west cloud.

APPENDIX B

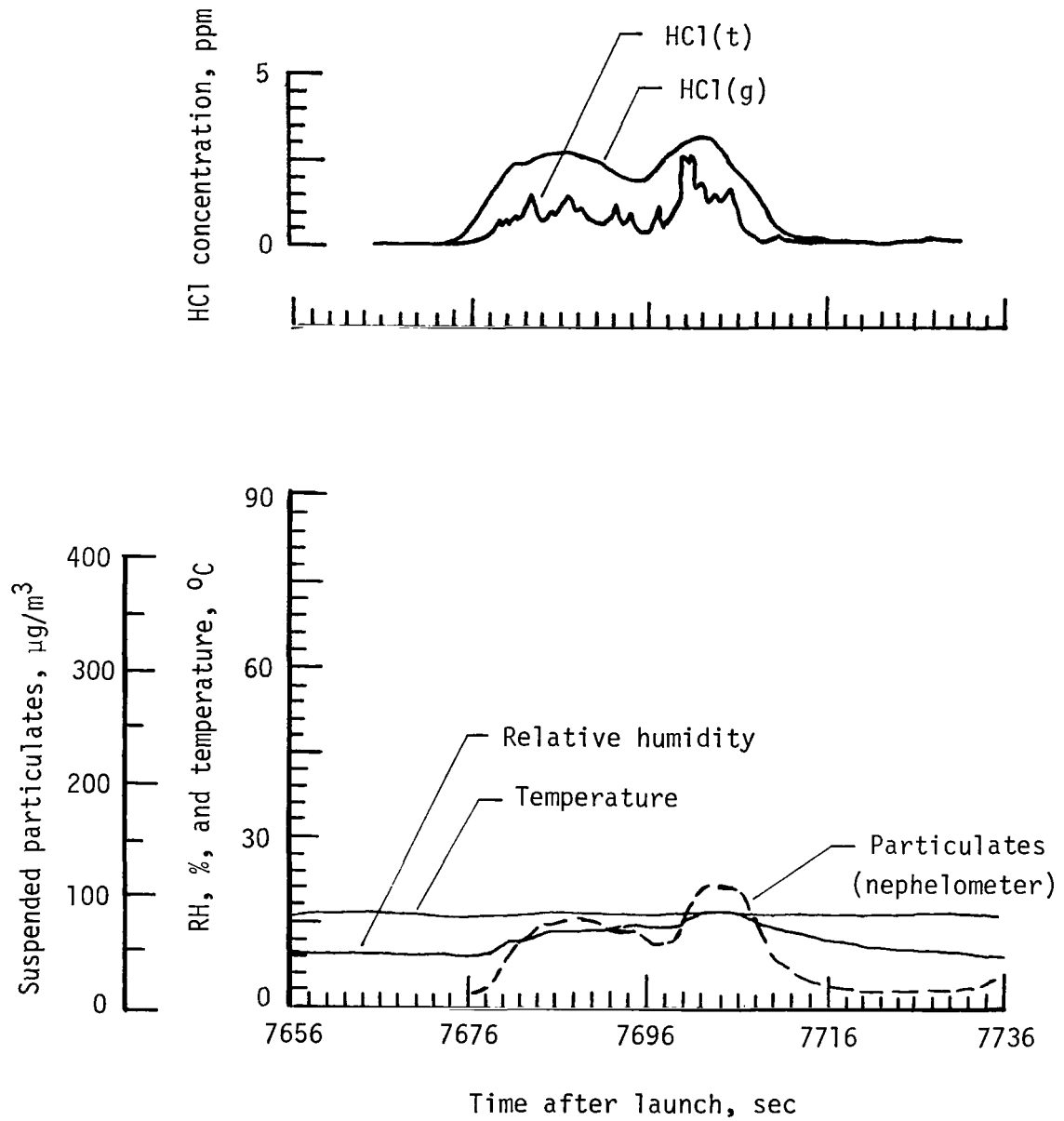


Figure B24.- Data of pass 31, west cloud.

REFERENCES

1. Hulten, William C.; Storey, Richard W.; Gregory, Gerald L.; Woods, David C.; and Harris, Franklin S., Jr.: Effluent Sampling of Scout "D" and Delta Launch Vehicle Exhausts. NASA TM X-2987, 1974.
2. Gregory, Gerald L.; Hulten, William C.; and Wornom, Dewey E.: Apollo Saturn 511 Effluent Measurements From the Apollo 16 Launch Operations - An Experiment. NASA TM X-2910, 1974.
3. Woods, David C.; and Chuan, Raymond L.: Characterization of Suspended Particles in the Space Shuttle Exhaust Cloud. Paper presented at the Third Symposium in Particulate Sampling and Measurement (Daytona Beach, Florida), Oct. 18-21, 1981.
4. Sebacher, D. I.; Gregory, G. L.; Bendura, R. J.; Woods, D. C.; and Cofer, W. R.: Hydrogen Chloride and Particulate Measurements in the Space Shuttle Exhaust Cloud. 1981 JANNAF Safety & Environmental Protection Subcommittee Meeting, CPIA Publ. 348 (Contract N00024-81-C-5301), Johns Hopkins Univ., Nov. 1981, pp. 251-257.
5. Environmental Impact Statement - Space Shuttle Program. NASA TM-82278, 1978.
6. Bowyer, J. M.: Rocket Motor Exhaust Products Generated by the Space Shuttle Vehicle During Its Launch Phase (1976 Design Data). Publ. 77-9 (Contract No. NAS 7-100), Jet Propul. Lab., California Inst. Technol., Mar. 1, 1977. (Available as NASA CR-154107.)
7. Gomberg, Richard I.; and Stewart, Roger B.: A Computer Simulation of the After-burning Processes Occurring Within Solid Rocket Motor Plumes in the Troposphere. NASA TN D-8303, 1976.
8. Bendura, Richard J.; and Crumbly, Kenneth H.: Ground Cloud Effluent Measurements During the May 30, 1974, Titan III Launch at the Air Force Eastern Test Range. NASA TM X-3539, 1977.
9. Gregory, Gerald L.; and Storey, Richard W., Jr.: Experimental Measurements of the Ground Cloud Effluents and Cloud Growth for the May 20, 1975, Titan IIIC Launch at Air Force Eastern Test Range, Florida. NASA TM-74044, 1977.
10. Wornom, Dewey E.; Woods, David C.; Thomas, Mitchel E.; and Tyson, Richard W.: Instrumentation of Sampling Aircraft for Measurement of Launch Vehicle Effluents. NASA TM X-3500, 1977.
11. Gregory, Gerald L.; and Moyer, Rudolph H.: Evaluation of a Hydrogen Chloride Detector for Environmental Monitoring. Rev. Sci. Instrum., vol. 48, no. 11, Nov. 1977, pp. 1464-1468.
12. Sebacher, Daniel I.: Airborne Nondispersive Infrared Monitor for Atmospheric Trace Gases. Rev. Sci. Instrum., vol. 49, no. 11, 1978, pp. 1520-1525.
13. Stephens, J. Briscoe; and Stewart, Roger B.: Rocket Exhaust Effluent Modeling for Tropospheric Air Quality and Environmental Assessments. NASA TR R-473, 1977.

14. Charlson, R. J.; Ahlquist, N. C.; Selvidge, H.; and MacCready, P. B., Jr.: Monitoring of Atmospheric Aerosol Parameters With the Integrating Nephelometer. *J. Air Pollut. Control Assoc.*, vol. 19, no. 12, Dec. 1969, pp. 937-942.
15. Tombach, Ivar: Measurement of Some Optical Properties of Air Pollution With the Integrating Nephelometer. AIAA Paper No. 71-1101, Nov. 1971.
16. Nadler, Melvin P.: Environmental Study of Toxic Exhausts. AFRPL-TR-76-13, U.S. Air Force, Feb. 1976. (Available from DTIC as AD A022 671.)
17. Wornom, Dewey E.; and Woods, David C.: Effluent Monitoring of the December 10, 1974, Titan III-E Launch at Air Force Eastern Test Range, Florida. NASA TM-78735, 1978.
18. Gomberg, Richard I.; Kantsios, Andronicos G.; and Rosensteel, Frederick J.: Some Physical and Thermodynamic Properties of Rocket Exhaust Clouds Measured With Infrared Scanners. NASA TP-1041, 1977.
19. Sebacher, Daniel I.; Wornom, Dewey E.; and Bendura, Richard J.: Hydrogen Chloride Partitioning in a Titan III Exhaust Cloud Diluted With Ambient Air. AIAA Paper 79-0299, Jan. 1979.
20. Pellett, G. L.; Sebacher, D. I.; Bendura, R. J.; and Wornom, D. E.: HCl in Rocket Exhaust Clouds: Atmospheric Dispersion, Acid Aerosol Characteristics, and Acid Rain Deposition. [Preprint] 80-49.6, *Air Pollut. Control Assoc.*, June 1980.
21. Pellett, G. L.: Analytic Model for Washout of HCl(g) From Dispersing Rocket Exhaust Clouds. NASA TP-1801, 1981.
22. Pellett, G. L.; and Staton, W. L.: Application of a Gaussian Multilayer Diffusion Model To Characterize Dispersion of Vertical HCl Column Density in Rocket Exhaust Clouds. NASA TP-1956, 1981.
23. Fenton, Donald L.; and Ranade, Madhav B.: Aerosol Formation Threshold for HCl-Water Vapor System. *Environ. Sci. & Technol.*, vol. 10, no. 12, Nov. 1976, pp. 1160-1162.

TABLE I.- ESTIMATION OF SPACE SHUTTLE EXHAUST PRODUCTS^a

(a) Solid engines (totals for two)

Species	Mass in cloud, kg	Nozzle exit plane flow	
		At nozzle exit plane, percent (mass)	Plume ^b at 1 km from exit plane, percent (mass)
Al ₂ O ₃	42 000 to 68 000	30.1	30.1
CO	34 000 to 54 000	24.1	(c)
HCl	30 000 to 48 000	21.2	18.9
N ₂	12 000 to 20 000	8.7	(d)
H ₂ O	13 000 to 21 000	9.3	28.6
CO ₂	5 000 to 8 000	3.4	41.2
Cl ₂	(c)	(c)	2.1
O ₂	(c)	(c)	(d)
NO	(c)	(c)	1.3
Other	5 000 to 7 000	3.2	1.1
Total	141 000 to 226 000	100.0	123.3 ^e

(b) Liquid engines (totals for three)

Species	Mass in cloud, kg	Nozzle exit plane flow	
		At nozzle exit plane, percent (mass)	Plume ^b at 1 km from exit plane, percent (mass)
H ₂ O	20 000 to 33 000	95.9	128
H ₂	700 to 1 000	3.5	(c)
Other	(c)	.6	.6
Total	21 000 to 34 000	100.0	128.6 ^e

^aFrom references 5 to 7.

^bAfterburning is complete.

^cLess than 300 kg or 0.1 percent.

^dAssumed to be part of air.

^eTotal is greater than 100 percent because of the chemical addition of air.

TABLE II.- FLIGHT PARAMETERS FOR SAMPLING STS-1 LAUNCH

Pass number	Time after launch, T + min	Altitude, m	Aircraft heading, deg (magnetic)	Aircraft time in cloud, sec
1	9	945	295	75
2	15	853	165	54
3	20	869	253	66
4	24	640	155	44
5	28	853	254	54
6	32	884	146	74
7	35	869	250	54
8	40	884	142	70
9	43	884	239	38
10	50	1372	233	120
11	55	1615	336	60
12	58	1676	240	58
13	63	1661	151	64
14	65	1661	242	34
15	70	1676	352	75
16	73	1676	261	22
17	81	1676	331	66
18	85	1753	283	54
19	92	1798	280	40
20	94	1768	97	58
21	96	1798	292	26
22	100	1813	250	26
23	105	1859	254	78
24	108	1859	87	80
25	110	1859	278	72
26	113	1859	82	40
27	115	1859	254	90
28	118	1859	73	40
29	119	1844	271	60
30	124	1844	270	60
31	128	1859	275	42

TABLE III.- AIRCRAFT INSTRUMENTATION, STS-1 LAUNCH

Species	Technique	Detection limit ^a	Time response to 90 percent of reading, sec
HCl(t)	Chemiluminescent	0.2 ppm	1
HCl(g)	Gas filter correlation	.2 ppm	1
Particulates	Nephelometer ^b	3.8 $\mu\text{g}/\text{m}^3$	1
Particulates	Quartz crystal microbalance	1 $\mu\text{g}/\text{m}^3$	2
Temperature	Resistance thermometer	.1°C	1
Dewpoint temperature	Cooled mirror	.1°C	NA ^c

^aAs flown for STS-1 mission.

^bUses a heated inlet to volatize liquid aerosols.

^cResponse stated in terms of dewpoint temperature change per unit of time; i.e., 1°C/sec.

TABLE IV.- QCM SIZING CHARACTERISTICS

Stage number	50-percent sizing cut point, μm	Effective sizing interval, μm	Geometric mean diameter, μm
1	30	60 to 30	42
2	15	30 to 15	21
3	7.5	15 to 7.5	10.7
4	3.7	7.5 to 3.7	5.4
5	1.8	3.7 to 1.8	2.6
6	1.0	1.8 to 1	1.34
7	.48	1 to .48	.69
8	.23	.48 to .23	.33
9	.13	.23 to .13	.17
10	.08	.13 to .08	.11

TABLE V.- SUMMARY OF STS-1 DATA FOR HCl AND PARTICULATES

Pass number	Maximum concentration			
	HCl(t), ppm (a)	HCl(g), ppm (b)	Particles, $\mu\text{g}/\text{m}^3$ (c)	$B_{\text{scat}}, \text{m}^{-1}$
1	14.9	3.5	668	17.6×10^{-4}
2	8.9	2.0	334	8.8×10^{-4}
3	5.6	1.2	332	8.7×10^{-4}
^d 4	1.0	<.2	180	4.7×10^{-4}
5	4.3	1.0	274	7.2×10^{-4}
6	5.0	1.5	284	7.5×10^{-4}
7	2.9	.6	253	6.7×10^{-4}
8	3.4	1.0	305	8.0×10^{-4}
9	3.3	1.0	264	7.0×10^{-4}
10	3.7	(e)	117	3.1×10^{-4}
11	6.4	4.7	175	4.6×10^{-4}
12	6.4	4.1	170	4.5×10^{-4}
13	3.6	4.0	121	3.2×10^{-4}
14	2.8	(e)	87	2.3×10^{-4}
15	4.6	4.5	160	4.2×10^{-4}
16	.5	(e)	37	0.9×10^{-4}
17	1.3	(e)	48	1.3×10^{-4}
18	2.5	2.5	109	2.9×10^{-4}
19	2.4	2.3	101	2.7×10^{-4}
20	2.4	2.6	112	3.0×10^{-4}
21	2.8	2.4	110	2.9×10^{-4}
22	1.5	2.0	84	2.2×10^{-4}
23	1.4	2.1	81	2.1×10^{-4}
24	.9	(e)	65	1.7×10^{-4}
25	4.1	3.6	112	3.0×10^{-4}
26	.8	(e)	58	1.5×10^{-4}
27	2.3	2.7	100	2.6×10^{-4}
28	.4	(e)	38	1.0×10^{-4}
29	1.7	2.5	86	2.3×10^{-4}
30	1.2	2.2	78	2.0×10^{-4}
31	2.5	3.0	110	2.9×10^{-4}

^aHCl(t) \equiv Total HCl (gaseous plus aqueous).

^bHCl(g) \equiv Gaseous HCl.

^cNephelometer data.

^dUnder cloud.

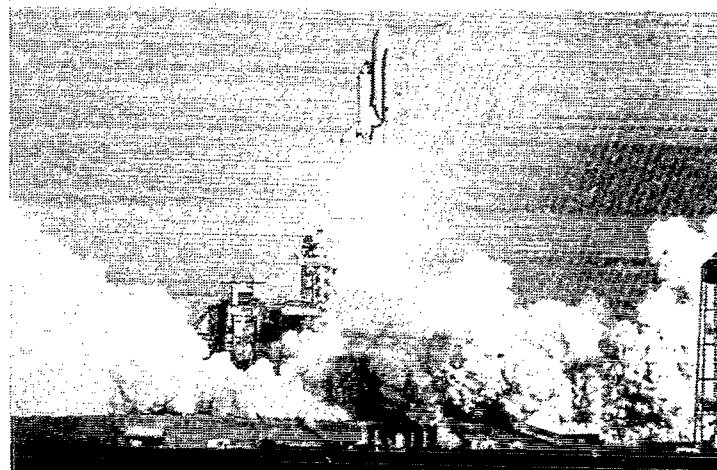
^eData loss.



7 min



3 min



Launch

L-82-201

Figure 1.- STS-1 cloud photographs, April 12, 1981.



L-82-202

Figure 2.- Sampling aircraft.

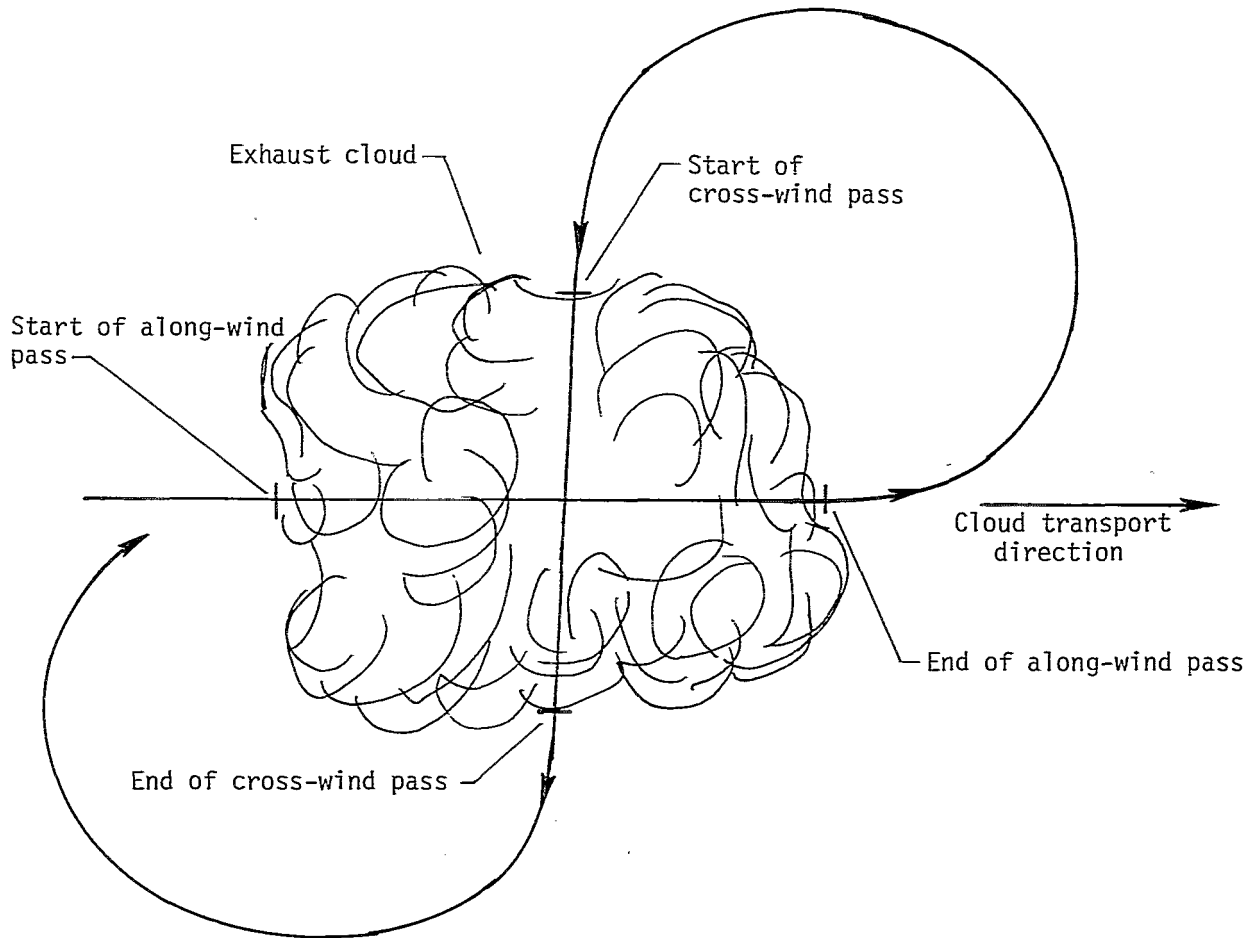


Figure 3.- Plan view of aircraft sampling plan.

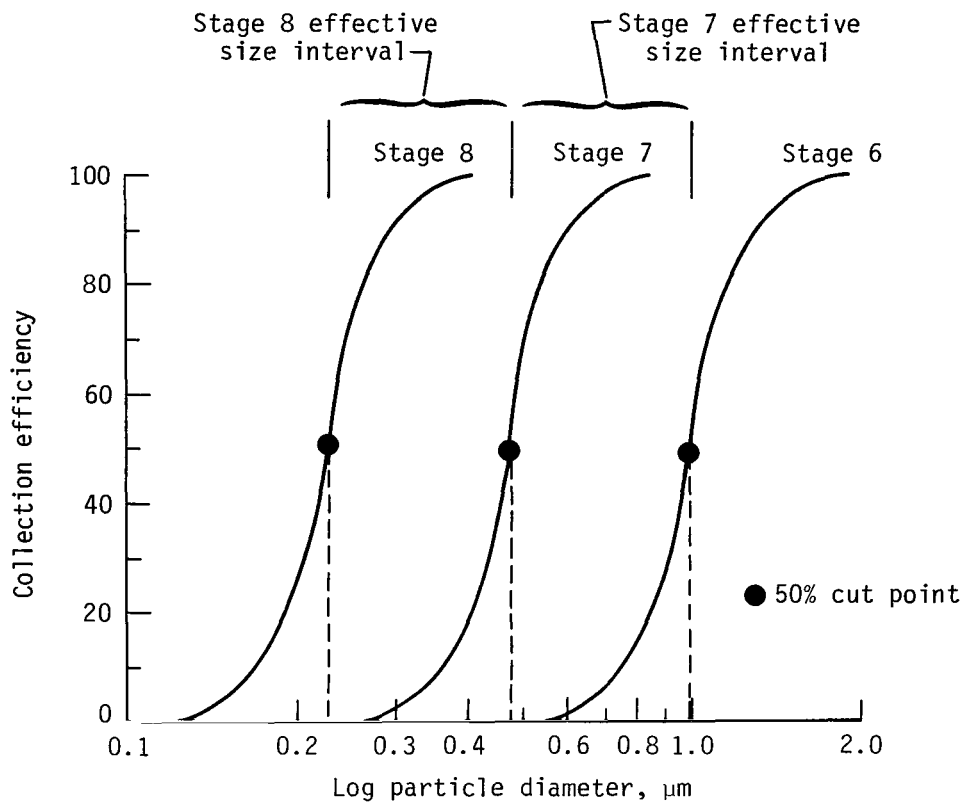


Figure 4.- Illustration of QCM sizing intervals.

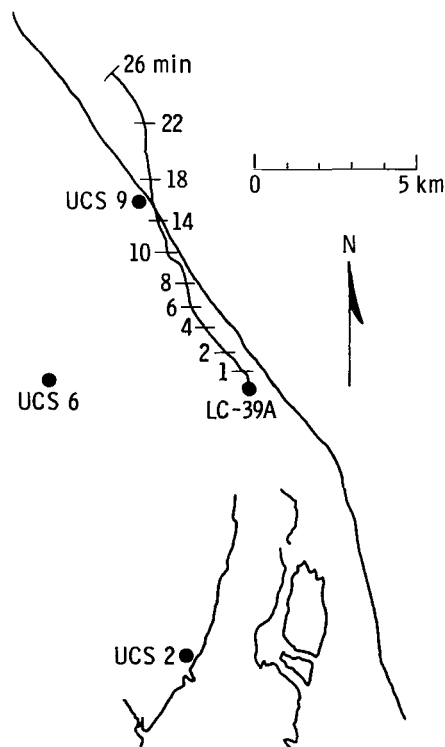


Figure 5.- North cloud trajectory.

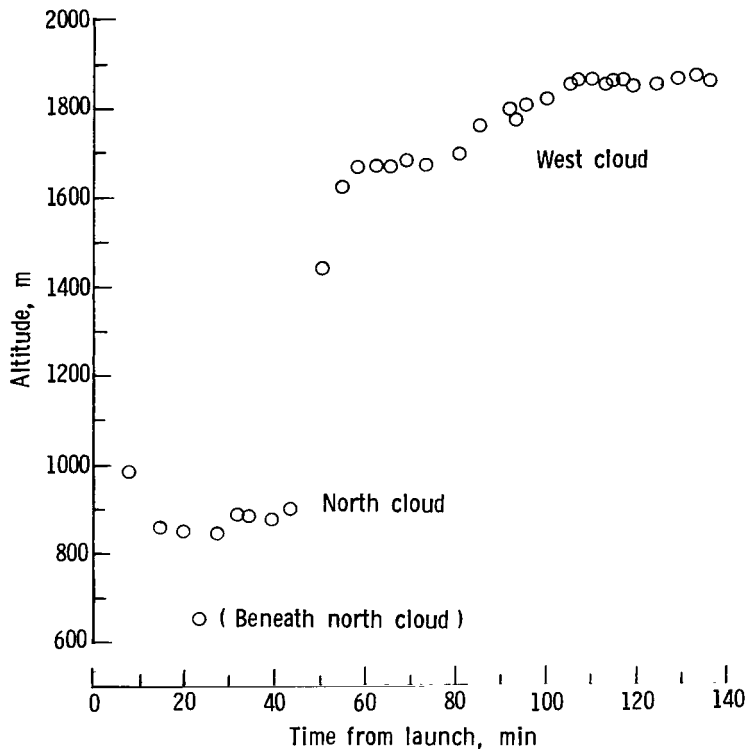


Figure 6.- Aircraft altitude during cloud sampling.

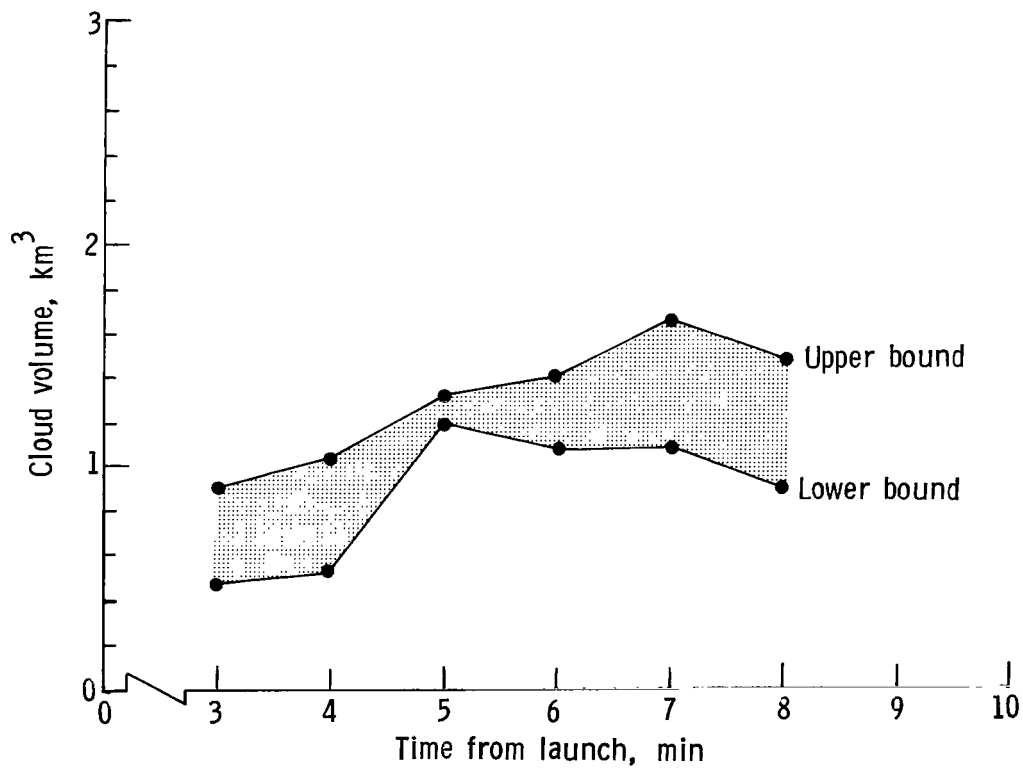


Figure 7.- Estimated volume for north cloud.

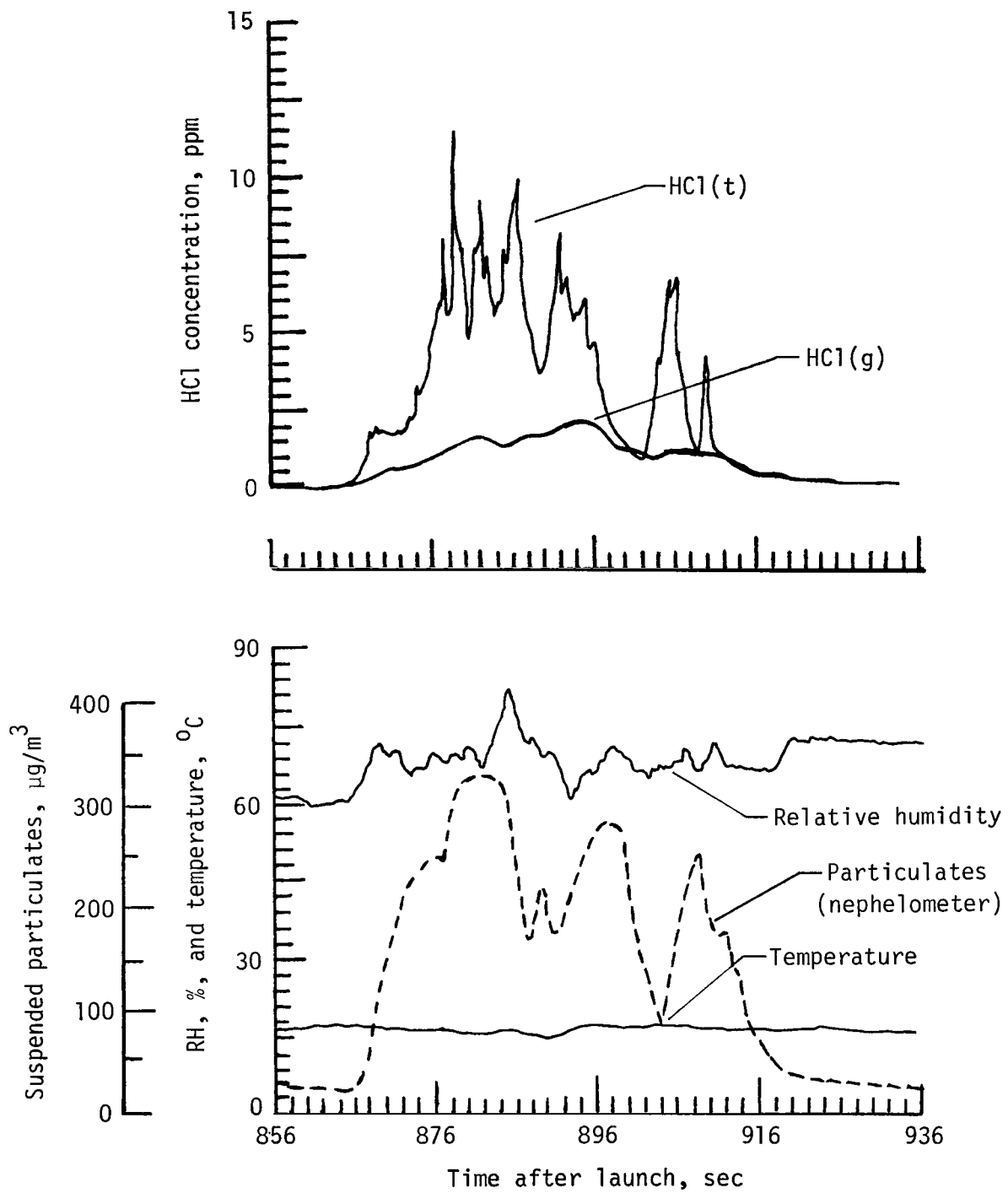


Figure 8.- Typical in-cloud data for north cloud, pass 2 at T + 15 min.

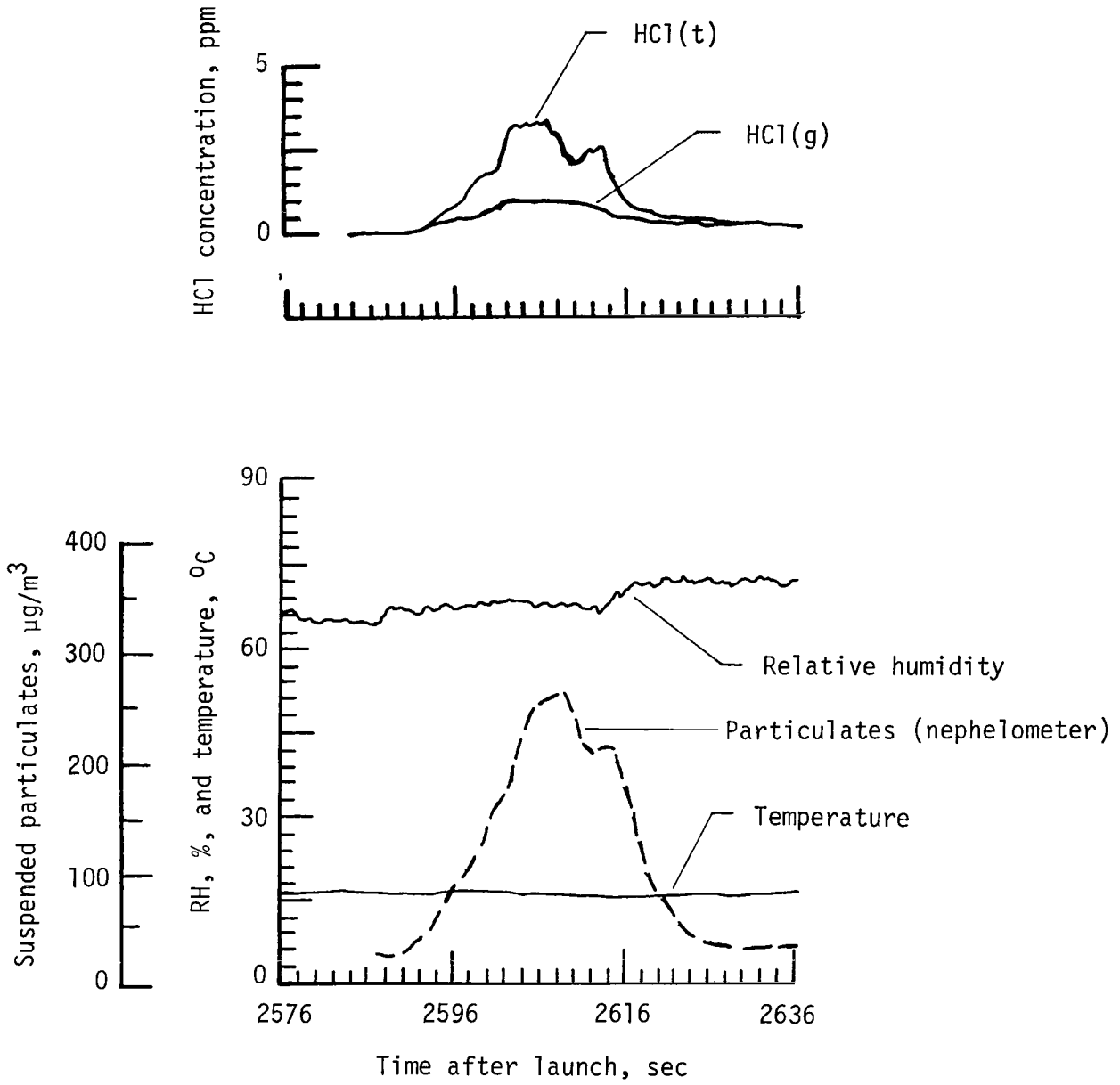


Figure 9.- Typical in-cloud data for north cloud, pass 9 at T + 43 min.

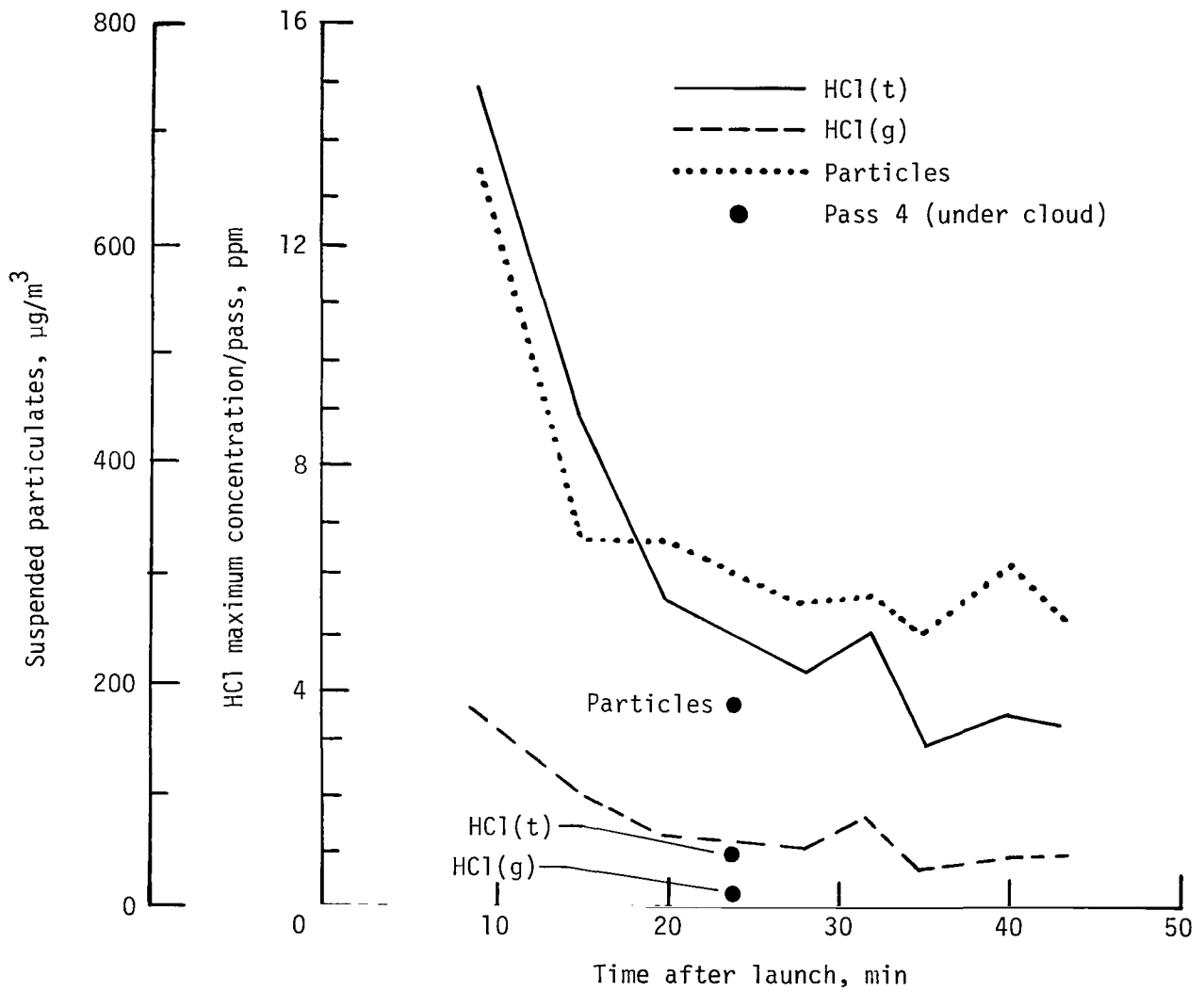
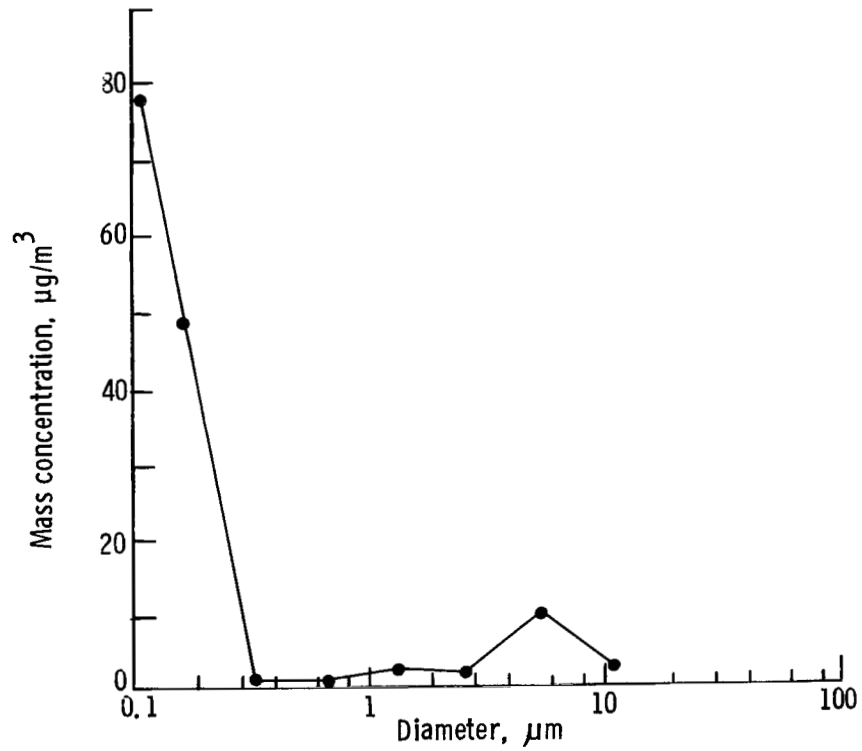
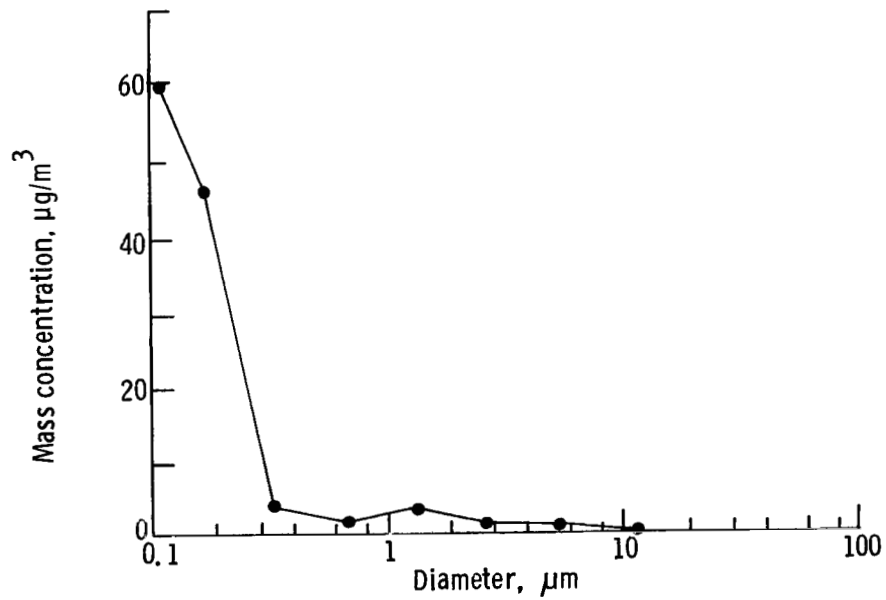


Figure 10.- Species decay with time, north cloud.



(a) Pass 2 at T + 15 min.



(b) Pass 9 at T + 43 min.

Figure 11.- Typical in-cloud particle size (QCM) data, north cloud.

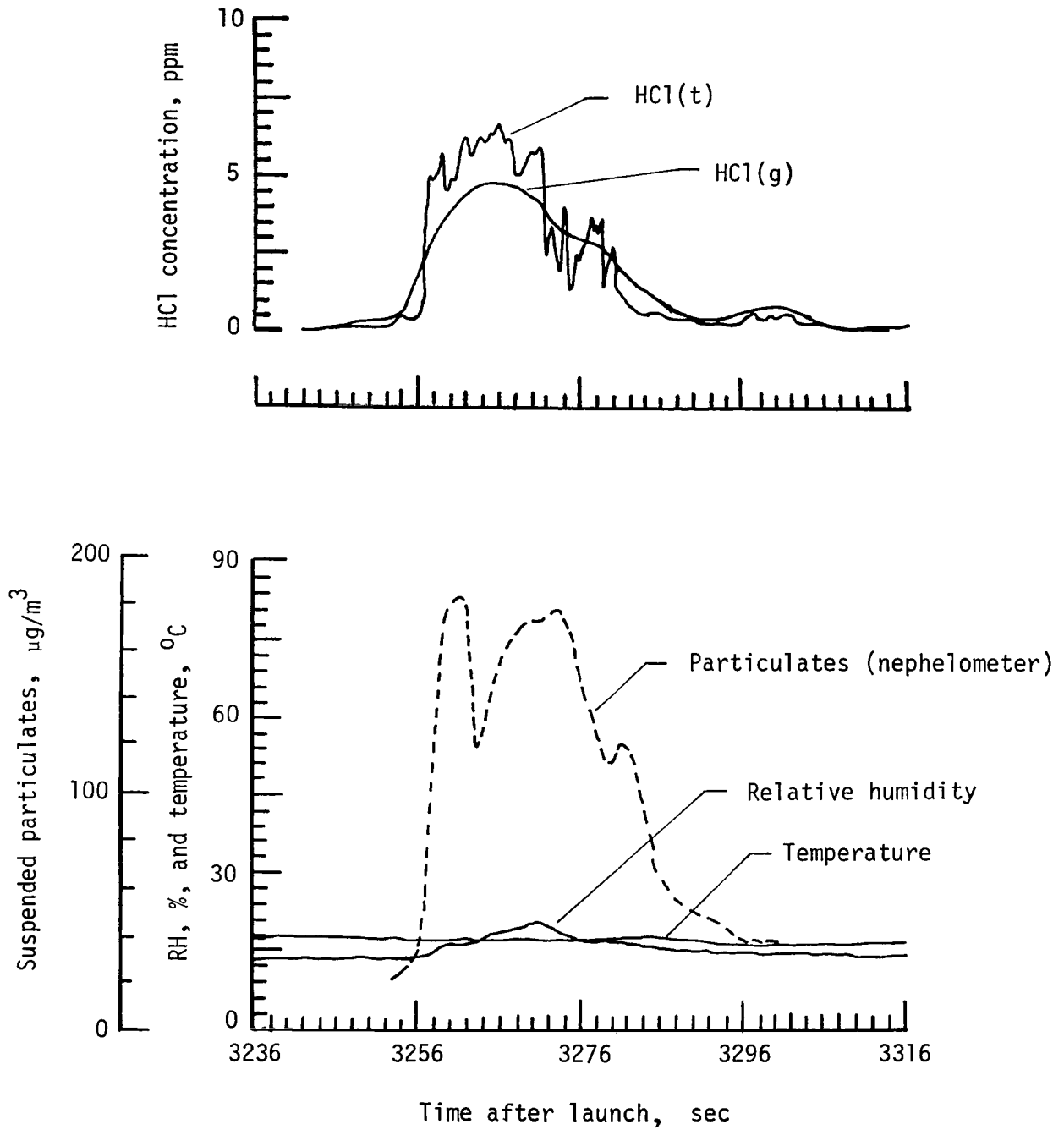


Figure 12.- Typical in-cloud data for west cloud, pass 11 at T + 55 min.

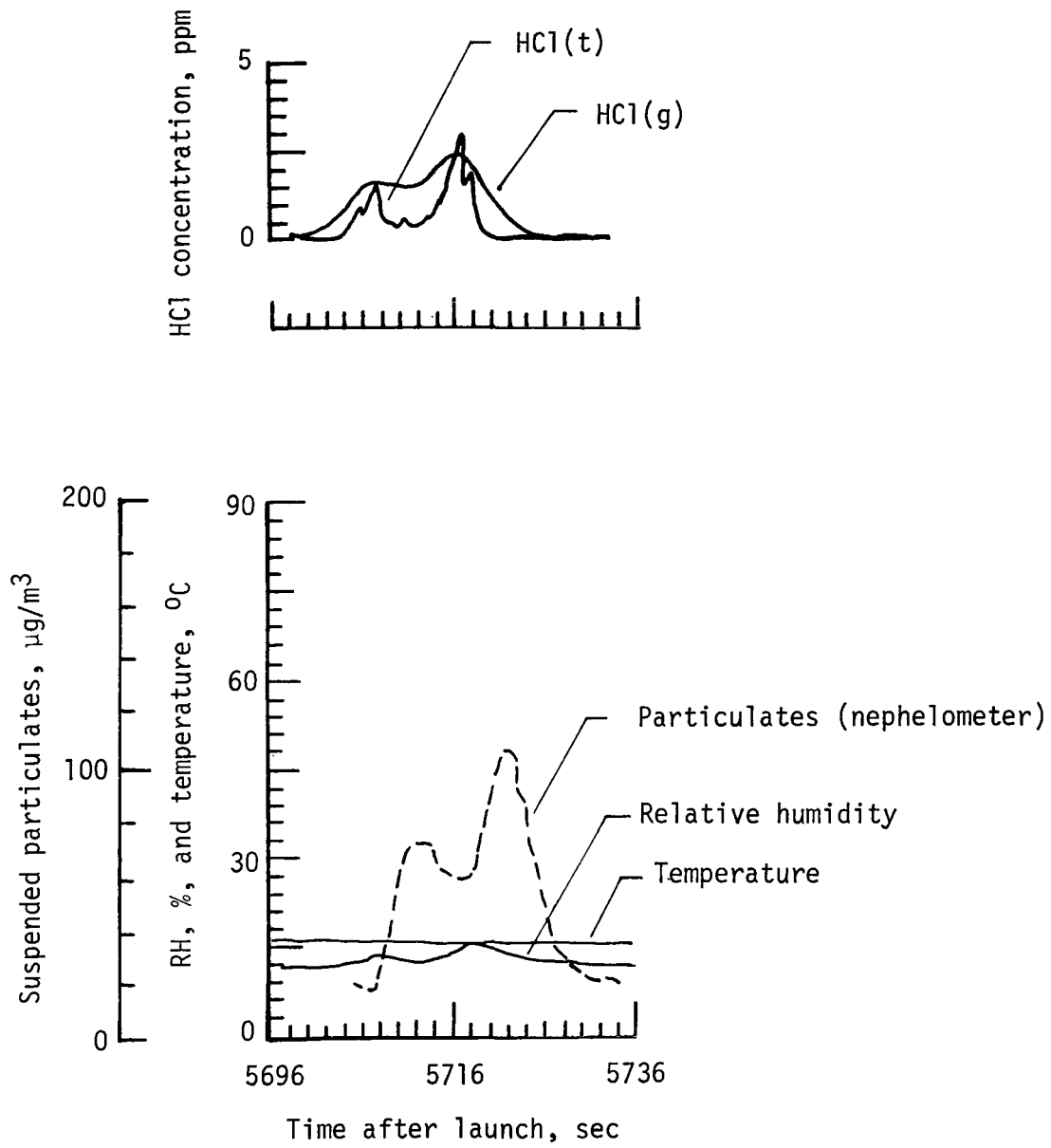


Figure 13.- Typical in-cloud data for west cloud, pass 21 at T + 96 min.

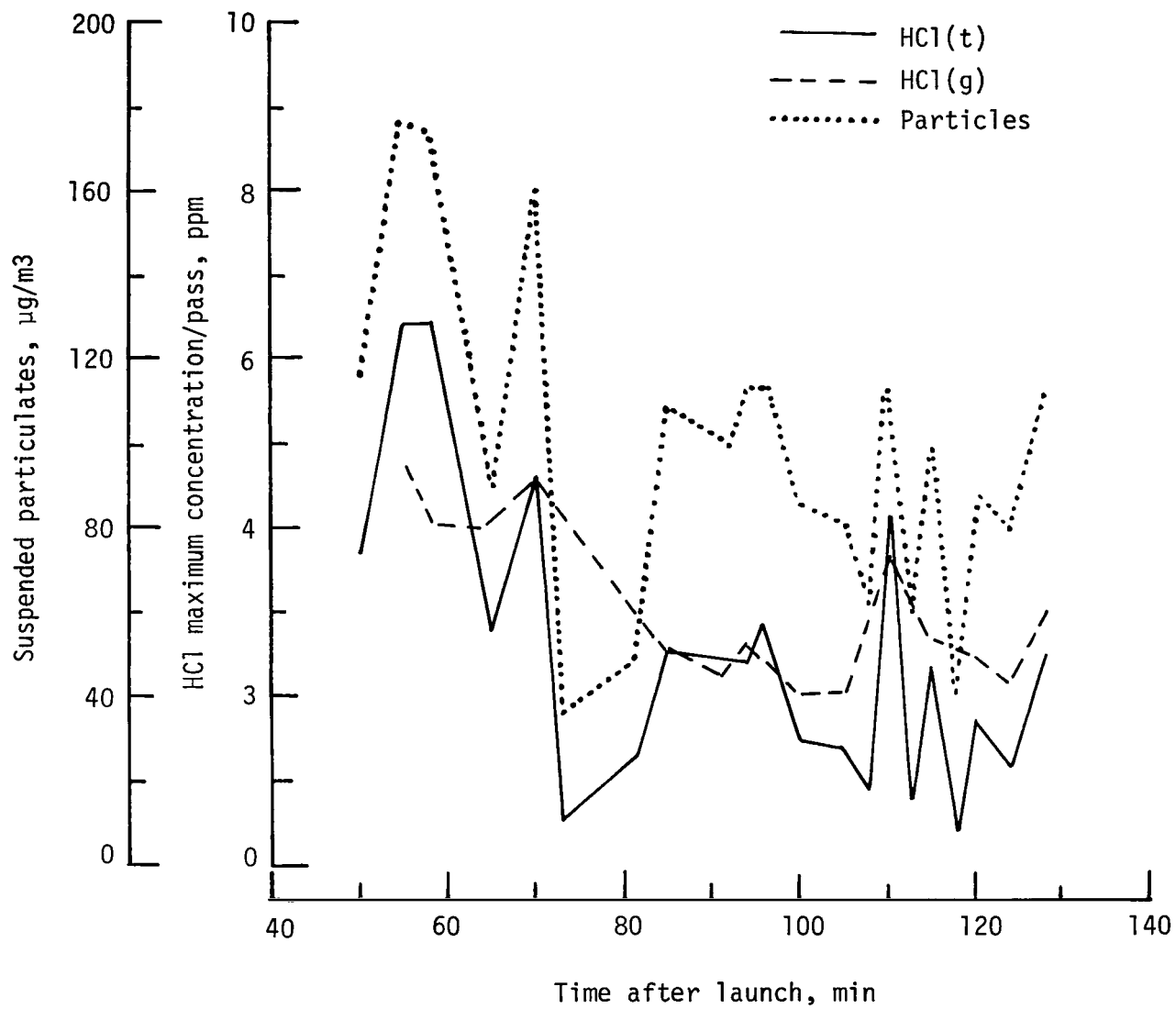
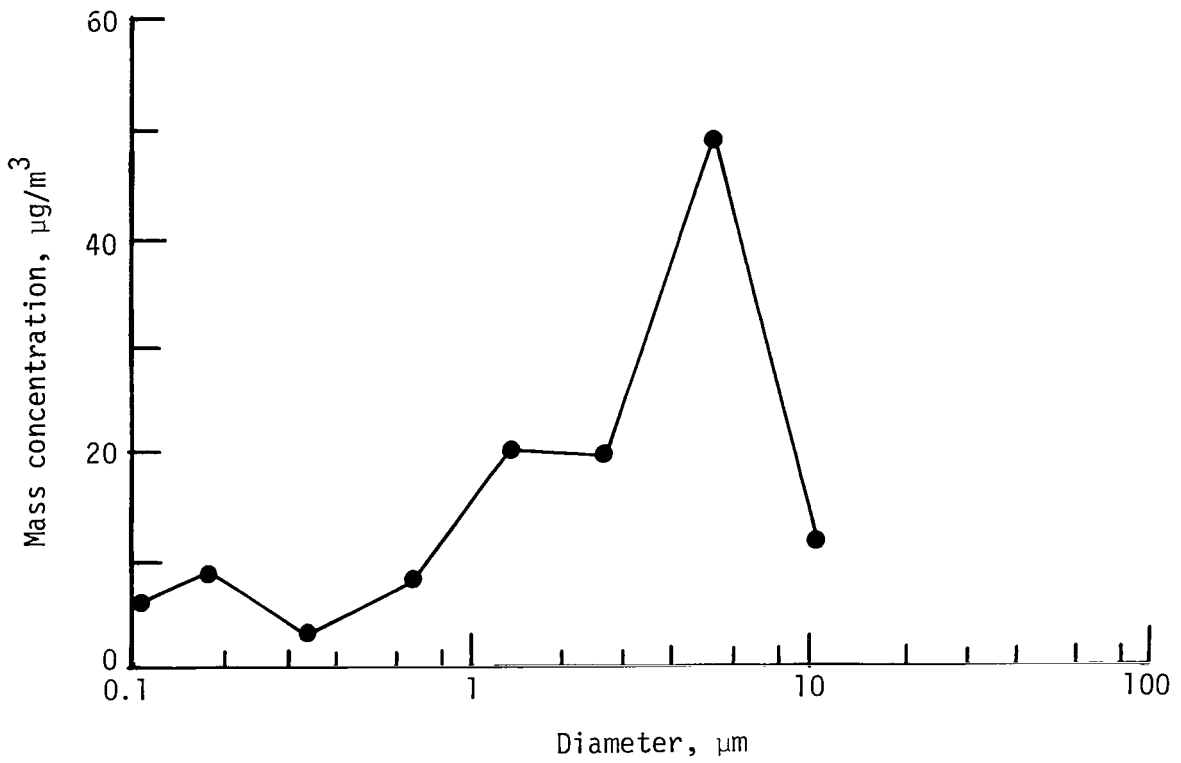
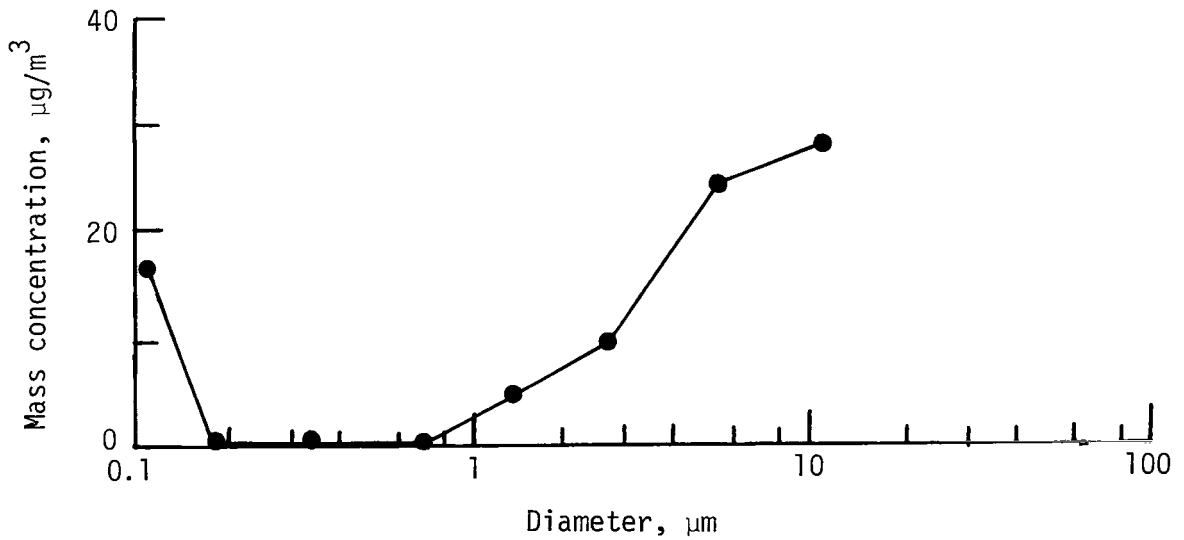


Figure 14.- Species decay with time, west cloud.

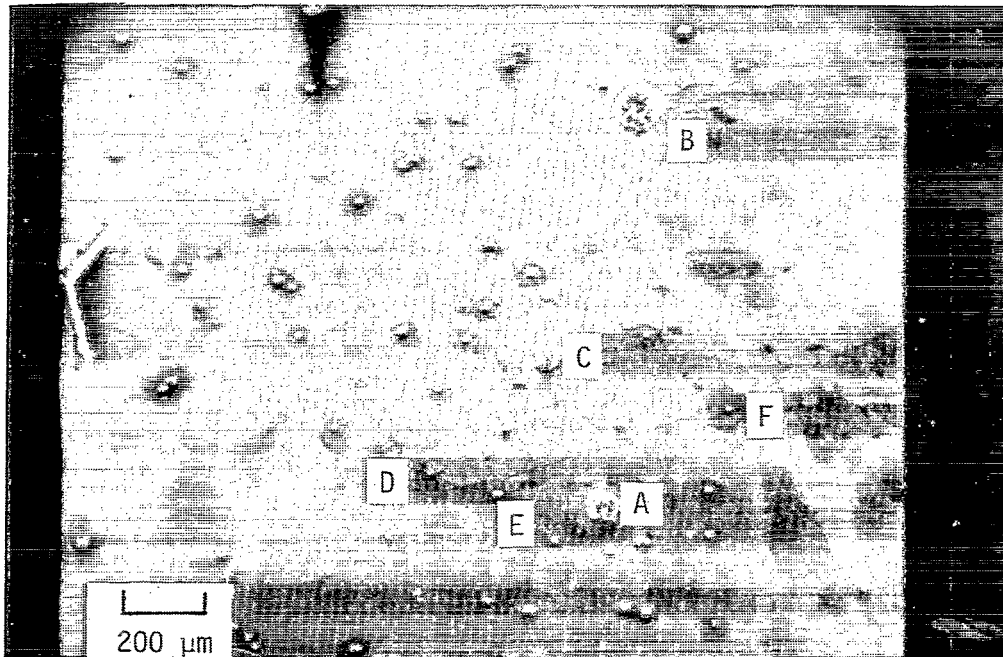


(a) Pass 11 at T + 55 min.

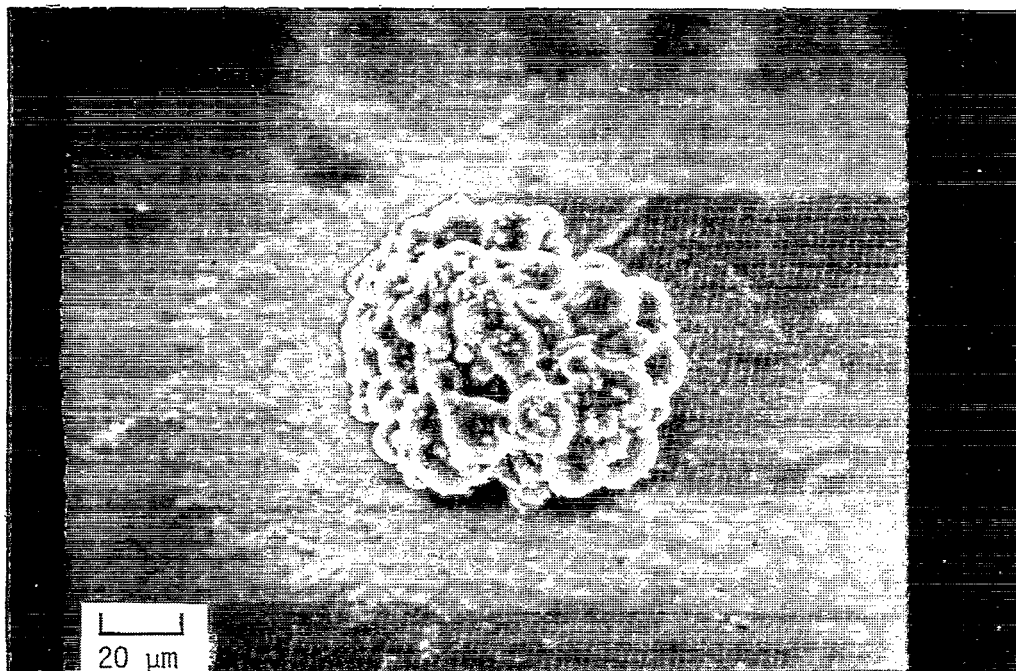


(b) Pass 21 at T + 96 min.

Figure 15.- Typical particle size (QCM) data, west cloud.



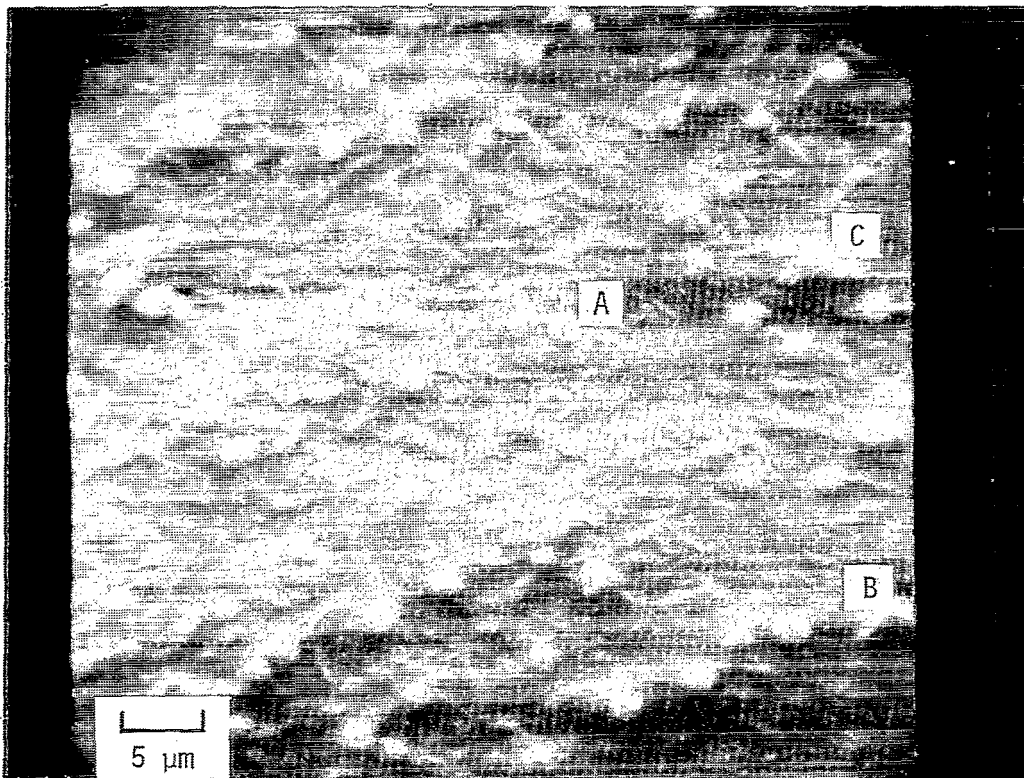
(a) Stage 1 particles.



(b) Enlargement of particle A.

L-82-203

Figure 16.- Scanning electron microscopy photographs of aluminum oxide particles collected on stage 1 of the QCM.



L-82-204

Figure 17.- SEM photograph of particles on stage 6 of QCM.

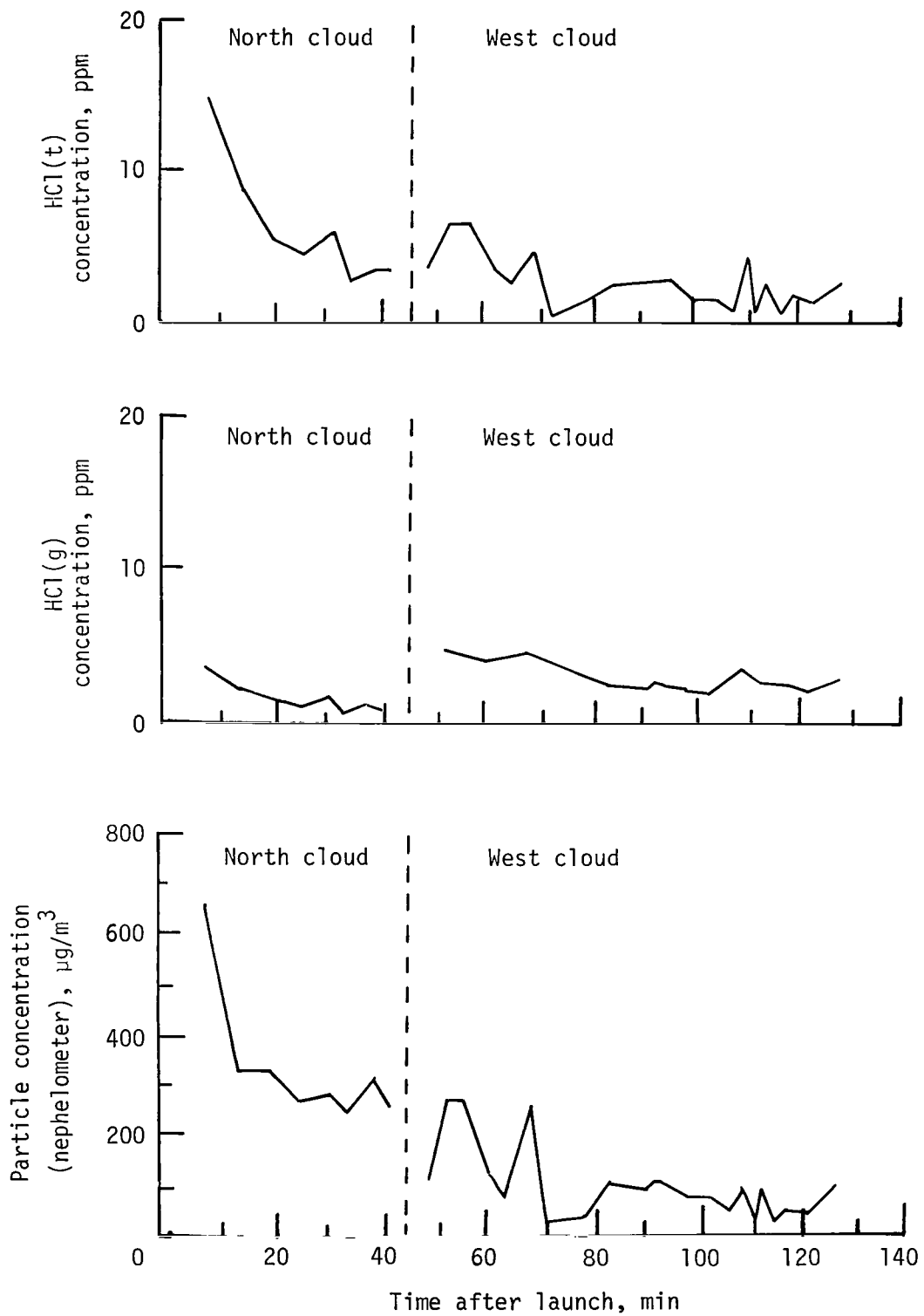


Figure 18.- Peak in-cloud concentrations for STS-1.

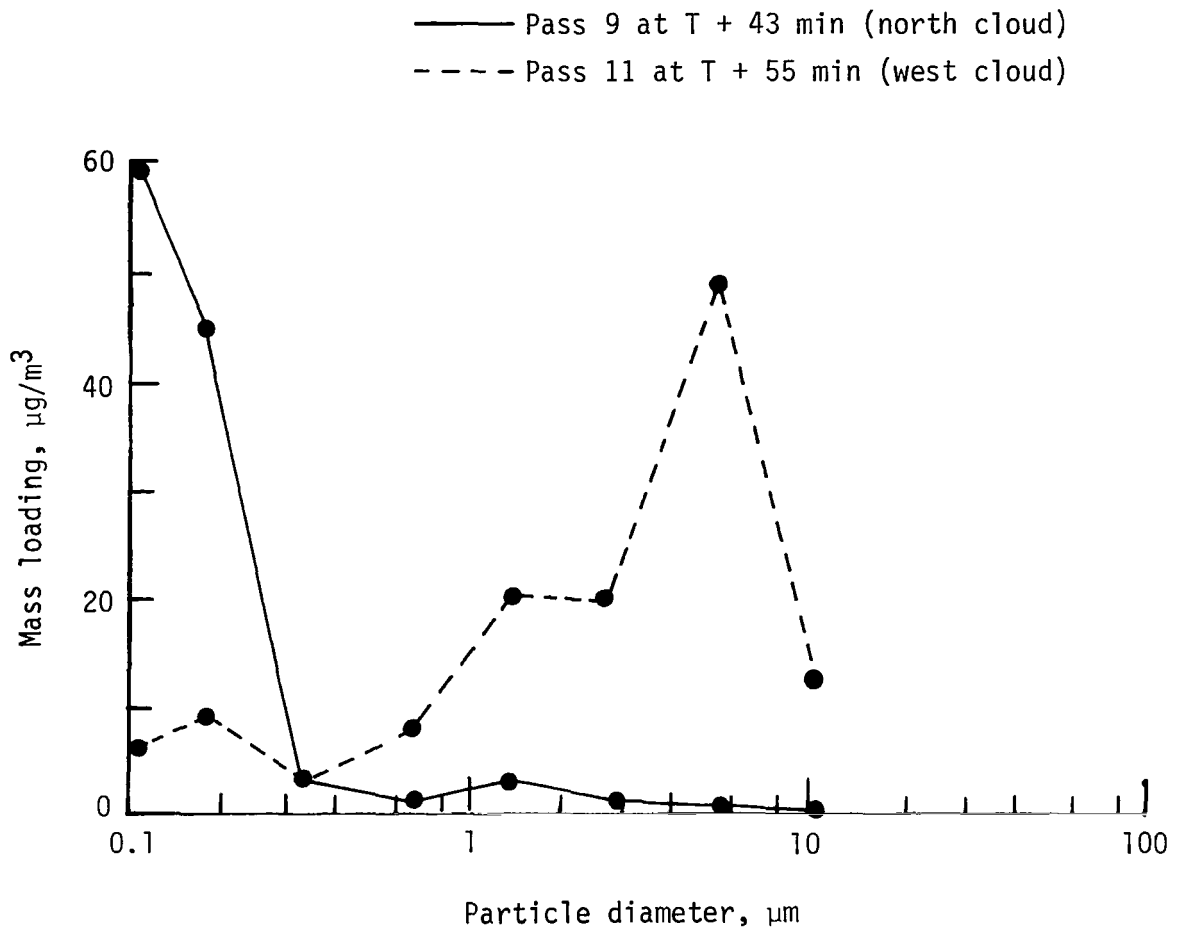


Figure 19.- Comparison of particle size distributions for north and west clouds.

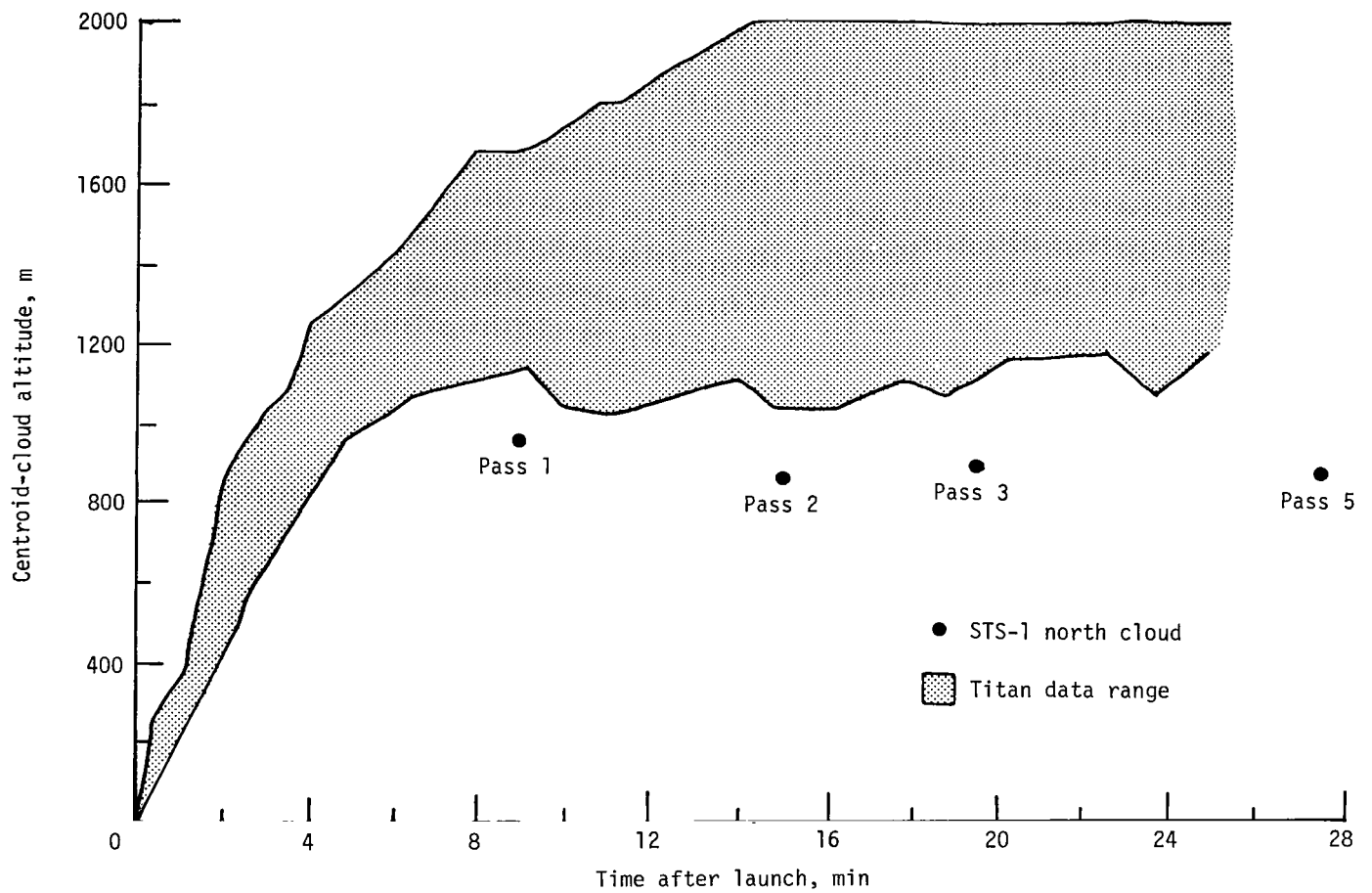


Figure 20.- Comparison of STS-1 and Titan cloud-centroid altitudes.

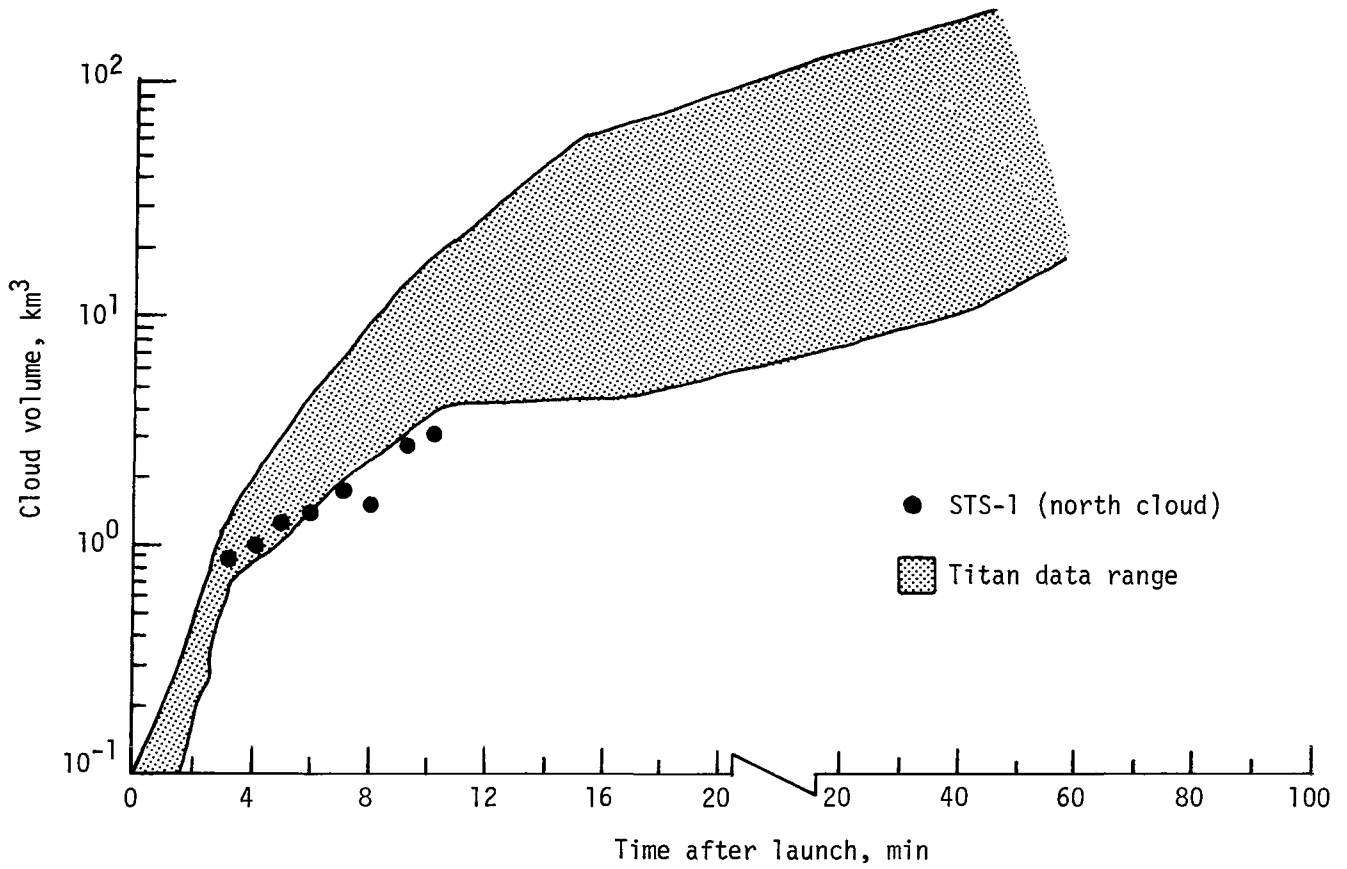


Figure 21.- Comparison of STS-1 (north cloud) and Titan cloud volumes.

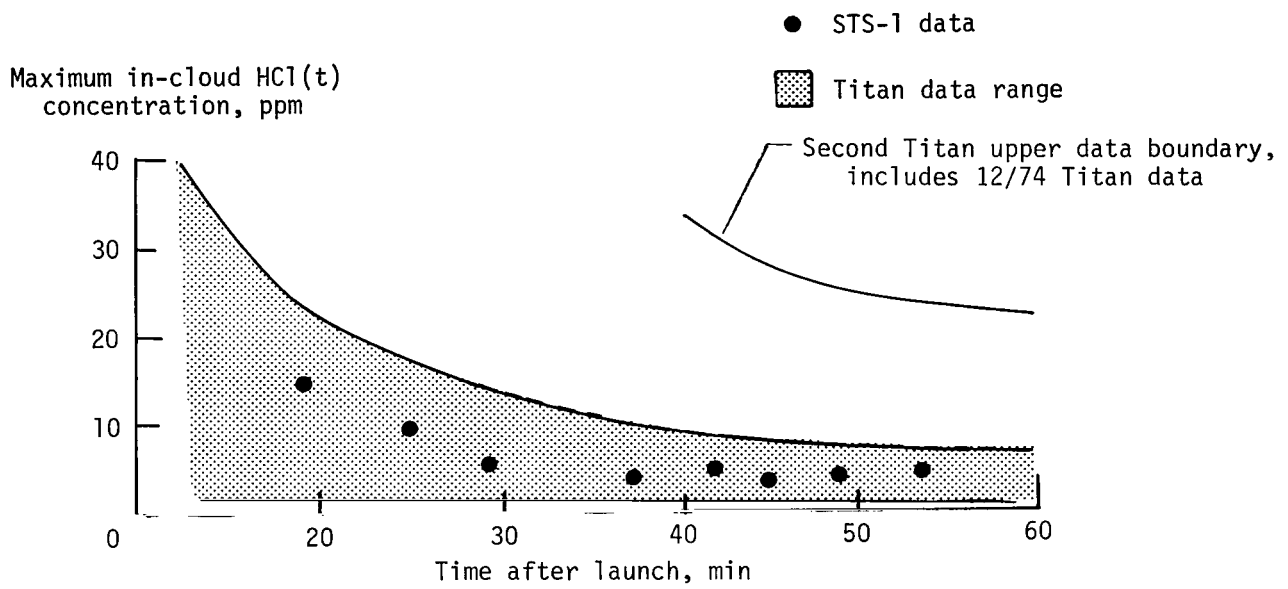
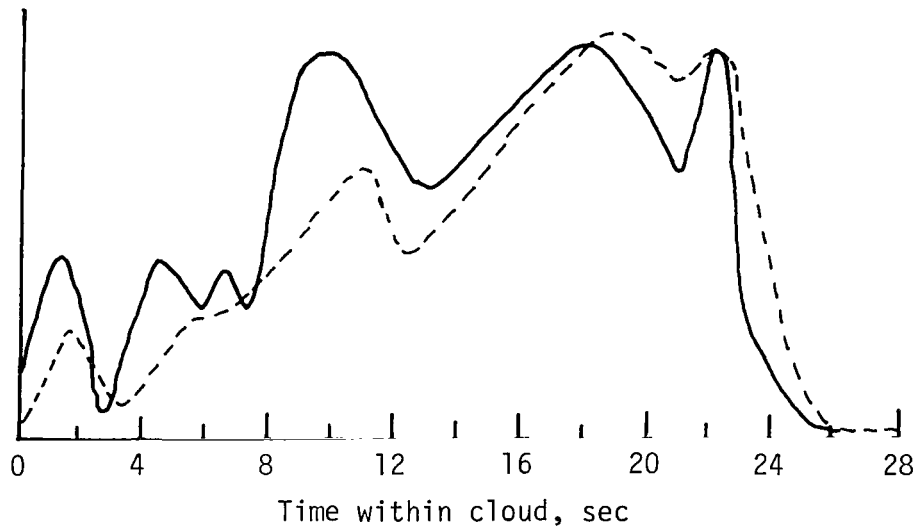


Figure 22.- Comparison of STS-1 and Titan HCl(t) maximum in-cloud concentrations.

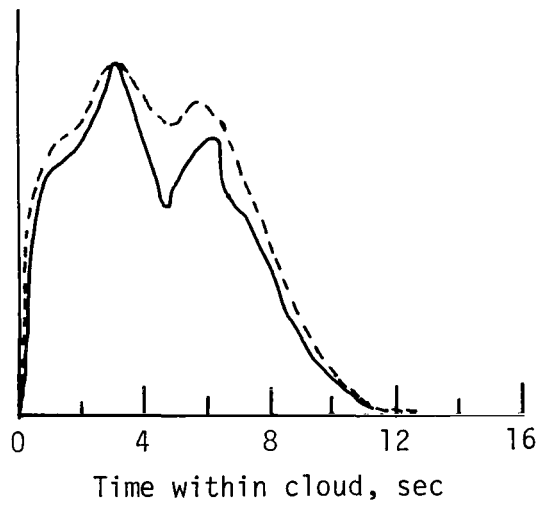
—— HCl(t)
----- Particulates (nephelometer)

Normalized concentration



(a) Pass 2 at T + 5 min.

Normalized concentration



(b) Pass 9 at T + 22 min.

Figure 23.- Titan data, December 1974 launch.

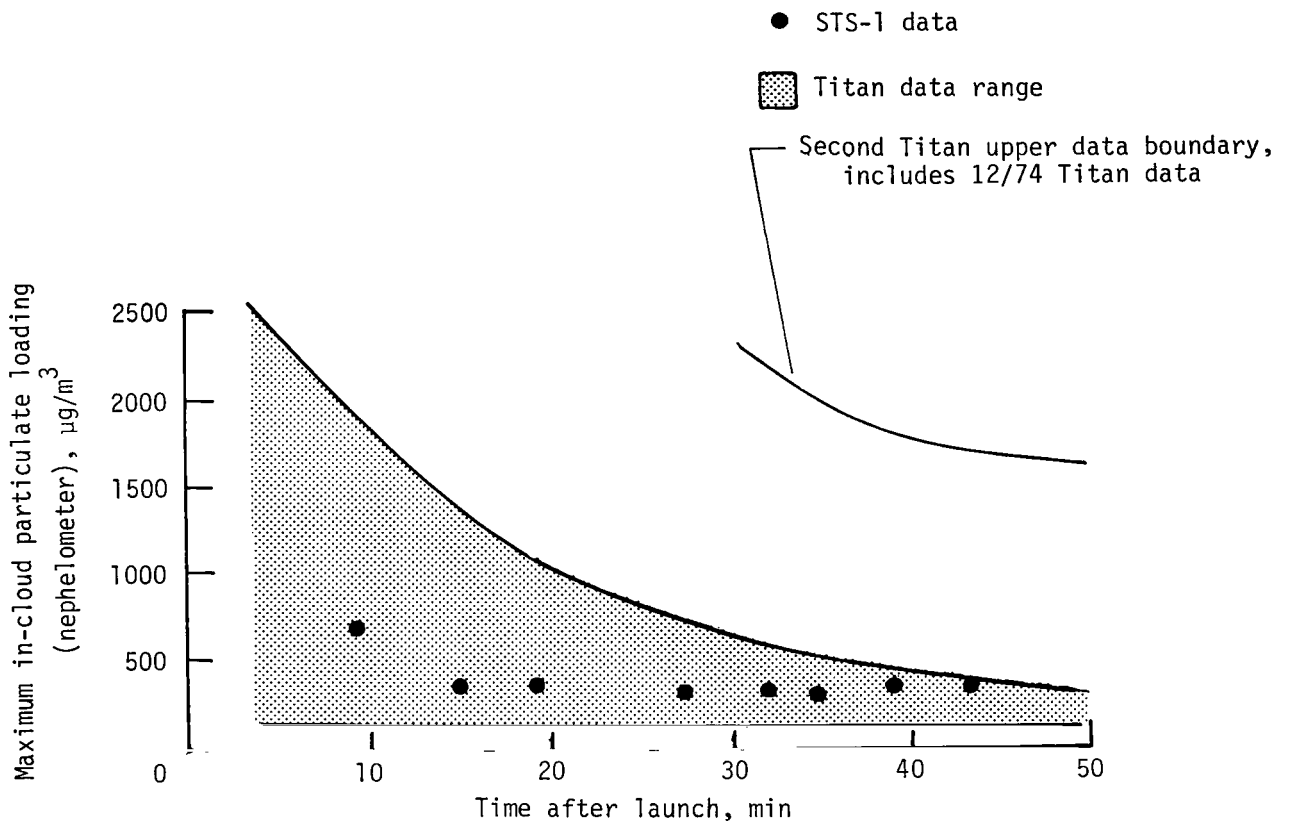


Figure 24.- Comparison of STS-1 and Titan particulate (nephelometer) maximum in-cloud loadings.

1. Report No. NASA TP-2090	2. Government Accession No.	3. Recipient's Catalog No.
4. Title and Subtitle AIRBORNE MEASUREMENTS OF LAUNCH VEHICLE EFFLUENT - LAUNCH OF SPACE SHUTTLE (STS-1) ON APRIL 12, 1981		5. Report Date January 1983
7. Author(s) Gerald L. Gregory, David C. Woods, and Daniel I. Sebacher		6. Performing Organization Code 925-81-01-01
9. Performing Organization Name and Address NASA Langley Research Center Hampton, VA 23665		8. Performing Organization Report No. L-15494
12. Sponsoring Agency Name and Address National Aeronautics and Space Administration Washington, DC 20546		10. Work Unit No.
15. Supplementary Notes		11. Contract or Grant No.
16. Abstract <p>The first Space Shuttle (STS-1) was launched from John F. Kennedy Space Center at 0700 eastern standard time, April 12, 1981. Launch vehicle effluent environmental impact activities included airborne measurements within the exhaust cloud from about 9 min after launch (T + 9) to T + 120 min. Measurements included total hydrogen chloride (gaseous plus aqueous) concentrations, particulate concentrations, temperature, and dewpoint temperature. The airborne measurements are summarized. A brief discussion of the physical growth and behavior of exhaust clouds is presented as well as the results of laboratory analysis of elemental composition of particulate samples collected by the aircraft. Observed results from the STS-1 launch are compared with earlier Titan III results. Shuttle effluent concentrations are found to be within the range of Titan III observations.</p>		13. Type of Report and Period Covered Technical Paper
17. Key Words (Suggested by Author(s)) Airborne sampling Effluent sampling Rocket vehicle exhaust Shuttle exhaust Air quality		14. Sponsoring Agency Code
19. Security Classif. (of this report) Unclassified		18. Distribution Statement Unclassified - Unlimited Subject Category 45
20. Security Classif. (of this page) Unclassified	21. No. of Pages 72	22. Price A04

National Aeronautics and
Space Administration

Washington, D.C.
20546

Official Business

Penalty for Private Use, \$300

THIRD-CLASS BULK RATE

Postage and Fees Paid
National Aeronautics and
Space Administration
NASA-451



S

4 1 10, E. 830105 S00903DS
DEPT OF THE AIR FORCE
AF WEAPONS LABORATORY
ATTN: TECHNICAL LIBRARY (SUL)
KIRTLAND AFB WA 37117

NASA

POSTMASTER:

If Undeliverable (Section 158
Postal Manual) Do Not Return